Re-evaluating the basis of clonal selection in germinal centres

Ziqi Long

Somerville College

University of Oxford

A thesis submitted for the degree of

Doctor of Philosophy

Trinity Term 2022

Abstract

Effective humoral responses rely on the development of high-affinity antigen-specific B cells. However, the naïve repertoire of antibodies usually shows low affinity. B cells need to improve their affinity in secondary lymphoid structures known as germinal centres (GCs) during infections, a process known as affinity maturation. In GCs, B cells undergo iterative rounds of somatic hypermutation in the dark zones (DZs) to diversify BCRs then exit cell cycle and move back to light zones (LZs) for affinity-based selection. In the LZs, it has long been considered that only selected cells could subsequently reenter cell cycle and move back to DZs, a process known as cyclic re-entry. Affinity enhancements are thought to be conferred via T cells providing help to the highest affinity LZ B cells to initiate cyclic re-entry, however, this hypothesis was never directly tested. Using fluorescent cell cycle reporter mice, we found neither T cells depletion nor MHCII deletion abolished the cyclic re-entry initiation in LZ cells and this process was not detectably restricted by general intra-GC competition. Concurrently, using BATF as a marker for recent T-B interactions, we found B cells needed to compete in order to receive T cell mediated refuelling in an affinity dependent manner. However, this process was also limited by B cells' intrinsic ability to acquire antigens. Consistent with the observations above, cyclic re-entry LZ cells were found to be heterogeneous at their BATF levels, further confirming cyclic re-entry initiation and receiving T cell mediated refuelling are two processes regulated independently. Our data is pointing towards a less binary selection mechanism in GCs, which confers proliferative advantage to higher affinity clones while allowing low-affinity cells to mature via more complex pathways so that antibody repertoires are matured for both affinity and clonal diversity.

Acknowledgements

First and foremost, I have been extremely fortunate to be supervised by Oliver Bannard in my DPhil studies. I received a tremendous amount of guidance and encouragement from Oliver in the last four years. Oliver has taught me everything about germinal centre, experimental techniques and how to think scientifically. If I can be considered as one step closer to being a confident and independent researcher, that would largely be owing to Oliver's supervisions and support. As a passionate and creative scientist, Oliver can give very detailed suggestions but he also gave me the freedom to investigate what I think is most interesting. Oliver encouraged me to pursue the career that I desired the most when I was unsure about the future, to which I remain forever grateful.

I am also sincerely grateful to my secondary supervisor Persephone Burrow. Seph has set me a role model as an insightful and diligent scientist to whom I am always looking up. She has been very approachable and has given me a great amount of fantastic suggestions for the project and encouraged me whenever I was in self-doubt. I am very thankful for the valuable feedback from my transfer examiners Jan Rehwinkel and Sarosh Irani as well as my thesis committee members Claus Nerlov and Terry Rabbitts throughout my DPhil studies. My college advisor, Richel Exley, has always been there to help.

I would like to thank all the past and present members of the Bannard lab. We have been a small but warm and supportive lab and I could not have imagined being in a better environment to spend four years doing research. In particular, I thank Adrien for his (sometimes dry) humour and jokes that made me laugh even on difficult experiment days. Besides, project discussions with him have always been insightful and interesting. We are also very lucky to have Ana, who has fantastic technical skills and supplemented them with her enthusiasm and high spirits. I am very grateful to Veera, who taught me all I know about microscopic work and image analysis. Although I never had the chance to meet Beth in the lab, she has laid a great foundation for our project. Elise and Mollie also contributed with excellent technical assistance. Our very first DPhil student in the lab, Isabelle, has set a model for me as a smart and hard-working DPhil student.

I am also very thankful to our wonderful staff in WIMM FACS facility, Paul, Craig, Sally and Kevin for answering all my questions about flow cytometry and for their help with my sorting experiments. I am very grateful to Roo, Jonathon and all other staff from BMS JR who trained me patiently for all my techniques and for their help with my mouse work.

Friends are the family we choose for ourselves. My DPhil life would have been a lot harder without Xiaorui. Although we are 8000 miles apart physically, she has witnessed all my ups and downs throughout the whole journey and is always there to listen. I have been very fortunate to be surrounded by friends throughout these years. Rong, really is my big sister and I received so much love from her. Zixi and Xiying, we have fought together side by side for four years and will miss these days. Also Qian, Yiran, Meng and Lisa, very very grateful that they could all be in my life. Some of our friends have moved on to their new life adventures but we remain close regardless of our geographical locations.

"There is no place like home." – L.Frank Baum. Last but not least, I would like to thank my parents, who set me great examples to look up to when I grew up and always supported me to the best of their abilities. They believe in actions speak louder than words, and I can feel their love through every detail, no matter where I am in the world. I have been gradually getting towards my dream and the person I want to be, and this is only possible because of my parents' love and support. Their unconditional love and support have been and will always be the source of my confidence and strength to face all the challenges in my life. Words just cannot express how much I love you.

Four-year DPhil study has not been an easy journey. Thanks to all the people I met I have been able to witness a great view and have the courage to try many things. This journey is now leading towards new adventures which I will remain forever curious about.

Contents

List of Figures

List of Tables

List of Abbreviations

AID . . . . . Activation induced cytidine deaminase.

BAFF . . . . . B cell activating factor.

BATF . . . . . Basic Leucine Zipper ATF-Like Transcription Factor.

BCR . . . . . B cell receptor.

BLNK . . . . . B cell linker protein.

BM . . . . . Bone marrow.

bnAbs . . . . . Broadly neutralizing antibodies

Btk . . . . . Bruton's tyrosine kinase

CSR . . . . . Class switch recombination

DC . . . . . Dendritic cell

DTR . . . . . Diphtheria toxin receptor

DZ . . . . . Dark zone

FDC . . . . . Follicular dendritic cell

FRET . . . . . Fluorescence resonance energy transfer

GC . . . . . Germinal centre

GFP . . . . . Green fluorescent protein

HEL . . . . . Hen egg lysozyme

ICOS . . . . . Membrane-bound inducible costimulator

ITAM . . . . . Immune receptor tyrosine-based activation motif

LZ . . . . . Light zone

MHCII . . . . Major histocompatibility complex class II

MBC . . . . . Memory B cell

NK cell . . . . Natural killer cell

NP 4-Hydroxy-3-nitrophenyl

OVA . . . . . Ovalbumin

PAGFP . . . . Photoactivatable green fluorescent protein

PC . . . . . Plasma cell

PRR . . . . . Pattern recognition receptors

S1PR2 . . . . . Sphingosine-1-phosphate receptor 2

SHM . . . . . Somatic hypermutation

SRBC . . . . . Sheep red blood cell

SW_{HEL} . . . . Switchable HEL

T_{FH} . . . . . Follicular helper T cell

T_{FR} . . . . . Follicular regulatory T cell

TLR . . . . . Toll-like receptor

Treg . . . . . Regulatory T cells

WT . . . . . Wild type

Chapter 1

Introduction

Contents

1.1 The immune system requires diversity to provide defence against endless pathogens

1.1.1 Innate and adaptive immune systems are two branches in the immune system

The immune system is a complex cellular network involving multiple types of cells and proteins that work together to protect the organism from diseases. It is responsible for recognizing non-self and harmful incoming pathogens across a diverse range, from viruses to eukaryotic parasites and eliminating them to maintain tissue homeostasis. In most vertebrates, the immune system involves two arms, the innate and adaptive immune systems.

The first line of defence is the innate immune system. This consists of a physical barrier, including skin and mucosal membranes, that physically blocks the entry of pathogens. If pathogens penetrate the physical barriers, the innate immune cells then utilize pattern recognition receptors (PRRs) to identify molecular signatures that belong to foreign pathogen-associated molecular patterns (PAMPs) or damaged-associated molecular patterns (DAMPs). PRRs fall into different subfamilies based on their structures; for example, the Toll-like receptors (TLRs) and the intracellular NOD-like receptors (NLR) that recognize a wide range of bacterial lipids, lipoproteins or microbial nucleic acids; important viral RNA sensor RIG-I-like receptors (RLRs) and the C-type lectin receptors (Kawasaki et al, 2014; Franchi et al, 2009; Rehwinkel et al, 2020). Once these receptors are activated by ligands, the downstream clearing process is quickly initiated by either direct killing or phagocytosis. As such, innate immunity has a fast response speed but only recognizes specific conserved patterns.

When pathogens breach surface barriers and are not immediately cleared at the site of invasion, the adaptive system next tries to resolve the infections with a more tailored response that is highly specific for each pathogen. This process

is orchestrated in highly organized and compartmentalized peripheral lymphoid organs, namely spleens and lymph nodes. A successful adaptive immune response is triggered and requires input from innate immunity. Various cell types such as dendritic cells (DCs) and macrophages from the innate immune system act as antigen-presenting cells for the activation of lymphocytes, not only displaying antigen but also directing differentiation and polarisation through appropriate cytokine release - thereby helping shape optimal adaptive responses (Jain et al, 2017). The adaptive immune system encompasses T and B lymphocytes that carry tremendous diversity in terms of pathogen recognition as a result of random somatic combinations occurring at the V(D)J loci. Adaptive immune responses have a delayed onset because the activation and expansion of T and B cells with the correct specificity require several days. An essential function of the immune system is to memorize the previously encountered pathogens to accelerate the response time for the next time. Despite the innate immune system having to some degree memory through memory-like natural killer cells (NK) and trained innate immunity, the vast majority of long-term antigen-specific memory resides in the adaptive immune system, with antigen-experienced memory T and B cells.

In adaptive immunity, T cells function through direct cytotoxicity effector functions, cytokine secretion or helper characteristics to promote B cell activities. At the same time, B cells are essential in humoral responses with their ability to differentiate into plasma cells that can secrete high-affinity antigen specific antibodies. B cells are constituted of two major subclasses – B1 cells and B2 cells. B1 cells are found less in lymphoid organs but predominantly in body cavities, such as peritoneal and pleural cavities. These cells are self-renewal and display innate immune system features by secreting natural antibodies (Baumgarth et al, 2010). While B2 cells constitute follicular and marginal zone B cells, they participate in the adaptive immune responses and produce antibodies following activation and receiving T cell help. These are the cells that we focus on in this thesis.

1. Introduction

Antibodies function either through direct neutralization of the pathogens or via effector functions, effectively orchestrating the responses from both innate and adaptive arms. Antibodies can be recognized by complement receptors or Fc receptors and then activate downstream phagocytosis or direct lysis, depending on the nature of the pathogens. Also, antibody-antigen complex recognition by these receptors could retrospectively enhance antigen uptake and presentation by DCs or follicular dendritic cells (FDCs), which activate T and B cells, respectively.

Structurally, antibodies are divided into variable regions that show significant diversity and constant regions, which determine the downstream signalling mechanisms. Based on the structure of the constant region, there are five isotypes of antibodies: IgD, IgM, IgG, IgE and IgA. Each one has different distribution and employs different effector functions. IgM and IgD are the first antibodies secreted during an immune response. B cells secreting these antibodies have not generally undergone extensive somatic hypermutation (SHMs), so they usually display low affinity. For IgM, the low affinity in each Fab interaction is compensated by its ability to form a pentameric structure, which results in high avidity. IgG is the main antibody isotype generated in the majority of immune responses and is widely distributed in most tissues in the body. Apart from direct neutralization, it can efficiently induce phagocytosis of the opsonized pathogens or activate the complement system. IgE mediates central responses in parasitic protection and allergy pathogenesis through the direct and indirect activation of mast cells, basophils, and eosinophils via Fc receptors FcεRI and FcεRII. Subsequent antigen binding to IgE on these cells leads to rapid degranulation and causes allergic reactions. IgA is mainly distributed on the mucosal surface in the intestines and respiratory tracts. However, most antibodies are not born with high affinity; they need to go through a Darwinian-like evolutional process to improve their binding effectiveness.

1.1.2 Importance of antibody affinity maturation

The development of antigen-specific antibodies is a critical feature of adaptive immune responses. B cells are facing an enormous challenge in generating antibodies with neutralizing activities against invading pathogens because there is an almost infinite number of epitopes to recognize. Naïve B cell repertoires are established in the bone marrow (BM) through VDJ gene recombination mediated by RAG recombinase and improper end joining. This process generates up to ~10^{15} antibodies with different specificities, and the adult human body uses a fraction of these antibodies to generate a B cell pool of ~5x10^9 cells (Briney et al, 2019).

For some pathogens and antigens, naïve B cell populations already contain cells expressing highly potent antibodies specific for both non-neutralizing and neutralizing epitopes that can elicit effective protection (Ju et al, 2020). However, this is not true for all targets and pathogens. Sometimes pathogens often make any important epitopes of vulnerability particularly hard to reach, highly variable or have similarities to self (for example, through self-glycan shielding), and/or by frequently mutating them to escape recognition. Consequently, no naïve repertoires contain all the antibody specificities required to confer absolute protection against all pathogens a person or animal might face.

In the first few days after an infection or immunization, antigen-specific naïve B cells quickly proliferate and differentiate into antibody-secreting plasmablasts. While the antibodies produced through these pathways can contribute to preventing pathogen dissemination, their affinities tend to be relatively low (MacLennan et al, 2003), and they are almost certainly limited in terms of the number of epitopes they bind "well". Herman Eisen first showed in the 1960s that the mean affinity of the antibodies in the serum increased over the course of an infection and after immunisation, indicating, besides VDJ recombination, the existence of a second mechanism for the antibodies to improve their recognition of antigens. This increase in affinity could not be readily explained by the presence of high-affinity germline

antibodies, indicating the antibodies are actually further diversified and evolving during immune responses. It was discovered that this process happens on a per molecule basis, suggesting this occurs on a genetic level. This process was later recognized as SHM taking place in lymphoid organs (Reynaud et al, 1991). Even functionally potent germline-encoded antibodies can be further improved this way, thereby reducing the number of antibody-secreting cells required for functional immunity. This process is termed affinity maturation and has two main goals: high affinity and vast diversity.

1.2 The antibody affinity maturation starts from naïve B cell activation and proliferation

1.2.1 The process of B cell activation

Naïve recirculating B cells are in G0 quiescent state, colonizing lymphoid organs in organized follicular structures and periodically recirculating through the lymphoid tissues via the lymphatic system and blood. During their residence in lymphoid tissues, naïve B cells are continuously surveying for cognate antigens. The lymphoid organs have highly compartmentalized structures to promote the retention and presentation of antigens to naïve B and other immune cells. When there are incoming pathogens/antigens, depending on their molecular weights, the small molecules are capable of freely diffusing into B cell follicles (Pape et al, 2007), while larger antigens are transported via endocytosis and exocytosis through subcapsular (SCS) macrophages into follicles (Carrasco and Batista, 2007; Junt et al, 2007; Phan et al, 2007). From here, immune complexes may be further transported into the parenchyma of the tissue by piggybacking on migrating lymphocytes using Fc and complement receptors, ultimately becoming deposited on FDCs. The FDCs then hold and display the intact antigens to B cells, providing opportunities for recognition. B cells may also sometimes directly encounter antigens for the first

time when presented by other cell types, including SCS macrophages and dendritic cells (Qi et al, 2006; Gonzalez et al, 2010).

Activation of naïve B cells starts when non-self antigens are encountered, with a second signal usually then required to confirm "foreignness" and permit rapid expansion of these activated B cells. When B cells recognize their cognate antigens via engaging their B cell receptors (BCRs), this leads to the activation of various downstream signalling pathways. For most of the incoming pathogens, BCR signalling alone is insufficient for full activation, and a second signal derived from T cells is required. The second confirmation signal is to avoid activating autoreactive B cells. Early activated B cells upregulate chemokine receptors CCR7 and EBI2 following BCR stimulation, allowing them to follow chemoattractant gradients of CCL21 and 25-hydroxycholesterols, respectively, and migrate toward the border between B cell follicle and T zone (Liu et al, 1991; Reif et al, 2002; Okada et al, 2005). T cells are primed and activated in T zones by dendritic cells displaying peptides from the same antigens (Philippe 2008). At the T-B border, activated B cells can present peptides derived from antigens on surface MHCII to T cells and receive help in the form of receptor ligations and local cytokine productions. The receptors include CD40-CD40L, ICOS-ICOSL and cytokines involving IL21, IL4 etc (Garside et al, 1998; Han et al, 1995; Zotos et al, 2010; Linterman et al, 2010). Following activation, B cells are significantly reprogrammed at the transcriptomic level to promote and control rapid proliferation, including upregulation of Fas (also known as CD95) (Allen et al, 2015). Fas ligand induces apoptosis in these fast dividing activated B cells if not balanced by the pro-survival signals from T cells (Koncz et al, 2012). This serves as an important checkpoint because proliferation left unchecked could ultimately lead to diffuse large B cell lymphoma (Razzaghi et al, 2021).

Some antigens with specific properties can directly stimulate B cells activation and proliferation without the need for a second signal from T cells, a process known as T-independent activation. These T-independent antigens fall into two categories,

type I and type II. Type I antigens can directly stimulate B cells through co-receptors such as TLRs. While type II antigens have highly multivalent structures, including polysaccharides, this multivalency can efficiently engage and crosslink BCRs for downstream activation (Vos et al, 2000).

Following the initial first round of intensive clonal proliferation, activated B cells potentially have three fates: they can differentiate into short-lived extrafollicular plasmablasts, secreting the first wave of antibodies following infections or immunizations, become extrafollicular memory B cells, or they can seed GCs. Initially, this fate decision process has been reported to be influenced by BCR affinity, with higher affinity cells preferentially selected into the plasmablast compartment (Paus et al, 2006). However, the generation of extrafollicular plasmablasts was later demonstrated to be an effect of proliferation of these cells rather than direct selection (Chan et al, 2009). Other studies demonstrated that cells with identical BCRs have equal capacity to differentiate into all three fates (Jacob et al, 1992; Chan et al, 2009). *In vivo* limiting dilution adoptive transfer-based studies have even shown that individual B cells can acquire multiple downstream effector fates (Taylor et al, 2015). Therefore, the initial round of clonal expansion following antigen stimulation generates extrafollicular effector populations and prepares for further rounds of diversification by seeding GCs.

1.2.2 BCR signalling transduction during B cell activation

BCRs are the receptors responsible for antigen recognition and the initial activation of naïve B cells. They are membrane-bound immunoglobulins (Ig) composed of two heavy and two light chains linked by disulphide bonds (surface antibodies). The heavy chain consists of three domains: the extracellular domain, a transmembrane domain and a short intracellular domain, while the light chains only have the extracellular structures. The Igs are associated with intracellular accessory proteins, Iga and Igb, also known as CD79a and CD79b, to propagate the extracellular BCR crosslinking signals across the plasma membrane. Then,

downstream intracellular components are activated through interactions with the immune receptor tyrosine-based activation motif (ITAM) on the cytoplasmic tails of Iga and Igb (Murphy et al, 2008).

The BCR signalling starts from cognate antigens engaging individual BCRs, followed by significant changes in BCRs from resting to activated states. However, contradicting observations have been made in the local multimeric BCR organizations following antigen stimulation and various models have been postulated. There are three major models depicting structural organizations. The major discrepancies arise from whether BCRs are in monomeric or multimeric structures. Klasener et al reported that resting BCRs are largely organized into clusters which dissociate from each other upon activation due to the increased rate of diffusion (Klasener et al, 2014). Meanwhile contradicting observations were made with super-resolution STED microscopy and fluorescence resonance energy transfer (FRET) that BCRs are monomeric in their resting states and crosslinking BCRs leads to the formation of local BCR clusters, facilitating efficient downstream signal propagation (Depoil et al, 2008; Gomes de Castro et al, 2019; Tolar et al, 2005). The third collision coupling model proposes that the increased BCR mobility upon activation promotes their probability of encountering kinases for signal transduction, under the assumption that BCRs and their co-receptors are segregated (Treanor et al, 2012). This model is built on the observation that the diffusion rate of resting BCRs is restricted by local actin filaments and depolymerization of actin filaments alone results in elevated BCR signalling (Treanor et al, 2010).

The initial substantial local BCR structural re-organization is accompanied by more conformational changes in the individual BCRs to allow signal transduction. Using FRET, Tolar et al. reported that upon antigen engagement, the cytoplasmic domains of BCRs undergo conformational changes to open up the structure, allowing the association of the first kinase Lyn to phosphorylate the ITAM domain (Tolar et al, 2005; Pierce et al, 2010). Following the phosphorylation of Lyn, the next step of phosphorylation on ITAM is carried out by Syk kinase. Syk kinase in turn

induces a cascade of phosphorylation and activation events, including B-cell linker protein (BLNK), Btk and phospholipase C (PLCr2), resulting in the activation of calcium release and protein kinase C (PKC) and NF-kB pathway activation (Oellerich et al, 2011). Concurrently, the PI3K pathway is activated by Lyn kinase phosphorylating CD19, which activates the mTORC1 pathway for biogenesis. The activation of these pathways results in transcriptional changes and the rapid growth and proliferation of activated B cells (Young et al, 2013).

1.3 The GC is the site for antibody affinity maturation

1.3.1 GCs are organized into two distinct compartments with specific phenotypes and events in each compartment

Following their initial activation, activated B cells have gone through intensive proliferation but bear zero or very few somatic hypermutations, therefore the affinity of their antibodies tends to be relatively low. Essentially, antibody specificity is restricted at this stage to the products of VDJ recombination in the BM, minus what was trimmed due to autoreactivity. It is estimated that up to 75% of immature B cells recognize self-antigens and so are removed before the maturation stage (Grandien et al, 1994; Wardemann et al, 2003). As such, there can be major functional gaps (i.e., of necessary affinity for effective Ab function) in the primary antibody repertoire that GCs can sometimes fill by improving the affinity and diversity of poorly reactive naïve B cells. In 1884, GCs were first described as aggregations of dividing lymphocytes by Walther Flemming. Later, GCs were identified to be organized secondary lymphoid loci that arise in the centre of B cell follicles in periphery lymphoid organs following infections and immunizations aimed at antibody affinity improvements. The migration of activated B cells from the periphery to the centre of follicles to seed GCs is controlled by the chemoattractant axis in the lymphoid

organs. Upon differentiation into GC B cells, they coordinately upregulate S1PR2 and downregulate EBI2, leading to their sequestration in the centre of follicles (Green et al, 2011; Green et al, 2012; Gatto et al, 2009, Pereira et al, 2009).

In GCs, antibody affinities are enhanced through iterative rounds of immunoglobulin variable region gene SHM and clonal selection, thereby generating bespoke antibodies for each pathogen encountered. The ultimate output from the affinity matured GC B cells is long-lived memory and plasma cells that confer immunity. GCs are divided into two zones; dark zones (DZs) and light zones (LZs) based on their anatomical features, with GC B cells making iterative interzonal movements. DZs are enriched with densely packed fast-dividing B cells so they appear darker during H&E stain, while in LZs, B cells are mostly quiescent, and LZs contain other essential cell types, including stromal-like FDCs and follicular helper T (T_{FH}) cells (Nieuwenhuis et al, 1984).

The physical separation of the GCs is coupled with different focuses on the events occurring in each zone to ensure efficient affinity maturation. DZs are the sites for rapid cell proliferation and SHM, where B cells proliferate and diversify their BCRs (Jacob et al, 1991; Hanna et al, 1964). Then, B cells with mutated BCRs are selected based on their BCR affinity in LZs. The whole affinity maturation follows a Darwinian-like evolution where random mutations followed by fitness-based selection lead to improvements at the general population level. However, the distinct separation of the events in different locations is probably not vital for them to take place in GC B cells. When the DZ/LZ axes are abolished by either ablating CXCR4 or FoxO1, they can still undergo SHM and seemingly DZ-like proliferation (Bannard et al, 2013; Sander et al, 2015). Cells without CXCR4 can still cycle between DZ and LZ phenotypes, indicating the existence of an intrinsic cellular programme that controls transitioning between the two states (Bannard et al, 2013). Despite the observations above, the physical separation of DZ and LZs has been postulated to have evolved for the efficient generation of high affinity cells. This hypothesis is supported by mathematical modelling studies showing

that rapid proliferation intercalated with resting selection periods could lead to optimal affinity maturation efficiency (Kepler and Perelson, 1993). Consistent with this, when the axes were disrupted, SHM levels were modestly decreased and cells that were unable to physically enter DZs appeared less competitive in terms of their long-term GC participation (Bannard et al, 2013). The exact way by which LZ/DZ promotes effectiveness remains an open question.

As compared to naïve B cells, GC B cells face unique challenges including a significant amount of genotoxic stress from SHM and the need for rapid selection. As such, they have substantially reprogrammed transcriptional networks to manage these stresses, starting from the upregulation of Bcl6 in antigen-activated B cells (Kitano et al, 2011). Bcl6 is the master transcription regulator for GC B cells and has various critical functions. First, GC B cells bear very high genomic mutational loads, induced by activation-induced cytosine deaminase (AID) activity during SHM. Bcl6 has been reported to protect cells from DNA damage induced apoptosis through direct suppression of P53, P21, ATR, and CHEK1 (Phan and Dalla-Favera, 2004; Phan et al, 2005; Ranuncolo et al, 2007, 2008). Bcl6 also inhibits pre-mature early differentiation into plasma cells by repressing the expression of lineage defining transcription factors Blimp1 (PRDM1/Prdm1) and IRF4 (Tunyaplin et al, 2004; Basso et al, 2010). Quick improvement in overall affinity requires a rapid turnaround in testing and eliminating unfit B cell clones. GC B cells are sensitized to apoptosis by Bcl6 induced downregulation of Bcl2 (Saito et al, 2009). Together with the general upregulation of apoptotic factors and downregulation of anti-apoptotic factors (Klein et al, 2003), GC B cells are prone to death if they do not receive survival signals from BCR and/or T cells. In addition, Bcl6 represses the expression of EBI-2 to restrict GC localization to the follicle centre (Shaffer et al, 2001; Pereira et al, 2009).

1.3.2 The DZ is the site of proliferation and BCR diversification through SHM

In DZs, GC cells undergo rapid cell divisions with a characteristic of short G1 periods, leading to their signature dark stain nuclei stain (Pae et al, 2021). GC B cells undergo SHM to introduce random mutations to the variable region of Ig genes, some of which are capable of enhancing their binding affinity towards the epitopes (Jacob et al, 1991; Kuppers et al, 1993). AID is the main enzyme initiating this process and also leads to class switch recombination (CSR) (Chaudhuri et al, 2003). SHM is considered to take place in DZs because DZ cells demonstrate high-level expression of AID both on transcription and protein levels (Victora et al, 2012; Caron et al, 2009).

AID catalyses SHM by inducing deamination of the cytosine residues, thus converting deoxycytiosine into deoxyuraciles, generating local U to G mismatches. Subsequently, depending on the recognition and repair mechanisms, different mutations can be introduced. If DNA polymerase directly replicates over the deaminated region, then the C:G pair is mutated straight to a T:A pair. If after deamination the uracil is recognized by uracil DNA glycosylase (Ung), then the Ung removes the uracil to create a basic site, followed by the base excision repair to close the lesion, generating a wider range of mutations (Lindahl et al, 1977). Alternatively, if the mismatch is recognized by the Msh2/Msh6 mismatch repair heterodimer, Exo1 is recruited to excise the surrounding base pairs (Liu et al, 2009). Following the excision of mismatched uracils, the Ig gene locus can be further diversified during the error-prone translesion repair process, by switching the error-free DNA polymerase δ and ε that is otherwise essential for the maintenance of genome integrity with the low-fidelity polymerase pol θ, pol η and pol ξ (Zhao et al, 2013; Saribasak et al, 2012). Ultimately, this programmed mutagenesis leads to a mutation rate of $1/10^3$, a million times higher than that in the genomic regions not targeted by AID (Kleinstein et al, 2003). Certain sequences in the variable regions are more likely to

be targeted by AID, known as the "hotspots" - WRCY and its reverse complement sequence RGYW where W is A/T, R is A/G and Y is C/T (Pham et al, 2003).

AID actively mutates the genome, therefore its activity requires strict regulation. Ectopic activation of AID can lead to translocation of the genes such as c-Myc and Bcl6 and ultimately leads to lymphomas in mature B cells (Migliazza et al, 1995; Martin et al, 2002; Okazaki et al, 2003). Its expression in mature B cells has been considered to be tightly restricted in only activated and GC B cells (Xu et al, 2007). However, there is evidence showing its expression also in immature B cells (Kuraoka et al, 2011; Meyers et al, 2011). In activated B cells, AID needs to be targeted only to Ig regions and not affect other genes. Hence AID is subject to multi-layer tight regulation to ensure its proper activities including nuclear translocation and post-translational phosphorylation (Ito et al, 2004; Basu et al, 2005; Pasqualucci et al, 2006).

On average, B cells divide 2-3 times in the DZ during each visit (Gitlin et al, 2014). When cells finish the previous cell cycle, there is a fate decision process in the early G1 where DZ B cells choose to either enter another cell cycle for continued clonal expansion and SHM or alternatively, if they have exhausted their proliferative potential, downregulate CXCR4, exit cell cycle, and migrate to LZ for affinity-based selection (Allen et al, 2004; Stewart et al, 2018). At this stage, the integrity of BCR signalling pathways plays an important role in allowing only B cells with functional BCRs to return to LZs (Stewart et al, 2018; Mayer et al, 2017). The above two studies used active Caspase3 stain and FRET apoptosis reporters, respectively, and demonstrated that DZ B cells with deleterious BCR mutations resulting in premature stop codon or frameshifts are prone to apoptosis in the DZs. Concurrently, various transcriptional and phenotypic changes occur to promote the transition from DZ to LZ cells, with most of these changes being controlled by intrinsic cellular programmes (Bannard et al, 2013).

1.3.3 LZ is the site for affinity mediated positive selection

1.3.3.1 LZs are enriched with different cell types important for the selection

As discussed in section 1.3.1, mature GCs are polarized into two distinct compartments, LZs and DZs, that GC B cells move back and forth between during the course of responses. LZs are characterized by the presence of specialised stromal FDCs, which makes the LZs appear lighter on nuclei stain, as well as T_{FH} cells (Jacob et al, 1991; Cyster et al, 2019; De Silva et al, 2015). DZs are primarily devoid of FDCs and instead can be identified by the massive amounts of B cell proliferation occurring there. While lacking classical FDCs, DZs have been shown to contain their own stromal cell population known as CXCL12-expressing reticular cells (also recently termed FDC2s) (Pikor et al, 2020).

When GC B cells return to LZs, they express their newly mutated BCRs, which they then try to test their affinity by acquiring antigens and presenting them on pMHCII complexes to T_{FH} cells and in turn, the outcome is the amount of T cell help they can receive (Victora et al, 2012). LZs are therefore considered to be the site for affinity-based positive selection and have the types of cells and structural organization needed to facilitate this process to happen efficiently. Structurally, the orientation of the GCs in the lymph nodes is such that the LZ is orientated directly underneath the subcapsular sinus, facilitating the antigen transport and accumulation from the circulating system into where they are most required in the GCs (Hauser et al, 2010). In this section, I will describe the main cellular "players" present in GC LZs and discuss what is currently known about their contribution to the selection process.

Follicular dendritic cells (FDCs)

FDCs bear important functions in the GCs structurally and functionally. Depletion of FDCs quickly disseminated GCs (Wang et al, 2011). Arguably the

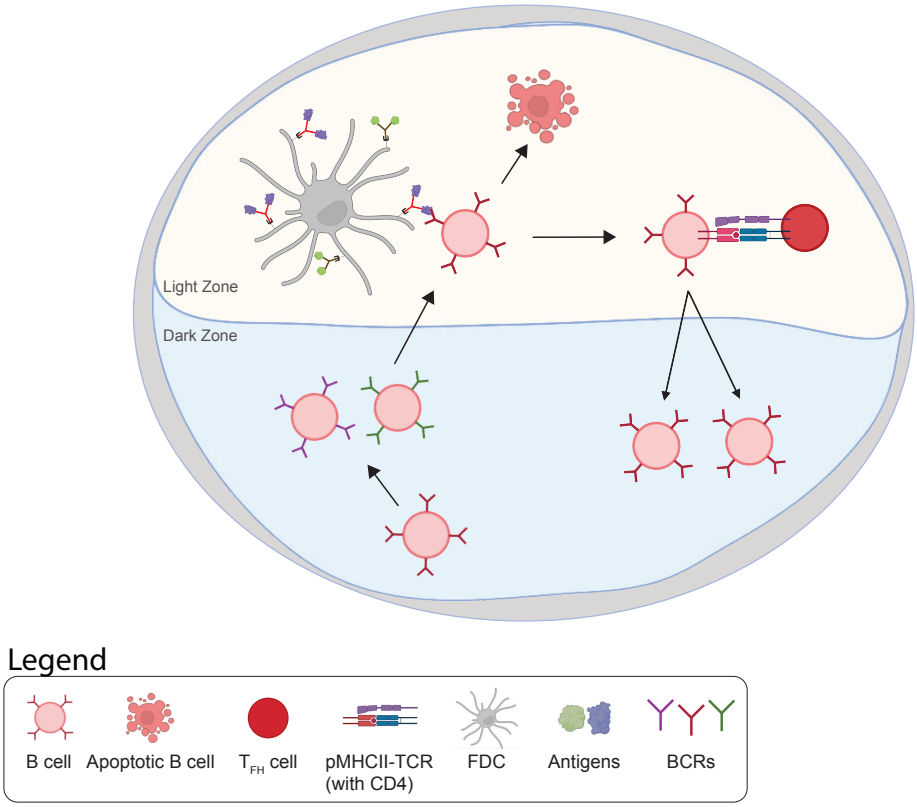

Figure 1.1: GC selection occurs in LZs in an affinity-based manner. Schematic diagram of the positive selection process in GCs. In DZs, GC B cells proliferate and undergo SHMs to diversify their BCRs. B cells then exit cell cycle and transition back into LZs. In LZs, cells acquire antigens with their newly mutated BCRs and present them to T cells on MHCII complexes. Higher affinity cells receive better/larger quantity and/or quality of T cell help are ultimately selected and return to DZ for further rounds of proliferation and mutations.

most important function for FDCs is to serve as a platform for antigen display in their native form against which LZ B cells can test their BCR affinities through antigen acquisition in readiness for presentation to T_{FH} cells. In LZs, antigens are trafficked into follicles through either conduits for small molecules or via subcapsular sinus macrophages for large complement coated antigens (Phan et al, 2007). FDCs capture and present intact antigens on their surface in the form of immune complexes captured by Fc receptors CD16/32 and CD23, as well as complement receptors CR1/2 (Qin et al, 2000; Liu et al, 1997). FDCs are capable of holding intact antigens for prolonged periods (>3 months), even when they have been cleared from

the broader circulatory system (Mandel et al, 1981). As a result, antigen availability is increased in the GCs which almost certainly will be important for prolonging GC responses and potentially for fostering more complex maturation pathways (Cirelli et al, 2017). To achieve long term retention, antigens are cycled through non-degradative endocytic recycling compartments in FDCs instead of simply being passively displayed as immune complexes on the cell surface (Heesters et al, 2013).

Apart from the role in antigen sequestration, FDCs are an important source of CXCL13 production, helping organise the GC and sequestering most CXCR5-expressing T_{FH} cells in LZs to facilitate B cell selection (Nishikawa et al, 2006; Ansel et al, 1999). FDCs have also been suggested to support the overall proliferation of the GCs, because inhibition of TLR4, which impairs FDC activation, causes defects in GC responses (Garin et al, 2010). However, it is likely that the innate signalling in GC B cells and/or other cell types were also affected.

Follicular helper T cells (T_{FH} cells)

T_{FH} cells are central players in mediating the selection process in LZs through affinity discrimination, and dysregulation of this population leads to unpaired GC responses and autoimmunity (Vinuesa et al, 2005). T_{FH} cells are a specific lineage of T cells that differentiate and reside in the B cell follicles and provide help to B cells locally to support the generation of plasma cells and memory B cells. The differentiation of T_{FH} cells from naïve T cells requires multiple-stage activation, and upregulation of Bcl6 (the same master transcription regulator for GC B cells) confers lineage commitment to T_{FH} phenotypes (Crotty et al, 2011). T_{FH} cells are characterized by their high-level expression of CXCR5 and PD1; these phenotypic markers also play important functional roles, with CXCR5 directing T_{FH} homing in the follicle and PD1 regulating T_{FH} differentiation and entry into GCs (Ansel et al, 1999; Haynes et al, 2007, Shi et al, 2018). GC T_{FH} cells, i.e., those cells that physically reach GCs, have been reported to have the highest expression level of these two markers in the T_{FH} population (Shulman et al, 2013).

T_{FH} cells regulate GC responses by differentially providing help to each LZ B cell based upon the strength of pMHCII-TCR interactions. T_{FH} cell help is provided in the form of receptor ligations (CD40-CD40L, membrane-bound inducible costimulator (ICOS-ICOSL)) and cytokine production (IL-21, IL-4) (Garside et al, 1998; Han et al, 1995; Zotos et al, 2010; Linterman et al, 2010; Cunningham et al, 2004). These stimuli instruct the formation, selection and ultimate output from the GCs by regulating the performance of B cells; disruption of any of these stimulations with blocking antibodies or genetic mutants leads to reduced GC proliferation and ultimate GC collapse (Mayer et al, 2017; Watanabe et al, 2017; Zotos et al, 2010). The importance of these stimuli in regulating final GC output was also demonstrated in studies where impaired IL-21 or IL-4 signalling showed defective antibody/plasma cell production (Ozaki et al, 2002; Yusuf et al, 2010). During the end stage of GC responses, it is generally considered that antigen exhaustion terminates GC responses (Cirelli et al, 2017). However, recent studies have unveiled the role of T_{FH} cells during this process, with a fraction of T_{FH} cells upregulating Foxp3 and adopting the regulatory T cell (Treg) phenotype to end GC responses by downregulating CD40L and ICOSL (Jacobsen et al, 2021).

The regulation of T_{FH} cells in GCs is dynamic. First, the diversity of epitopes recognized by T cells is enhanced through the mobility of T_{FH} cells between GCs. This contrasts with GC B cell behaviour since there is minimal movement of GC B cells between different loci. The mobility of T_{FH} cells between GCs has been shown by intravital imaging studies that "photo-converted" PAGFP expressing T_{FH} cells in one GC and tracked their movement over the time, with converted T cells being subsequently found in neighbouring GCs (Shulman et al, 2013). A follow-up study by another group suggested that this GC hopping behaviour may not be general T_{FH} behaviour and might occur more commonly for reactivated memory T_{FH} (Suan et al, 2015). Secondly, it was recently shown that T_{FH} cells are not as quiescent as previously considered, and that the T_{FH} repertoire may also undergo substantial changes during the course of GC responses. It is generally thought that there is limited cell division in the GC T_{FH} compartment after their establishment.

However, it was shown that T_{FH} cells continued to incorporate EdU, and that T_{FH} cells themselves are subject to a form of affinity-based selection that determines their extent of clonal expansion (Merkenschlager et al, 2021). As such, the changes in the T_{FH} TCR repertoire over time could also shift the clonal repertoire of GC B cells. Besides T_{FH} cells regulating the selection of B cells in the GCs, B cells are counteractively regulating T_{FH} cell functions. It is reported that the steady-state maintenance of T_{FH} cells requires constant input from GC B cells through antigen presentation and stimulation of TCR as well as co-receptor interactions (Baumjohann et al, 2013). As such, in GCs, B cells are not only being regulated by different cell types, but they can also feedback into the niche environment constantly. How T_{FH} cells mediate positive selection will be discussed later in this section.

Follicular regulatory T cells (T_{FR})

In 2011, a new population of Treg cells was identified by their characteristic co-expression of Foxp3 and Bcl6. These cells share the same phenotypic characteristics of high-level PD1 and CXCR5 expression as T_{FH} cells and are termed T_{FR} cells. They have been shown to suppress GC responses by limiting the expansion of non-antigen specific B cells (Chung et al, 2011; Linterman et al, 2011). Moreover, T_{FR} cells have also been reported to limit the generation of autoreactive IgE B cells and limit plasma cell differentiation, as well as spontaneous GC generation (Clement et al, 2019; Sage et al, 2016; Gonzalez-Figueroa et al, 2021). Gonzalez-Figueroa et al employed a $Bcl6^{fl/fl}$ Foxp3-Cre conditional knockout mouse line to deplete T_{FR} cells in GCs following immunization, and found that T_{FR} cells could repress plasma cell differentiation, and reduce the expression level of ICOSL on B cells, potentially counteracting the help provided by T_{FH} cells (Gonzalez-Figueroa et al, 2021). Therefore, T_{FR} cells provide an additional layer of negative regulation besides the passive regulation of antigen availability.

1.3.3.2 The cyclic re-entry model for positive selection in GCs

A central function of GCs is to promote affinity maturation by selecting the products of SHM based on their antibody affinities. Affinity-based selection can occur in just one of two ways; through preferential survival (avoidance of death) or favoured growth of higher affinity cells (Shlomchik et al, 2019). It has long been thought that the former represents the main affinity driving force in GCs, with most reviews and papers referring to the "cyclic re-entry" model. This framework was first proposed in a seminal mathematical modelling paper by Kepler and Perelson in the early 1990s. According to their modelling, the optimal efficiency of mutation accumulation for affinity maturation was achieved by intercalating periods of rapid mutation and proliferation with periods of mutation free rest stage and selection. This linked well with BrdU chase experiments from 3 decades earlier that had shown that DZs rather than LZs were the main sites of proliferation in GCs, but that cells in the latter compartment were derived from the former. Hence, the physical separation of GCs into DZs and LZs was proposed to facilitate the compartmentalization of mutation/proliferation and selection, respectively (Kepler and Perelson, 1993).

Apparent further support for the cyclic re-entry model (of selecting for survival in LZs) came from the observation by Maclennan and colleagues that crosslinking their BCRs *in vitro*, while also providing anti-CD40 stimulation, prevented the death of human tonsillar LZ cells - known at the time as centrocytes, with apoptosis being the pre-determined fate for these cells if not rescued. This suggested that cells failing selection would mostly die immediately from neglect (Liu et al, 1989). More recently, photoconversion techniques were used to tag PAGFP-expressing LZ or DZ cells in situ and to subsequently track their movement over the proceeding hours. In 4-6hrs, a substantial (50-70%) of DZ cells moved physically into LZs, while only 10-30% of LZ cells returned to DZs in the same period. As such, there was a net flux of cells in the DZ to LZ direction, which added support to the notion that cells failing selection might die while still in LZs (Victora et al 2010; Meyer-Hermann et al, 2012). As such, the positive selection process was proposed

to occur in LZs and directly cause cells to migrate back to DZs and return to a proliferative state (cyclic re-entry). A critical and immediate next question is what "selects" cells for cyclic re-entry. Various inputs have been considered to drive this process, and the key players are discussed below.

1.3.3.3 BCR signalling alone was not sufficient for GC positive selection

Antibody affinity maturation involves preferentially selecting B cells with higher affinity BCRs. Therefore, a seemingly obvious and direct approach to achieve this would be for cells to be selected based on the strength of BCR signalling that they receive. For many years the field assumed that direct antigen sensing would be the way affinities are measured, with supporting evidence including that BCR stimulation (together with CD40 ligation) rescues LZ cells from apoptosis *ex vivo* (Liu et al, 1989). As Kepler and Perelson phrased it, "antigen bound by proliferating cells is no longer available for other cells to use". The idea that small subsets of LZ cells preferentially engage antigen is supported even by more recent studies using modern genetic reporters, where subsets of the LZ that are preferentially enriched with high affinity cells show evidence of more BCR signalling (Mueller et al, 2015). However, it is difficult to separate the contribution from BCR signalling directly from advantages conferred at the point of T cell interactions. Instead, various studies have questioned the extent and importance of BCR signalling in driving affinity-based selection. Elegant live 2-photon imaging studies carried out by Allen et al revealed that B cells could not be seen blocking other B cells' access to antigens on FDCs, disfavouring the hypothesis above. Instead, they observed that T_{FH} cells are far less abundant in GCs than B cells and that T-B interactions are transient and rare, providing the first *in vivo* evidence that T cells may be the main player in discriminating affinity and selecting GC B cells (Allen et al, 2007).

Following up on these proposals, Victora and colleagues performed a critical set of experiments that demonstrated that BCR signalling alone is not sufficient to drive antibody affinity maturation if the amounts of T cell help received are

normalised. The authors used anti-DEC205-peptide antibody conjugates to drive equivalent antigen presentation by all GC B cells through a BCR independent pathway (Victora et al, 2010). Interestingly, and consistent with it playing a minimal role in selecting for affinity, BCR signalling in fact seems to be diminished or much repressed in GC B cells due to high phosphatase activity from GC B cell specific AKT-kinase driven negative feedback loop (Luo et al, 2019; Khalil et al, 2012). More recent studies have revealed that this involves a certain amount of signal "rewiring" in GC B cells, in which BCR engagement does not lead to Nfkb activation as it does in naïve cells but rather triggers PI3k-Akt induction (Luo et al, 2018). In contrast, CD40 instead leads to Nfkb induction, which would be consistent with T cells rather than B cells triggering a key selection event. Optimal induction of c-Myc, a key player in selection (discussed later in section 1.3.3.7), requires synergism from both pathways. At this stage, the role of BCR during selection seemed to be only the endocytic receptor for antigen internalization.

1.3.3.4 The role of T cell help in driving cyclic re-entry in GC LZs to carry out positive selection

The T cell centric model for selection gained interest when BCR signalling and antigen access appeared to not be the main driving force. A subsequent alternative mechanism by which antigen engagement through the BCR could support selection is via presentation to T_{FH} cells and the receiving of "help". T cell help has been shown to be of central importance in regulating GC outputs by initiating and sustaining GC responses, since the disruption of T-B interaction leads to early dissolution of GCs (Victora et al, 2010; Gitlin et al, 2014; Gitlin et al, 2015; Turner et al, 2017; Turner et al, 2018).

Following antigen acquisition in LZs, GC B cells process them and present peptides to T cells. Given that the amounts of antigen that B cells acquire and present is likely to be proportional to the affinity of the BCRs, high affinity cells should be capable of retrieving more antigens from FDCs and receiving more T

cell help (Batista et al, 2000). The question then became whether T cells would be capable of discriminating B cell affinity based on these interactions alone, and whether that is how antibody affinity enhancements are promoted. This hypothesis was supported by the observation that T_{FH} cells are far less abundant in GCs that B cells and that T-B interactions are transient and rare, suggesting interaction with T_{FH} cells is likely to be highly competitive and affinity dependent (Allen et al, 2007). As such, it was proposed that high affinity B cells are preferentially selected as a result of them out-competing their neighbours in receiving T cell help delivered in short-lived intercellular contacts (Victora et al, 2010; Shulman et al, 2013; Crotty et al, 2011; Allen et al, 2007).

Experimental support for the above model was provided by Victora et al. in their seminal 2010 study. Here, an *in vivo* system was established to allow antigen loading into B cells without stimulation of BCR to independently study the contribution of T_{FH} and BCR signalling during positive selection. They used the anti-Dec205-peptide approach to augment antigen presentation in small proportions of the GC population without touching their BCRs. When B cells were supplemented with extra antigen through this approach, these cells were found to preferentially accumulate in DZs, suggesting T cells are involved in selecting LZ cells to return to DZ and possibly promoting their clonal expansion once there. Follow-up live imaging studies have confirmed that enhanced antigen presentation by this approach leads B cells to engage in more frequent and longer T cell contacts (Shulman et al, 2014). While some groups have questioned whether this approach might be "super-physiological", for many these important sets of experiments were taken as direct proof that high affinity B cells are preferentially selected as a result of them presenting higher amount of pMHCII complexes to T cells and receiving better/larger quantities of T cell help. This allows the selected cells to preferentially undergo cyclic re-entry, leading to their ultimate enhanced survival (Victora et al, 2010; Shulman et al, 2013; Crotty et al, 2011; Allen et al, 2007, Meyer-Hermann et al, 2012).

1.3.3.5 Roles for T cells beyond controlling cyclic re-entry and controversies related to the T cell centric model

Although experimental evidence so far suggests T_{FH} cells are selecting cells to undergo cyclic re-entry as the mechanism behind the positive selection, later on, several studies revealed additional ways by which T cells may promote GC B cell expansion. In two consecutive studies, T_{FH} cell help was found to be associated with the overall proliferative state of the B cells even after they return to DZs. Using an inducible H2B-mCherry division counter system, the authors demonstrated that strong T cell help stimulates the expansion of GC B cell clones by shortening cell division time and elongating their DZ dwelling time (Gitlin et al, 2014; Gitlin et al, 2015). This higher proliferative state is possibly sustained by higher metabolic activities in these cells resulting from T cell-dependent upregulation of the mTORC1 and c-Myc related pathways that feed into biogenesis and cell growth (Ersching et al, 2017, Finkin et al, 2019). These studies suggest that, beyond driving cyclic re-entry, T cell help levels may also control the overall performance of DZ cells in terms of preferential growth and DZ dwell time. In this case, higher affinity cells can outcompete the low affinity cells due to their better capability to expand faster in GCs.

Given that the strength of T cell help instructs positive selection, possibly the local strength of pMHCII-TCR interactions plays an important role in GC positive selection. However, the density of surface MHCII was controlling B cells' GC entry but not during GC selection, as shown by the haploinsufficiency of MHCII or cells with H2-O deficiencies, which is a chaperone for MHCII and negatively regulates the loading of MHCII (Yeh et al, 2018; Draghi et al, 2010). It is possible that this is due to the occupancy of the MHCIIs by antigen-derived peptides on GC B cells being less than that of the activated B cells.

In conclusion, these observations are in support of a selection model where higher affinity B cells are better at antigen acquisition and presentation, allowing

them to preferentially receive higher amounts, and/or better quality, of T cell help than lower affinity competitor cells. Original studies suggested that T cell help probably directly promotes LZ cell cyclic re-entry and return to DZs, and more recent studies revealed additional/alternative roles of T cells in promoting/controlling cell growth and cell proliferation related pathways, thereby supporting selected cells to have longer dwell times in DZs. Ultimately higher affinity clones are preferentially selected and expanded.

1.3.3.6 T cell help is self-reinforcing for efficiency

LZ cells are specifically equipped for the selection process in various aspects. First, they upregulate CD83, which antagonizes the MARCH1, a ubiquitin ligase and targets MHCII for degradation (Bannard et al, 2016). As such, LZ cells have more stabilized MHCII expression, facilitating antigen presentation and interactions with T cells. This is somewhat analogous to changes reported for dendritic cells during their maturation from sampling to T cell stimulating phases. Moreover, T cell help acquisition was shown to act as a positive feedback loop with B cells, also stimulating T cells to promote stronger interactions. More specifically, CD40 agonism resulted in rapid upregulation of ICOSL in GC B cells, leading to a feed-forward loop that results in calcium release in T_{FH} cells triggering more CD40L externalization, facilitating them for stronger T-B interactions (Liu et al, 2014). pMHCII stimulation of TCR upregulates LFA-1 in T_{FH} cells and in turn, promotes the interactions with ICAM on GC B cells (Zaretsky et al, 2017). High affinity cells have also been suggested to create a gradient of chemokines (CCL22) that attract T_{FH} cells locally, potentially increasing the probability of further interactions, although how such gradients function when the producing cell is migratory is not clear (Liu et al, 2021). Similarly, CD40 is upregulated in c-Myc$^+$ LZ B cells, reinforcing the helped cells to receive more T cell help (Nakagawa et al, 2021).

1.3.3.7 Transcription factors/proteins involved in positive selection for cell proliferation and DZ maintenance

c-Myc

c-Myc is one of the most important transcription factors for GC-positive selection. In both innate and adaptive immune systems, c-Myc regulates the maturation, activation and differentiation of many immune cells by acting as a signalling hub, integrating inputs from various pathways including PI3K, Jak/STAT, and beta-catenin pathways (Gnanaprakasam et al, 2017). More specifically, in immature and naïve lymphocytes, c-Myc acts as a division timer to report the integrative strength of the stimuli (Marchingo et al, 2014; Heinzel et al, 2017). However, its role in GC B cell regulation was not well appreciated, because bulk RNA sequencing revealed that GC B cells did not have a higher level of c-Myc than quiescent follicular B cells (Klein et al, 2003).

The central importance of c-Myc to GC positive selection was revealed in two back-to-back studies that demonstrated it to be transiently upregulated only in a small fraction of LZ GC B cells, and where inhibition of c-Myc activity was shown to be sufficient to cause GC collapse (Calado et al, 2012; Dominguez-Sola et al, 2012). The upregulation of c-Myc is associated with an elevated level of cell cycle genes and preferential enrichment of these cells in the plasmablast compartment, indicating its role in positive selection (Calado et al, 2012; Dominguez-Sola et al, 2012). Levels of c-Myc expression, and the activities of its downstream pathways, have since been shown to be key factors in translating the strength of T cell help received by B cells into the extent of downstream cell growth and proportional expansion in DZs (Victora et al, 2010; Finkin et al, 2019). More specifically, Finkin et al demonstrated that the level of c-Myc expression was proportional to the amount of T cell help received, and that higher levels of c-Myc were associated with larger LZ cell sizes and stronger proliferative potential in DZs (Finkin et al, 2019). As such,

it was proposed that selected LZ cells display this biased c-Myc$^+$ state (Calado et al, 2012; Dominguez-Sola et al, 2012; Victora and Nussenzweig, 2022).

Besides T cell help providing CD40 receptor ligation, BCR signalling could also contribute to the optimal induction of c-Myc, potentially allowing c-Myc to integrate signals from different upstream pathways and act accordingly (Luo et al, 2018; Nowosad et al, 2016). Overall these studies indicate that the strength of interaction with T cells dictates the amount of c-Myc expression, which further feeds into the downstream biosynthesis pathways, allowing these B cells to accumulate metabolites for faster proliferation once back into DZs.

mTORC1

Besides c-Myc, the mTORC1 complex is another essential regulator in sensing growth-stimulating signals and stress and then triggers biosynthesis/cell growth and cell proliferation when conditions are favourable by phosphorylating 4E-BP1 and ribosomal protein S6 kinase (S6K) (Marin et al, 2011, Sengupta et al, 2010). Similar to c-Myc, optimal induction of mTORC1 in GC B cells also requires signals from both BCR crosslinking and CD40L stimulation (Luo et al, 2018).

The importance of mTORC1 in GC positive selection was demonstrated by its role in inducing cell growth for clonal expansion and accumulation in DZ of positively selected B cells (Ersching et al, 2017). Mechanistically, Ersching and colleagues postulated a hypothesis of anabolic growth in GC B cells, in which the mTORC1 driven cell growth only occurs in the LZ prior to rounds of proliferation with minimum biogenesis in each cell cycle in DZs. The supporting evidence comes from the experiments in which mTORC1 inhibitor rapamycin was given at different time points following synchronized B-T interactions. When rapamycin was given a short period of time following B-T interactions (before LZ cell growth started), the size of subsequent DZ clonal bursts reduced significantly. However, there was minimal blocking effect of DZ proliferation if rapamycin was administrated after ribosomal protein pS6 had been optimally induced by mTORC1. On the

other hand, hyperactivation of mTORC1 resulted in smaller DZ B cells than usual because cells proliferated faster than their growth capacity, possibly due to the enhanced expression of cyclin D3 (Ersching et al, 2017, Pae et al, 2021). Hence the biosynthesis and, therefore, mTORC1 pathway is vital for the cells to proliferate in the DZs efficiently.

AP4

Although c-Myc has been demonstrated to be the important master regulator for positive selection, levels of Myc quickly diminish after B cells move away from T cells (Calado et al, 2012; Dominguez-Sola et al, 2012). Hence the subsequent DZ cell cycle progression is sustained by downstream target genes, one of which is the transcription factor AP4. c-Myc induces AP4 expression and AP4 is reported to maintain cell cycle progression in the DZ by sustaining the transcription of cell growth and proliferation-related genes. Consistent with this, deficiency in AP4 reduces the proliferation potential of B cells in DZs (Chou et al, 2016).

FoxO1 and BATF

The cyclic re-entry process must involve two stages: the entry of resting G1 LZ cells back into cell cycle (S phase), followed by upregulation of DZ genes and programs. One critical DZ transcriptional regulator is FoxO1, which supports the transcription of various key genes linked to the DZ program, including *Cxcr4*. GCs B cells lacking FoxO1 due to conditional deletion almost completely lack DZs (Dominguez-Sola et al, 2015; Sander et al, 2015).

FoxO1 is subject to post-translational regulation, including cellular localisation and regulated degradation (Sander et al, 2015; Inoue et al, 2017). In LZs, FoxO1 activity is largely repressed as a consequence of its phosphorylation, which is probably triggered by BCR signalling upstream of subsequent PI3K-AKT, leading to its nuclear export (Su et al, 2011; Yusuf et al, 2004). Mutations that over-activate BCR signalling result in the suppression of normal FoxO1 activities, such

as Syk mutations that disrupt its phosphorylation and degradation, resulting in an accumulation of LZ cells (Davidzohn et al, 2020). Then, FoxO1 has been considered to be re-activated in recently selected LZ cells, based on experimental evidence showing co-localisation of nuclear FoxO1 and c-Myc in a small subset of LZ cells (Sander et al, 2015). However, despite FoxO1 being essential for the DZ phenotype, GC sizes are normal in its absence. Moreover, SHM and cell proliferation still occurred in the FoxO1 deficient GC B cells when most of these cells displayed an LZ phenotype, albeit at lower frequencies. The antibody affinity and titres were also affected (Inoue et al, 2017). Hence, it is possible that DZ phenotypes and activities in the DZ (such as SHM and inertial proliferation) are regulated independently, and although DZ/LZ segregation is not absolutely essential for these DZ activities, it is important for the efficiency of affinity maturation.

One of the reported targets of FoxO1 is *Batf* (encoding BATF). BATF displays a FoxO1-dependent upregulation in a small fraction of LZ cells, and these $BATF^{high}$ cells are more active in cycling. Conditional deletion of BATF in a mixed bone marrow chimera setting confirmed a preferential loss of DZ cells and less proliferation in the LZ in its absence. In accord with this, ectopic expression of BATF in GC B cells lacking the FoxO1 gene restored the proliferation defect, despite the polarization defect remaining, suggesting BATF is an essential target of FoxO1 for DZ proliferation (Inoue et al, 2017). In summary, positive selection is thought to induce the activity of various transcription and translation regulators that then support more active metabolic states necessary for clonal expansion as well as promoting DZ maintenance.

Cyclin D3

After interactions with T_{FH} cells, B cells upregulate c-Myc and mTORC1 pathway related genes, which promote cell cycle re-entry and the subsequent DZ expansion (Calado et al, 2012; Dominguez-Sola et al, 2012; Finkin et al, 2019; Ersching et al, 2017). However, the upregulation of these pathways is mainly

restricted to LZs cells, suggesting this information needs to be translated into the proliferative potential in other formats and some proteins may act as the cell division counter in DZs. Pae et al. demonstrated that in DZs, S phase entry and subsequent proliferation do not require immediate T_{FH} cell-derived signal, a process that was referred to as "inertial" cell cycles. This sustained proliferation is dependent on cyclin D3, whose expression is mainly restricted to DZ cells. Cyclin D3 deficient cells failed to expand in DZs following strong T cell stimulation in the previous LZ visit. Given cyclin D3 acts in a dose-dependent manner, the authors concluded it is possible that cyclin D3 translate the accumulative strength of T cell help that cells received in LZs into the extent of DZ expansion (Pae et al, 2021).

1.3.3.8 GCs have been shown to have a permissive environment

While the cyclic re-entry model provides an appealing conceptual framework for how higher affinity B cells can be strongly favoured in responses, it does have some potential limitations. Although antibody affinity is of great importance to its effectiveness, direct neutralization of pathogens also requires antibodies to recognize particular epitopes that are also involved in pathogenic processes. In addition, the best neutralising antibodies are not necessarily the highest affinity clones (Schieffelin et al, 2010). Therefore, a selection mechanism that is solely focussed on affinity may not always generate the most protective antibodies. Moreover, conceptually, it is not clear that always strongly favouring the highest affinity cells at the expense of diversity would be beneficial for several reasons. If the antibody responses are only focused on the highest affinity clones, it is likely to bias the responses towards a few most highly expressed or easily accessible epitopes and miss some of the important functional epitopes. This is because many pathogens "hide" their key epitopes, or make them appear to the host as self, as a strategy to evade immune recognition (Tas et al, 2016). Complex maturation pathways may be required to develop antibodies against these epitopes, and they can be easily outcompeted if affinity is the only selection criterion. Pathogens could also evolve to avoid easy recognition by the

antibodies, as exemplified by the recent fast mutating SARS-CoV2 virus to escape from the recognition by neutralizing antibodies (Cao et al, 2022). As such, an optimal antibody response should have high affinity and unlimited diversity to recognize any epitopes from a given response. While it is difficult to reach both at the same time, a balance is required for effectiveness.

Recent insights gained into the development pathways of broadly neutralizing antibodies (bnAbs) against viruses also supports the points made above. Due to the heavy glycan shield on HIV envelope proteins, the molecular similarity between some of the viral proteins to the host and a high mutation rate, HIV broadly neutralizing antibodies have only been found in 25% of the untreated infected people 2-3 years after infection (Stamatatos et al, 2009). VRC01 is one of such bnAb that recognizes the CD4 binding site on the envelope protein. The germline precursor of VCR01 requires more than 60 mutations to achieve full neutralizing potential – several fold higher than typical mutation loads in other antibodies (~15-20 variable region mutations in the heavy chain) (Tiller et al, 2007; Li et al, 2011). As such, a more permissive selection mechanism must exist to sustain B cells expressing these bnAbs in GCs for them to accumulate all necessary mutations, a phenomenon that is not easily explained according to cyclic re-entry-based selection models.

Two studies directly addressed the question of how much clonal and affinity diversity is maintained in GCs. According to models in which selection is stringent and only permits the highest affinity cells to survive each day, one might expect GCs to quickly become dominated by only a few more competitive clones. However, when this was assessed during complex responses to pathogen-derived protein antigens, high levels of clonal diversity were found even at quite late stages of the responses. Consistent with Eisen's original results, overall average antibody affinities did improve over the responses however individual antibody affinities showed up to ~100-1000-fold differences between different clones, and 10-20-fold within clones (Kuraoka et al, 2016). This significant intra- and inter-clonal diversity in affinity revealed the sustenance of lower affinity clones in GCs despite competition from

neighbours and suggested that affinity maturation does not come at the expense of supporting clonal and affinity diversity. Similar experiments from Tas et al. revealed striking affinity ranges present even in individual GCs (Tas et al, 2016). Hence, there ought to be a certain level of permissiveness in the GCs to provide help and sustain these low affinity cells, which is difficult to reconcile with the cyclic re-entry model. Consistent with this notion, even low affinity cells also have the chance to become c-Myc$^+$, a marker for positive selection, and also an indicator of strong recent interactions with T cells (Nakagawa et al, 2021).

To summarize, the cyclic re-entry model assumes that selection acutely rescues LZ cells from otherwise pre-determined immediate apoptosis, with only the highest affinity cells surviving each LZ visit. However, this model is difficult to fit with observations of how antibodies often develop. The studies described herein demonstrated that artificially enhancing T-B interactions in LZs leads to the preferential expansion of these B cells possibly due to their higher expression level of c-Myc and higher activity in mTORC1 pathways (Victora et al, 2010; Ersching et al, 2017; Finkin et al, 2019). Therefore, the current selection model needs to be revised to take into consideration of the current studies to accommodate a certain degree of permissiveness in the selection process.

1.4 The outputs from GC responses are plasma cells and GC-derived memory B cells

Ultimately, antibody affinity maturation is only useful to immune responses if GCs generate two important cell types – memory B cells and plasma cells. In the following sections, how cells are selected for these two fates is discussed.

1.4.1 Plasma cells are responsible for the production of high affinity antibodies

An important output from GCs is long-lived plasma cells (PCs) for the production of high affinity antibodies. Long-lived plasma cells eventually downregulate BCR and MHCII and home to the bone marrow where they can be maintained for decades. Compared with GC B cells, plasma cells display significant phenotypic and transcriptional differences to meet the specific requirements for extreme productive antibody production (Piskurich et al, 2000).

The consensus for PC selection in GCs is considered to be affinity-based. Over the course of the responses, PC precursors arise from high-affinity clones in GCs, resulting in an overall higher antibody affinity in the PC compartment than that in the GC B cell compartment (Kuraoka et al, 2016; Phan et al, 2006). This is considered to be an active selection process because solely promoting the survival of GC B cells by expressing anti-apoptotic Bcl2 transgene does not naturally lead to an expansion in the PC compartment (Smith et al, 2000). The driving force for the selection of GC B cells into PC fate was first considered to be a strong dose of T cell help, demonstrated by the expanded plasmablast compartment after enhanced B-T interactions (Victora et al, 2010). However, T cell help was subsequently argued to be sometimes dispensable for the initial stage of PC differentiation, in two studies showing that Blimp-1, a critical lineage commitment factor of PC fate, can be induced even when T cell help was acutely removed via ablation or depletion. In contrast, T cell help may be required for later differentiation process as Blimp1^{+} cells commit to becoming fully-fledged PCs, probably driven by stimulations other than the CD40-CD40L (Krautler et al, 2017; Radtke et al, 2019). Meanwhile, a critical role for Ag-BCR engagement (and probably signalling) was shown for the generation of pre-plasma cells (Blimp1-low GC B cells); this was demonstrated blocking antigen access for SW_{HEL} BCRs using a high affinity (Hy10*) monoclonal antibody (Ise et al, 2018). As such, a revised model proposes the PC selection to be a two-step process.

BCR signalling provides the initial selection cues for plasma cell differentiation and the ultimate fate commitment requires confirmation from T cell derived signals.

The location of where the PCs are generated remained elusive. One fate decision model in GCs is that cyclic re-entry or differentiation into PCs are fate bifurcations occurring in the LZ depending on the strength of T cell help received (Ise et al, 2018). This is supported by the observations that small frequencies of high-affinity PC precursors ($Bcl6^{low}$, $CD69^{high}$ and $IRF4^{+}$) were identified in the LZs, whose appearance was dependent on and proportional to the strength of T cell help (Ise et al, 2018, Krautler et al, 2017, Zhang et al, 2018). However, later, most of the early Blimp-1^{+} precursors were shown to display a DZ phenotype, suggesting that differentiation into PC is not an alternative fate of cyclic re-entry and may occur in the DZ (Radtke et al, 2019).

The extensive changes in the transcriptional network occurring during PC differentiation involve repression of transcription factors maintaining GC B cell identity (including PAX5. Bach2, AID) and activation of PC promoting transcription factors (Ise et al, 2019). One of the key transcription factors involved in the initial differentiation and later PC maintenance is IRF4, whose upregulation can be driven by strong CD40 and BCR signalling feeding into NF-kB pathways (Klein et al, 2006; Ochiai et al, 2013; Luo et al, 2018). Subsequently, IRF4 upregulation represses Bcl6 and various other genes, preparing the cells ready for GC egress (Saito et al, 2007). In addition to its transcription repressor activities, the expression of Blimp-1 may be dependent on IRF4 (Kwon et al, 2009; Sciammas et al, 2006; Sciammas et al, 2011), although some GC B cells have been found to induce Blimp-1 gene expression without detectable *Irf4* increases (Radtke et al, 2019). Blimp-1 regulates various aspects of PC functions, including repression of c-Myc transcription possibly to terminate active cell cycle progression in PCs and upregulating XBP-1 to regulate unfolded protein response and ER stress to match the requirements of intensive antibody productions capacity (Calado et al, 2012; Lin et al, 1997; Reimold et al, 2001; Todd et al, 2009).

1.4.2 Memory B cells receive less T cell help and are overall of lower affinity in exchange for a broader diversity

Memory B cells are the second "effector cell" of the humoral immune response. Antibodies secreted by long-lived PCs may not always be sufficient to prevent secondary infections, especially when pathogens themselves mutate as a result of immune pressure. For these reasons, memory B cells (MBCs) represent a critical second line in antibody-based immunity, retaining the capacity to be rapidly recalled when required.

As such, an important role of MBCs is to keep the breath of BCR diversity in the immunological memory to better prepare us for the next challenge from similar pathogens. Most of MBCs have GC origin but they can be derived without participating in GC responses (Suan et al, 2017; Takemori et al, 2014). MBCs can be found in various locations after their generation. A significant proportion of them reside in lymphoid organs and recirculate. But they are also reported in the local tissue and organs, possibly for rapid local activation (Maclean et al, 2022; Gregorie et al, 2022).

On average, MBCs tend to accumulate fewer mutations in their variable region and are generated throughout primary immune responses, but with a probable bias to early stages (Blink et al, 2005; Akkaya, et al, 2020; Palm et al, 2019; Weisel et al, 2016). Compared with PCs, which tend to display high affinity towards their cognate epitopes, MBC BCR pools have lower average affinities – a probable trade for the broader reactivity and the ability to quickly mutagenize towards pathogens with slight differences (Shinnakasu et al, 2016; Suan et al, 2017; Laidlaw et al, 2017; Wang et al, 2017). This was initially demonstrated with the SW_{HEL} system in which the memory B cells were more enriched in the low-affinity GC B cells (Phan et al, 2006). Later, direct unbiased measurements of antibodies derived from memory B cells made during responses to complex protein antigens were made using biolayer interferometry (BLI), revealing that many or even most

memory B cells bind to antigens with affinities too low to detectably measure with commonly used assays (Viant et al, 2020).

The preferential representation of low-affinity cells in the MBC compartment implies a lower selection threshold. It has been postulated that lower affinity cells that could not acquire sufficient T cell help to be sustained in GCs may choose this fate passively rather than being actively selected. Indeed, Overexpression of a Bcl2 transgene to promote survival in MBC deficient mouse models can restore this population to some extent (Smith et al, 2000; Inoue et al, 2021; Laidlaw et al, 2021). Perturbations in the ability of GC B cells to receive T cell help (for example, an inability to respond to IL-21 or migrate into DZs) results in an accumulation of MBCs that is disproportionate to GC size (Linterman et al, 2010; Zotos et al, 2010; Bannard et al, 2013). Also, pre-MBCs tend to be the most quiescent population in LZs, displaying lower metabolic activities, which matches their lower proliferative state – possibly an indicator of receiving minimal T cell help (Wang et al, 2017; Inoue et al, 2020).

GC B cells undergo substantial changes on the transcriptomic and epigenetic levels when they differentiate into memory B cells. Upregulation of Bach2 is associated with MBC differentiation (Shinnakasu et al 2016). The Bach2 level was reversely correlated with the amount of T cell help and therefore the authors postulated that lower affinity cells received a lower amount of T cell help, which in turn upregulates Bach2 which promotes the choice in those cells towards MBCs. Other transcription factors involved include HHEX, Tle3 etc (Laidlaw et al, 2020).

Besides quickly differentiating into plasma cells upon reactivation, MBCs retain the potential to participate in the secondary GC during recall responses, despite the fraction joining GCs varied between studies. Two studies have reported a minimum number of MBCs were recruited to secondary GCs during rechallenge, and these GCs were still largely composed of activated B cells from the repertoire (Benson et al, 2009; Dogan et al, 2009). While others reported that the MBCs

could compete with newly activated B cells in secondary GCs and clonally expand (Viant et al, 2020; Wong et al, 2020).

1.5 How the balance between affinity and diversity is achieved for antibody affinity maturation

Optimal antibody responses should be both high affinity and diverse. For pathogens where VDJ recombination does not generate good germline antibodies for this purpose, GCs probably play an important role in generating a host's only good/potent antibodies (e.g. HIV). However, it is clear that even naïve B cell repertoires often encode reasonably high affinity antibodies against certain "simpler" pathogens, so what is the role of the GC here? Given the quick mutational rate for some of the pathogens, it might be easy for them to develop escape mutations. Hence another important function of affinity maturation is to also expand the diversity of BCRs to maximise the coverage of the pathogens. This would involve improving antibodies that are already specific but of too low an affinity to be functional (filling functional holes in the repertoire).

As a consequence, a central question in antibody affinity maturation is how do GCs maintain a certain level of diversity in their repertoires while promoting the selection of high affinity clones? The cyclic re-entry model explains nicely how GCs preferentially select high affinity B cells, because only the most competitive LZ cells would reach the selection threshold required for surviving and returning to DZs. However, it is less easy to explain with this model how diversity is supported – which might leave major holes in the functional antibody repertoire. Conceptually, GCs also need to retain some amount of permissiveness to maintain low and moderate affinity clones in order to permit complex maturation pathways that are slower to develop. How that might occur if only the best 10-30% of cells survive each cyclic re-entry step is not clear.

In recent years, various studies greatly extended our understanding of GC clonal diversity and revealed that GCs could nurture high and low affinity cells concurrently. As such, our current understanding of how positive selection occurs in GCs may be far from complete. In this thesis, we are thus re-evaluating the model that affinity maturation occurs by B cells competing in a stringent manner for cues that drive their cyclic re-entry, and we are directly testing the roles of TFH cells in regulating the selection process.

Chapter 2

Materials and Methods

Contents

2.1 Reagent tables

Antibodies	Clone	Brand	Catalog No.
BV785-B220	RA3-6B2	Biolegend	103246
APCCy7-B220	RA3-6B2	Biolegend	103224
PE-B220	RA3-6B2	Biolegend	103208
Biotin - IgD	11-26c.2a	Biolegend	405734
APCCy7-IgD	11-26c.2a	Biolegend	405716
PECy7-CD95	Jo2	BD Biosciences	557653
Pacific Blue-GL7	GL7	Biolegend	144614
FITC-GL7	GL7	Biolegend	144604
BV785 - CD3e	145-2C11	Biolegend	100355
AF647-CD86	GL1	Biolegend	105020
PerCP/Cy5.5-CD86	GL1	Biolegend	105028
BUV395-CD86	GL1	BD Biosciences	564199
Biotin-CD83	Michel-19	Biolegend	121504
AF647-CD83	Michel-19	Biolegend	121514
PE-CXCR4	2B11	Thermo Fisher	12-9991-82
Biotin - CXCR4	2B11	Thermo Fisher	13-9991-82
Rabbit anti-BatF	D7C5	CST	8638s
PE-IRF4	IRF4.3E4	Biolegend	646403
FITC-I-Ab	AF6-120.1	Biolegend	116406
AF647-I-Ab	AF6-120.1	Biolegend	116412
APCCy7-IgKappa	RMK-45	Biolegend	409504
AF647-CD45.1	A20	Biolegend	110720
BV785-CD45.1	A20	Biolegend	110743
PerCP/Cy5.5-CD45.1	A20	Biolegend	110728
BV785-CD45.2	104	Biolegend	109839
PerCP/Cy5.5-CD45.2	104	Biolegend	109828
FITC-BrdU	3D4	Biolegend	364104
PECy7-CD4	GK1.5	Biolegend	100422
FITC-TCRb	H57-597	Biolegend	109206
Pacific Blue-CD44	IM7	Biolegend	103020
APCCy7-CD62L	MEL-14	Biolegend	104428
PE-CD62L	MEL-14	Biolegend	104407
AF647-PD1	29F.1A12	Biolegend	135229
FITC-PD1	29F.1A12	Biolegend	135214
Biotin-CXCR5	2G8	BD Biosciences	551960
Donkey Anti-Rabbit IgG AF647		Thermo Fisher	A31573
Anti-Mouse Ea52-68 Biotin	eBioY-Ae	Thermo Fisher	13-5741-85
Anti-CD40L	MR1	Biolegend	106516
Anti-FITC alkaline phosphatase		Jackson ImmunoResearch	200-052-037

Table 2.1: Antibodies

SW_{HEL} mice	Phan et al., 2003
I-$Ab^{loxp/loxp}$ mice	Hashimoto et al., 2002
Rosa26-CreERT2 mice	Ventura et al., 2007
$Aicda^{wt/cre}$ mice	Robbiani et al., 2008
Rosa26-loxp-stop-loxp-DTR mice	Buch et al., 2005
R26p-Fucci2 mice	Abe et al., 2013
OT-II transgenic mice	Barnden et al., 1998
C57BL/6 mice	Oxford University core breeding facility
B6SJLCD45.1 mice	Oxford University core breeding facility
TCRb/d$^{-/-}$ mice	Mombaerts et al., 1992; Itohara et al., 1993
CD79a-CreERT2 mice	Hobeika et al., 2015
CD4-Cre mice	Lee et al., 2001
Nur77-GFP mice	Moran et al., 2011

Table 2.2: Animal models

2.2 Mouse models

$MHCII^{fl/fl}$, R26-CreERT2, R26p-Fucci2, SW_{HEL}, $Aicda^{wt/Cre}$, R26-loxp-stp-loxp-DTR, CD79a-CreERT2, OTII, *TCRb/d*$^{-/-}$, Nur77-GFP, c-$Myc^{GFP/+}$ and CD4-Cre mice have been described previously. C57BL/6 and B6SJL.CD45.1 mice were purchased from the University of Oxford core breeding facility. All mice were >6 weeks of age at the time of experimentation, and mixes of male and female mice were used.

All mice were bred and housed in specific pathogen-free facilities at the Biomedical Sciences Facility at the University of Oxford. All experiments were performed under the authorization by a project license granted by the UK Home Office and were also approved by the Institutional Animal Ethics Committee Review Board at the University of Oxford.

To generate mixed bone marrow chimeric mice, B6SJLCD45.1 or C57BL/6 host mice were lethally irradiated twice at 4.5 Gy dose for 300 s with a 3-4hrs rest in between. Mice were injected i.v. with a mixture of sex matched CD45.1 WT and CD45.2 bone marrow, the ratios of different cell types are listed in the table below. Recipient mice received drinking water containing antibiotics (0.16mg/mL

Enrofloxacin (Baytril), Bayer Corporation) for 4 weeks after irradiation. Mice were rested for > 8 weeks to allow bone marrow reconstitution before experiments.

R26-CreERT2 x MHCII$^{fl/fl}$ CD45.2 80% (target freq.)	WT CD45.1 20% (target freq.)
R26-CreERT2 x MHCII$^{fl/fl}$ x Fucci2 CD45.2 60%	Fucci2 CD45.1 40%
R26-CreERT2 x MHCII$^{fl/fl}$ x c-Myc$^{GFP/+}$ CD45.2 60%	c-Myc$^{GFP/+}$ CD45.1 40%
AID-Cre x Rosa26-DTR CD45.2 80%	WT CD45.1 20%
AID-Cre x Rosa26-DTR CD45.2 45%	WT CD45.1 55%
AID-Cre x Rosa26-DTR CD45.2 80%	Fucci2 20%
AID-Cre x Rosa26-DTR CD45.2 80%	Nur77-GFP CD45.1 20%

Table 2.3: Mix BM chimeras

2.3 Immunisations, treatments and adoptive transfers

Immunisation

For polyclonal responses, mice were immunized with sheep red blood cells (SRBCs) (Fisher Scientific). Each mouse received ~2-3x10^8 defibrinated SRBCs diluted in 300ul PBS by i.p. injections.

Treatments

For HEL-specific GC responses, 1x10^5 HEL-binding MHCII$^{fl/fl}$ x CD79a-CreERT2 SW$_{HEL}$, SW$_{HEL}$ or SW$_{HEL}$ x Fucci2 cells were transferred into congenic C57BL/6 or B6SJLCD45.1 hosts by intravenous injection. Mice were immunized one to three days later with 50ug of HEL or HEL^{3X} conjugated to SRBCs (HEL-SRBCs)(Phan et al, 2003). For staining control mice the same number of OTII cells were co-transferred by i.v. injections. The following day mice were immunized with 25ug HEL-OVA/Ribi (Sigma, S6322) (Allen et al, 2007). All immunuzations were carried out by i.p. injections. Spleens were harvested 8 or 9 days after immunization.

For adoptive T cell transfer experiments, splenocytes from CD4-DTR donor mice were transferred into sex matched *TCRb/d$^{-/-}$* recipients by iv injections. Splenocytes from one donor mouse were transferred into three recipient mice. Recipient mice were immunized with SRBCs supplemented with 10ul/ml LPS (Sigma-Aldrich, L6529) on the following day. Mice were excluded from analysis if

the percentage of T cells ($CD4^+$ $TCRb^+$) was more than 0.4% splenocytes left after DT treatment, which was an indication of incomplete T cell ablation.

For tamoxifen (Sigma, T5648) treatment, 2mg tamoxifen was dissolved in 200ul solvent (10% ethanol plus 90% corn oil), sonicated briefly and given to mice by i.p. injections at indicated time points.

For DT (Calbiochem) treatment, mice received single i.p. injections of 0.75ug DT in 300ul of PBS or PBS alone at various time points.

For *in vivo* BrdU (Sigma-Aldrich, B5002) and EdU (Biosynth Carbosynth, NE08701) labelling experiments, mice received 2mg BrdU (300ul of 6.6mg/ml stock in PBS) or 1mg EdU (300ul of 3.3 mg/ml stock in PBS) by i.p. injections at indicated time points.

For anti-CD40L antibody treatment, each mouse received a single i.p. injection of 0.5mg anti-CD40L antibody in 300ul PBS at indicated time points.

For Ibrutinib (Selleckchem, S2680) treatment, Ibrutinib was provided through two intraperitoneal injections of ibrutinib (0.25 mg per mouse), separated by 3 hours. Ibrutinib was dissolved in CAPTEX 355 (1.56 mg/ml; ABITEC) and further diluted in phosphate-buffered saline (PBS) before use.

2.4 Flow cytometry and cell sorting

Single cell suspensions were prepared by meshing spleens through 40µm cell strainers. For each sample, $1.5*10^7$ splenocytes were washed with FACs buffer (PBS, 1% fetal bovine serum (Sigma), 5mM EDTA) and stained with the relevant antibodies. BrdU staining was performed following the fixation/permeabilization reagents from the BD BrdU flow kit according to the manufacturer's instructions but using the Mobu-1 antibody clone (Thermo Fisher Scientific) for BrdU/EdU double labelling experiments. Intranuclear BATF and IRF4 staining was performed on cells

permeabilised using the Invitrogen Foxp3 / Transcription Factor Staining Buffer Set (Invitrogen). Active caspase 3 staining was performed on cells permeabilised using the Fixation/Permeabilization Solution Kit (BD bioscience). All permeabilization steps were performed with an overnight incubation at 4°C. Samples were analyzed using BD LSR Fortessa, LSR Fortessa X20, Fortessa Symphony, or LSR II machines. Analysis was performed with Flowjo (Treestar Inc.).

2.5 Immunohistochemistry and immunofluorescence

Spleen fragments were snap-frozen in O.C.T. mounting medium (Tissue-Tek). Cryostat sections (7 or 10 µm) were cut and fixed with ice-cold acetone (10 min) before drying for >1 hour. For immunohistochemistry (IHC), slides were subsequently rehydrated in tris-buffered saline (TBS) with 0.1% BSA and stained for >3 hours with the relevant antibodies in TBS/blocking serums. Secondary stains were performed for >1 hour. Enzyme conjugates were developed using Sigma Fast DAB and Fast Blue substrates before mounting with Aqua-Mount. For immunofluorescence (IF), slides were rehydrated in PBS/0.1% BSA and stained for >3 hours with antibodies in PBS/blocking serums, washed, and stained with secondary reagents (>3 hours). IHC images were acquired using an Echo Revolve microscope, and IF images were acquired with 10× Axioscan (Zeiss). Frequencies of T_{FH} cells were quantified as the number of $PD1^+$ cells per mm^2 GC area.

2.6 Single-cell RNA sequencing

Single cell suspensions of splenocytes were prepared and stained with antibodies as in section 2.4. Then populations of interest were single cell index sorted into 96 well plates using 85um nozzle. Each well contained 4ul lysis buffer (2ul 0.4% Triton

X+ Rnase Inhibior, 1ul dNTP (10mM), 1ul Oligo dT (10uM), 0.01ul ERCC Spike in). Sorted plates were stored at -80°C until next step of processing.

The library construction was carried out by Dr Neil Ashley in the Single Cell Facility in the Weatherall Institute of Molecular Medicine.

Reverse transcription was carried out by adding the following reactions mix to each well: 0.5ul SuperScript II reverse transcriptase (200U/uL), 0.25ul Rnase inhibitor (40U/uL), 2ul Superscript II first-strand buffer (5x), 0.5ul DTT (100mM), 2ul Betaine (5M), 0.06ul MgCl2 (1M), 0.1ul TSO (100uM), Nuclease-free water 0.29ul. The PCR programme was the following: 90mins at 42°C, 15mins at 72°C and hold at 4°C.

Then 15ul pre-amplification mastermix (12.5ul KAPA Hifi HS Ready Mix (2x), 0.125ul ISPCR primers (10uM), 2.375ul Nuclease-free water) was added to each well. The following PCR programme was used: initial denaturation 98°C 3mins; 23cycles with 98°C 20s, 67°C 15s, 72°C 6mins; final extension 72°C 5mins and finally kept at 4oC. PCR products were purified with Ampure XP beads following manufacturer's instructions. The quality of cDNA library was check with Agilent high-sensitivity DNA chip as per manufacturer's instructions.

Next cDNA library was tagmented with Nextra XT DNA Library Prep Kit. 0.125ng cDNA was tagmented in a total volume of 5ul, containing 2.5ul tagmentation buffer (2x) and 1.25ul Amplicon Tagment mix. The plates were incubated at 55°C for 5min then returned to 4°C for storage. 1.25ul NT buffer was added to each well and plates were incubated at room temperature for 5mins. Indexing primers were added to cDNA fragments using the Nextera XT kit according to manufacturer's instructions. PCR products were purified with Ampure XP beads again. The concentration of cDNA library was determined using Qubit dsDNA HS Assay Kits. Library was pooled and sequenced.

2.7 Single-cell RNA sequencing data analysis

After sequencing runs, the FASTQ files were first processed in Partek software. Reads were subject to pre-alignment QC and then aligned to the genome with STAR. Gene counts were generated after post-alignment QC. Gene counts were then imported into Seurat for downstream analysis. Filtering was carried out to exclude cells with >5% mitochondiral genes. Next batch correction was carried out to remove differences caused by different batches of sample processing and sequencing runs. Normalization and dimensional reduction were then performed on the data sets. Then various downstream analyses were carried out.

2.8 Statistical analysis

First the normality of the experimental data set was determined by Shapiro-Wilk normality testing. Individual statistical analysis was carried out as specified in each figure legend. Statistical significance: *p <0.05, **p <0.01, ***p < 0.001, ****p < 0.0001. All statistical analyses were calculated in Prism 8 software (GraphPad).

Chapter 3

Cyclic re-entry initiation can occur independently of acute cognate T cell interactions

Contents

Positive selection in the GCs has long been thought to involve LZ cells needing to "initiate" cyclic re-entry each time they enter LZs. This concept was originally derived from the modelling studies of Kepler and Perelson showing

the optimal efficiency of mutation accumulation for affinity maturation could be achieved through the physical separation of locations for mutation/proliferation and selection in GC DZs and LZs, respectively, to intercalate periods of rapid mutations and rapid proliferations with resting selection, then having the selected cells re-entering GC DZs (Kepler and Perelson, 1993). This preferential "cyclic re-entry" thereby favours B cells expressing higher affinity BCR variants, and drives antibody affinity maturation.

Various inputs and processes have been considered to be controlling this positive selection process. The first candidate was the competition between B cells for antigen acquisition in which B cells compete for access to the antigens laden on FDCs (MacLennan et al, 1994). However, later on, it was revealed by two-photon microscopy that no prolonged interactions between B cells with FDCs were observed, suggesting that B cells are not blocking each other's access to antigens (Allen et al, 2007). In the same study carried out by Allen et al., T cell help was proposed to be the limiting factor, given the rareness of stable B-T interactions in GCs (Allen et al, 2007). Higher affinity B cells are thus more likely to receive a larger amount of T cell help because they are expected to acquire more antigens from FDCs, which would lead to more MHCII-peptide complexes (Batista et al, 2000). This was later seemingly supported by the findings that enhancing antigen presentation without BCR stimulation in LZs led to the significant accumulation of these cells in DZs, proposing that T cell help is essential for driving proliferation in GC B cells (Victora et al, 2010).

However, as elegant and informative as these studies were, none were aimed at directly testing whether or not selection cues are required for the cyclic re-entry initiation process itself. The conclusions were reached based on the observations that helped cells undergo preferential expansion in DZs (Victora et al, 2010; Gitlin et al, 2014; Gitlin et al, 2015). While this may mean that B-T cell interactions are required for selecting LZ cells to re-enter cell cycle, it also remains plausible that B cells that receive better quality and/or quantity of T cell help could undergo preferential

expansion in the DZ because it could also induce the expression of growth-related factors such as c-Myc and Cyclin D3 in GC B cells (Victora et al, 2010; Calado et al, 2012; Dominguez-Sola et al, 2012; Finkin et al, 2019; Pae et al, 2021).

The GC has long been considered to be a highly competitive environment, with up to 70% - 90% of cells failing to return to DZs following each LZ visit (Victora et al, 2010; Victora et al, 2012; Meyer-Hermann, et al, 2012). As such, it is expected only the fittest cells (highest affinity) can be selected for cyclic re-entry in LZs. However, as discussed earlier in the main introduction, GCs retain a considerable level of permissiveness in the selection process, as exemplified by the high clonal diversity even at relatively late stages of GC responses, and the existence of extremely highly mutated HIV-1 broadly neutralizing antibodies, none of which can be explained by a selection model that is overly stringent on affinity (Tas et al, 2016; Kuraoka et al, 2016; Mesin et al, 2016; Sok and Burton, 2018).

In order to dissect the association between specific selection cues and cyclic re-entry initiation, a high-resolution method is required for identifying the cells engaged in this process after manipulating key selection cues with different approaches. Therefore, in this Chapter, we started by investigating the involvement of T_{FH} cells in driving cyclic re-entry initiation in LZs.

3.1 Applying a genetic cell cycle based reporter mouse model to identify cells that are initiating cyclic re-entry

In order to examine what are the inputs that LZ cells need to receive to initiate cyclic re-entry, an approach was needed to identify cells engaged in this event. The mouse model we chose to use is Fucci2 (Fluorescent Ubiquitination-based Cell Cycle Indicator) (Abe et al, 2013). This mouse model allows for the identification of cells at various stages of the cell cycle based on the differential expression and accumulation of two reporter proteins. Our lab previously validated the fidelity of this model in

GC B cells and used it to follow cells at different cell cycle stages in DZs (Stewart et al, 2018). Therefore, we considered if we could also utilize this same approach to identify LZ cells transitioning from the late G1 stage back into early S phase, since this would be the first stage of cyclic re-entry. One key advantage of the Fucci2 model over other cell cycle identification approaches is that it allows not only for distinguishing different cell cycle stages, but also provides information about relative time spent in that phase. This approach also has the advantage of allowing cell cycle stage discrimination without the need for fixation or nucleotide analogue treatment.

We first sought to validate the appropriateness of the Fucci2 mouse model for tracking cyclic re-entry initiation in LZs. Fucci2 mice were immunized with the model T-dependent antigen sheep red blood cells (SRBCs) to induce GCs and polyclonal responses were analyzed close to the response peak on day 8. GC B cells were gated as $B220^{+}$, IgD^{low}, $CD95^{+}$, and $GL7^{+}$ by flow cytometry. LZ cells are identified as $CXCR4^{low}$ $CD86^{high}$ and DZ cells as $CXCR4^{high}$ $CD86^{low}$ GC B cells (Allen et al 2004, Victora et al 2010), as shown in Figure 3.1A. These Fucci2 mice carry a bicistronic Rosa26 driven transgene consisting of mVenus and mCherry fused to the ubiquitinylation domains of Geminin (hGem(1/110)) and Cdt1(hCdt1(30/120)), respectively (Abe et al, 2013). As such, cells start their journey as mVenus and mCherry double negative immediately after mitosis, and then mCherry accumulates throughout G1. Therefore, the intensity of mCherry is correlated with the time that the cell has spent in G1. mCherry starts to degrade at the onset of S phase and degradation completes by mid-late S phase/G2, whereas mVenus expression is upregulated when cells are entering S phase and terminates during mitosis (Fig. 3.1B).

In DZs, B cells undergo repetitive divisions without a prolonged G1 rest period (average of 2-3x), which has been referred to as "inertial" cell cycling (Gitlin et al, 2014; Gitlin et al, 2015; Pae et al. 2021). This rapid proliferative process is thought to be triggered and regulated by T cell mediated selection cues received within LZs, but occurs independently of selection cues once started as a result of

retained cyclin D3 expression in combination with the metabolic reserves following c-Myc induction in the LZ (Calado et al, 2012; Dominguez-Sola et al, 2012; Finkin et al, 2019). Consequently, DZ cells initiate S phase from a relatively "early" G1 state, evident from their intermediate mCherry intensities at the point of mVenus expression (Fig. 3.1C). An alternative fate to cell division is DZ cells exiting cell cycle, down-regulating CXCR4 and migrating back to LZs, which occurs ~8-10hrs post-mitosis (Stewart et al, 2018). Because such cells are resting for more extended periods than those undergoing inertial cycling, they have higher levels of mCherry (Fig. 3.1C). Therefore, consistent with expectations, LZ cells initiating cyclic re-entry can be clearly identified as a distinct mCherry^{high} mVenus^{+} early S phase population, as indicated by the red gate in Figure 3.1C. The dashed line is included for visualisation purposes, aiding the comparison of the mCherry intensity differences between inertial and cyclic re-entry populations. The "cyclic re-entry" gate was drawn relatively broadly in this figure; however, for the reasons outlined above, the very earliest S phase cells will be those with the lowest mVenus intensity. Together, these data demonstrate that the Fucci2 reporter line represents an appropriate model for our task of identifying LZ cells at the point they initiate cyclic re-entry.

3. Cyclic re-entry initiation can occur independently of acute cognate T cell interactions

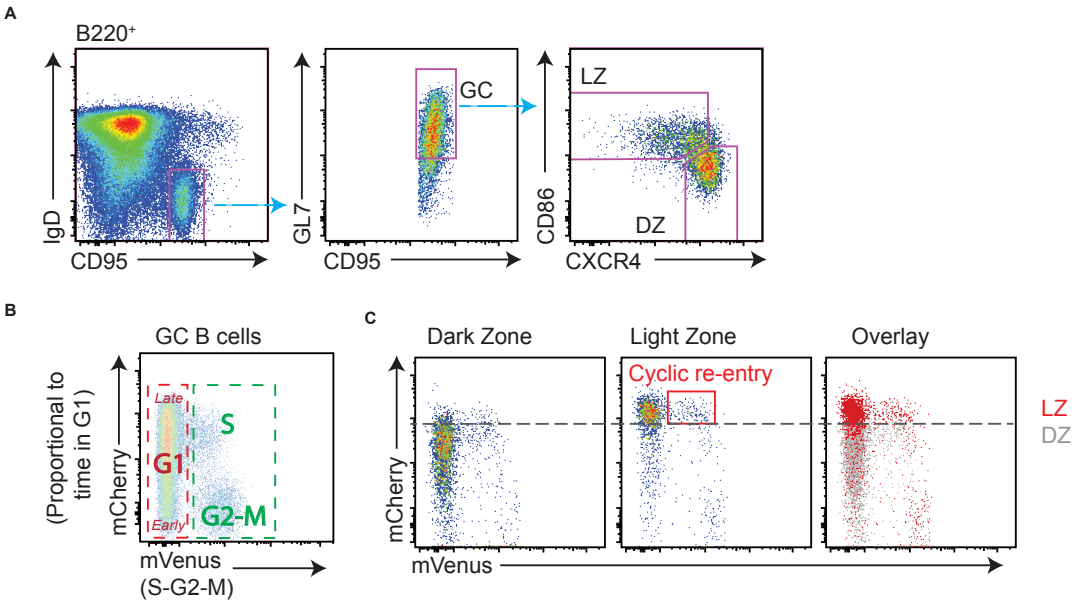

Figure 3.1: Identification of light zone cyclic re-entry cells in Fucci 2 mice. SRBC immunized GC responses in Fucci2 mice were analysed on day 8. (A) Gating strategy for splenic GC B cells, DZ and LZ populations identified as shown. (B) G1 cells and S-G2-M cells are gated as shown. mCherry levels accumulate with time post-mitosis, and mVenus accumulates with time in S phase; as such, early S phase cells are mCherry^{high} mVenus^{+}. (C) LZ cells are mostly resting and therefore have higher mCherry levels than DZ cells. The dashed line is provided to aid comparison. LZ cells initiating cyclic re-entry (early S phase) are identified by the red box. An overlay of DZ and LZ cells is shown on right.

3.2 Cyclic re-entry initiation remains unaffected when T cells are depleted from GCs

Having established an approach for identifying cells engaged in cyclic re-entry, we wished to test the assumptions of cyclic re-entry models that cyclic re-entry initiation only occurs if LZ B cells have successfully acquired a threshold level of T cell help.

To answer this question, we established a system that allows the deletion of T cells from established GCs. CD4-Cre^{+} mice were crossed to R26-loxp-stp-loxp-DTR mice (Lee et al, 2001; Buch et al, 2005). CD4-Cre^{+} Rosa26-loxp-stp-loxp-DTR mice express Cre-recombinase in all CD4^{+} T cells, which excises the stop cassette before

a human diphtheria toxin receptor (DTR) transgene to activate its expression. To note, the DTR expression also occurs in cells with a history of CD4 expression, such as $CD8^+$ T cells. The DTR expression renders cells susceptible to apoptosis quickly after DT treatment, permitting lineage specific cell deletion. We transferred naïve splenocytes from CD4-Cre^+ Rosa26-loxp-stp-loxp-DTR mice into mice lacking all T cells ($TCRb/d^{-/-}$) (Mombaerts et al, 1992; Itohara et al, 1993). Mice do not have endogenous DTR expression, therefore only the transferred $CD4^+$ cells are ablated after DT. The recipient mice also carried the R26-Fucci2 transgene, allowing cell cycle tracking. The development of GCs is a strictly T cell dependent process so GCs do not usually form spontaneously in these TCR knockout mice. However, transferred T cells and subsequent immunization with SRBCs supplemented with LPS permitted GC formation in these animals (Fig. 3.3 A). Six or eight days after immunization, mice received DT treatment by i.p. injections at indicated time points, followed by analysis on day 8 or 10, with a schematic diagram shown in Figure 3.2A.

Our examination of the dependence of T cells for cyclic re-entry initiation started by assessing the T cell deletion efficiency in this model. T_{FH} cells were identified as $B220^-$, $CD4^+$, $TCRb^+$, $PD1^{high}$ and $CXCR5^{high}$ by FACS analysis. T cell deletion was rapid, efficient and specific, with a more than 10-fold reduction in the number of T_{FH} cells within the first 24hrs after DT treatment and retained at 48hrs (Fig. 3.2, B and C) (Radtke et al, 2019). This 48hrs treatment was then chosen because GCs were allowed to further develop for a significant period of time without T_{FH} cells so that any phenotypic changes related to cyclic re-entry could appear but GCs had not yet collapsed. Deletion efficiency was also confirmed with immunohistochemistry (IHC), which is more direct visualization of both the number and location of T_{FH} cells. To do this, frozen spleen blocks were sectioned serially and stained with T and B cell markers. B cell follicles were demarcated by IgD and GCs by GL7, respectively. PD1 was stained to label T_{FH} cells in slides sectioned adjacently and T_{FH} cell numbers were quantified. The results are consistent with FACS data that the deletion was highly efficient (Fig. 3.2, D and E).

3. Cyclic re-entry initiation can occur independently of acute cognate T cell interactions

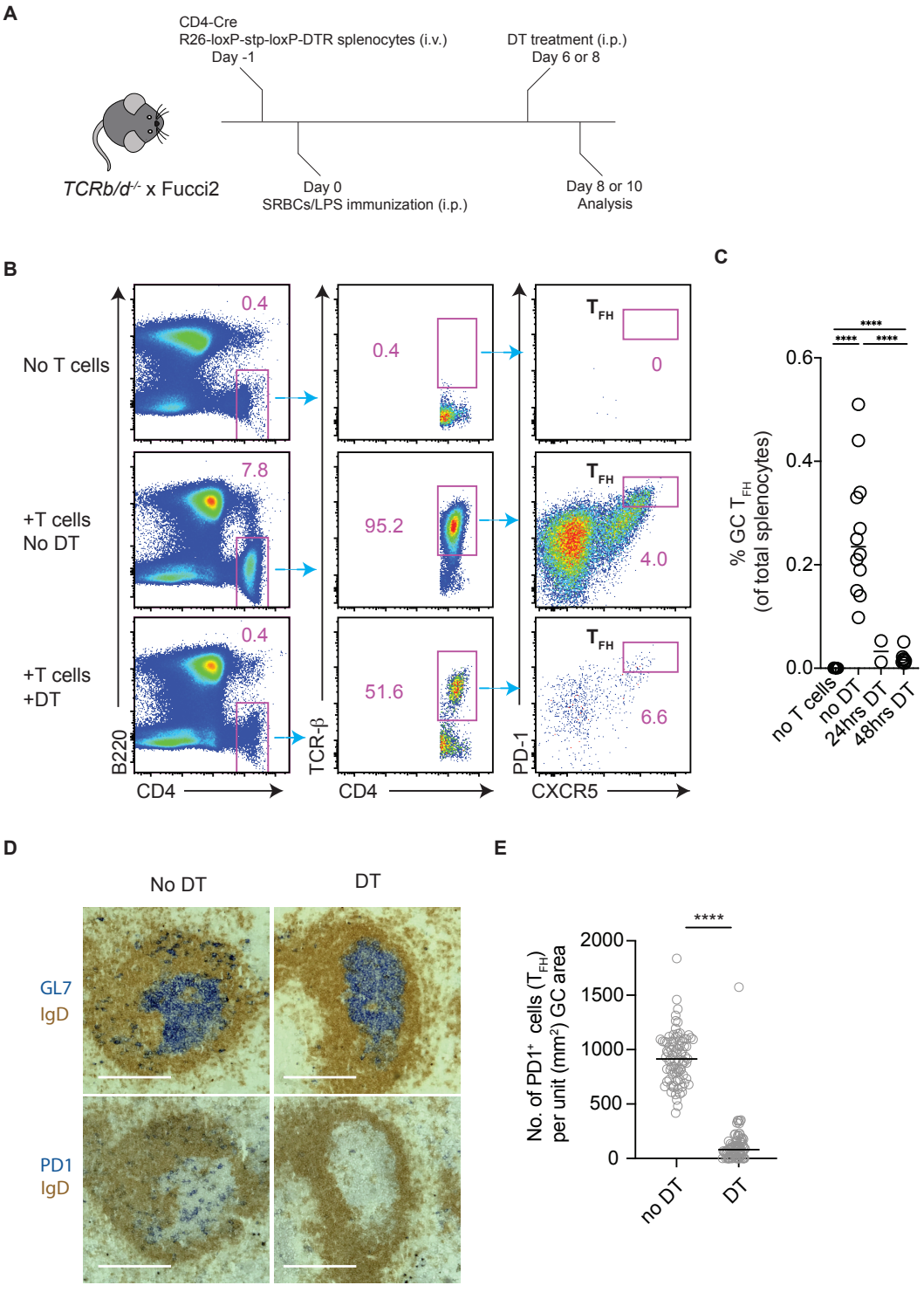

Figure 3.2: Establishment of a system to deplete T cells from established GCs. CD4-Cre^{+} R26-loxp-stp-loxp-DTR naïve splenocytes were adoptively transferred into sex matched *Tcrb/d*$^{-/-}$ Fucci2 recipients by i.v. injections, which were subsequently immunized with SRBCs supplemented with LPS (i.p.). Mice received DT or PBS 24 or 48hrs before spleen harvest on day 8 or day 10. (A) The schematic diagram of the experiment layout. (B) Splenic GC T_{FH} cells were gated as shown, (C) and quantitated. (D) The relative absence of PD1^{+} T_{FH} cells in GL7^{+} GCs was determined by IHC (scale bar, 220um), (E) and enumerated. Each point is a single GC, pooled from 5-6 mice/condition from five experiments. Statistical analysis was Mann-Whitney U test. ****$p < 0.0001$

3. Cyclic re-entry initiation can occur independently of acute cognate T cell interactions

Having established that DT treatment leads to a paucity of T_{FH} cells in GCs within one day, we next investigated the impact of T cell ablation on GC size and on cyclic re-entry initiation by remaining LZ cells. We did not observe any differences in GC sizes 48hrs after DT treatment, contrary to previous reports, where 48hrs of MHCII blockade led to shrinkage in GC sizes (Fig. 3.3A) (Pae et al, 2021). This difference could be due to several reasons. First, Pae et al used MHCII blocking antibodies to block B-T interactions, which could have different kinetics compared to DT-mediated cell death. The difference in the time that GCs have been functionally deprived of B-T interactions could contribute to this difference in observation. Additionally, in our adoptive transfer model, GC B cell frequencies showed some degrees of variation, which could also conceal some subtle differences.

Meanwhile, DT treatment did not cause any changes to the sizes of LZs (No DT 33±0.9%; +DT 35±1.1%) and there was a clear population of LZ cells identified as $mCherry^{high}$ $mVenus^{+}$ transitioning from late G1 state into early S phase after DT treatment (Fig. 3.3B, left). Late G1 cells and the late S-G2-M cells were also identified by the dashed purple gates and dashed orange gates, respectively (Fig. 3.3B, right). Surprisingly, there was no detectable change in the frequencies of early S phase LZ cells 48hrs after T cell ablation (Fig. 3.3C, middle). The percentages of late G1 cells as well as the frequencies of cells completing the cell cycle while remaining in LZ (the late S-G2-M population) after DT were also not affected (Fig. 3.3C, left and right). Although most cyclic re-entry initiating LZ cells would be expected to upregulate CXCR4, migrate to DZ and finish the cell cycle once in the DZ, there have been reports of these small populations of cells completing cell cycle in the LZ (Zotos et al, 2021; Hauser et al, 2007; Gitlin et al, 2014). Hence the normal frequencies of cells in any cell cycle stage after DT treatment possibly reflect that LZ cells do not show any defect in cell cycle progression despite receiving minimal or no support from T cells. Thus, these data suggest that the assumption that LZ B cells must receive cues from T cells prior to re-entering cell cycle, and that this is achieved only when strong cumulative help signals are reached, may not be correct.

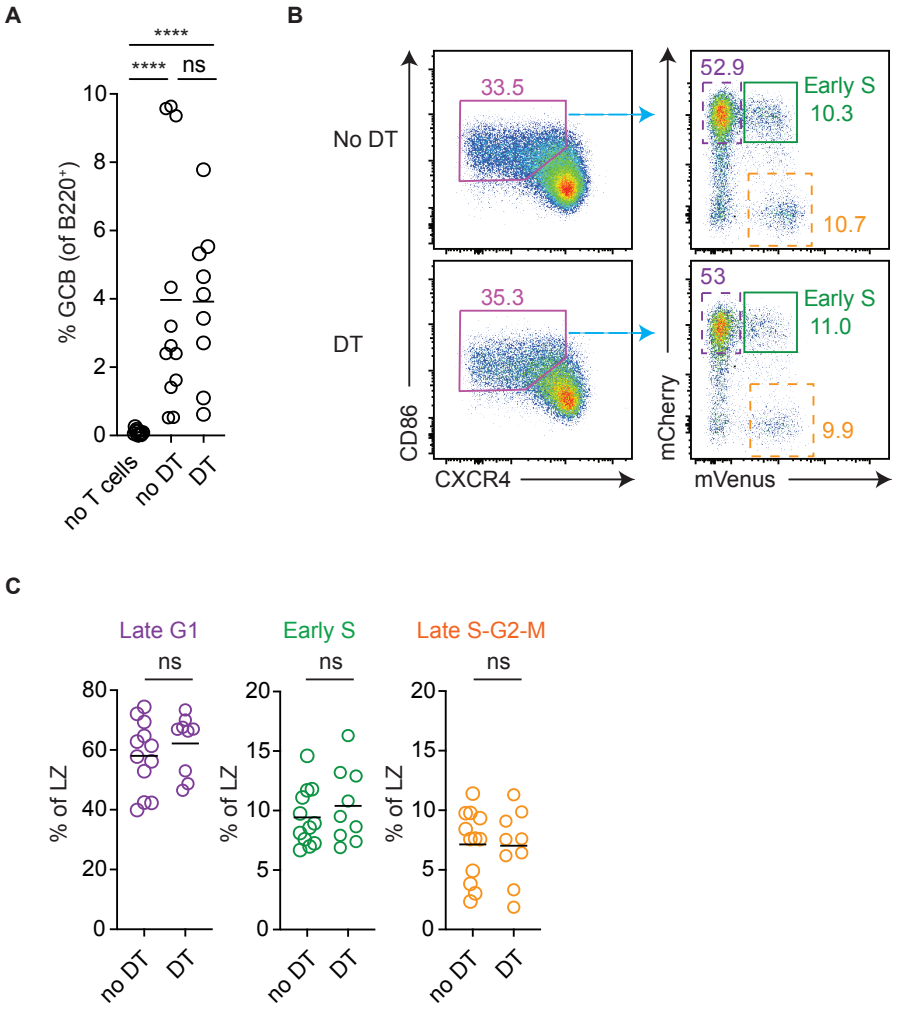

Figure 3.3: GC T_{FH} cell availability does not acutely restrain LZ B cells cyclic re-entry initiation.
Same experiment regimen as outlined in Figure 3.2. (A) Frequencies of GC B cells (IgD^{low} $CD95^{+}$ $GL7^{+}$) in mice that received no T cells, or received T cells and were subsequently treated DT or carrier alone 48hrs before analysis. (B) LZ cells were identified (left) and frequencies of early S phase cells were identified by the green gates, as well as late G1 (dashed purple gates), late S-G2-M (dashed orange gates) (right) and quantitated (C). Results are representative (B) or pooled (A, C) from 5 independent experiments each with 1-3 mice per condition. Analysis, Mann-Whitney U test (A) or unpaired student's T test (C, no DT vs DT). ****$p < 0.0001$

3.3 Cyclic re-entry is largely insensitive to MHCII deletion

3.3.1 Establishing and validating a genetic model to delete MHCII from GC B cells

We were surprised to find that LZ cells could still initiate cyclic re-entry in settings where T cells were much reduced, because it was generally assumed that such cells are limiting in number and that LZ B cells must have successfully competed for help from T cells in order to initiate cyclic re-entry. However, the T cell deficient/adoptive transfer model may mask subtle differences in changes of cyclic re-entry initiation, and certain GC regulatory networks may be rewired in this setting because this model was comparatively unphysiological. In this system, the competitive GC environment has been changed because most of T cells are depleted all at once so that B cells do not face competition from other B cells to interact with T cells. Moreover, despite T cell depletion being very efficient, it was not absolute, and a small number of T cells persisted (~1/10 normal frequency).

Prompted by these concerns, and given the central importance of the previous findings, we next sought to perturb B-T interactions in a different way, by deleting MHCII from a subset of GC B cells. We first established a mouse line whose MHCII can be conditionally deleted through the provision of tamoxifen, by crossing *H2-Ab1*$^{fl/fl}$ (hereafter referred to as MHCII$^{fl/fl}$) mice to R26-CreERT2^{+} mice (Hashimoto et al, 2002; Ventura et al, 2007). Tamoxifen administration activates the CreERT2 recombinase. CreERT2 then recognizes the loxP sites inserted up and downstream of the exon1 of MHCII alleles, resulting in the gene excision and hence MHCII knockout. In order to make internal comparisons of any phenotypes between MHCII-deleted and MHCII^{+} B cells, we generated mixed bone marrow (BM) chimeric mice with MHCII$^{fl/fl}$ R26-CreERT2^{+} CD45.2 and congenic WT CD45.1 cells. The targeted frequencies of these mixed BM chimeras were 60%:40% in slight favour of MHCII$^{fl/fl}$ R26-CreERT2^{+} cells.

3. Cyclic re-entry initiation can occur independently of acute cognate T cell interactions

To validate this approach, GCs were established by SRBC immunizations, with MHCII deletion achieved by the delivery of tamoxifen after GC formation at different time points post-immunization (Fig. 3.4A). These polyclonal responses were analyzed on day 8. There was a quick deletion of MHCII from a subset of GC B cells 24hrs after tamoxifen, and the proportion of MHCII-deleted cells increased at 48hrs (Fig. 3.4B). Notably, there was no further reduction in the level of MHCII in the $MHCII^{neg}$ gate 48hrs after tamoxifen, suggesting the MHCII deletion was complete for some cells within 24hrs of Cre activation. The existence of WT cells helps to maintain a close to normal competitive environment in the GC.

To further confirm that loss of detectable surface MHCII led to the expected loss in antigen presenting capability, we stained for peptide-MHCII complexes after MHCII deletion. We performed similar MHCII deletion experiments but in settings where B cells carried the HEL-specific SW_{HEL} BCR (*CD79a*-$CreERT2^{+}$ $MHCII^{fl/fl}$ SW_{HEL} B cells) (Phan et al, 2003; Hobeika et al, 2015; Moran et al, 2018). CD79a is BCR associated protein alpha chain so in these mice, MHCII deletion can be induced in BCR expressing cells (Hobeika et al, 2015). On day 8 of the immunisation-induced response (40 hrs post-tamoxifen), splenocytes were harvested and cultured *ex vivo* for 2 hrs with HEL-Ea-GFP, a peptide-protein conjugate composed of cognate antigen HEL and a well-defined peptide Ea52-68 as well as GFP (Pape et al, 2007). Antigen uptake can be measured by detecting GFP fluorescence, while the Ea52-68 peptide presented on I-Ab can be detected with the Y-ae monoclonal antibody (Murphy et al, 1989). Control cells were cultured with a HEL-BSA conjugate, which still leads to BCR crosslinking but without Ea52-68 peptide uptake. The MHCII-deleted GC B cells showed the same amount of GFP acquisition compared with $MHCII^{high}$ cells but had no detectable Y-ae staining, indicating that antigen uptake was normal in these MHCII-deleted cells but they were unable to present peptide antigen (Fig. 3.4C).

To complement the antibody staining, we also assessed whether MHCII-deleted GC B cells could functionally present peptide antigens to T cells. For this purpose,

3. Cyclic re-entry initiation can occur independently of acute cognate T cell interactions

we used OTII T cells, which have transgenic TCR that recognizes Ovalbumin (OVA) peptide 323-339 presented on I-Ab (Barnden et al, 1998). MHCII$^{fl/fl}$ R26-CreERT2^{+} mice were immunized with SRBCs to form GCs and MHCII^{high} and MHCII-deleted GC LZ B cells were FACS sorted on day 8, 24hrs after tamoxifen treatment. Naïve OTII T cells were also purified by FACS. MHCII^{high} and MHCII-deleted cells were co-cultured with OTII cells *ex vivo* in supplement with exogenous OVA peptide for 12hrs. Levels of early activation markers (CD69 and CD25) were then assessed on OTII cells. MHCII^{high} LZ cells were able to stimulate the upregulation of these early activation markers on OTII cells, while MHCII-deleted cells failed to do so, indicating there were no functional MHCII-TCR interactions hence an undetectable level of MHCII in MHCII-deleted cells. The baseline was set with OTII cells cultured alone (Fig. 3.4D). In conclusion, we confirmed with various methods that MHCII deletion can be quickly induced by tamoxifen injection and MHCII-deleted cells faithfully lost the ability to present peptides to T cells.

3. Cyclic re-entry initiation can occur independently of acute cognate T cell interactions

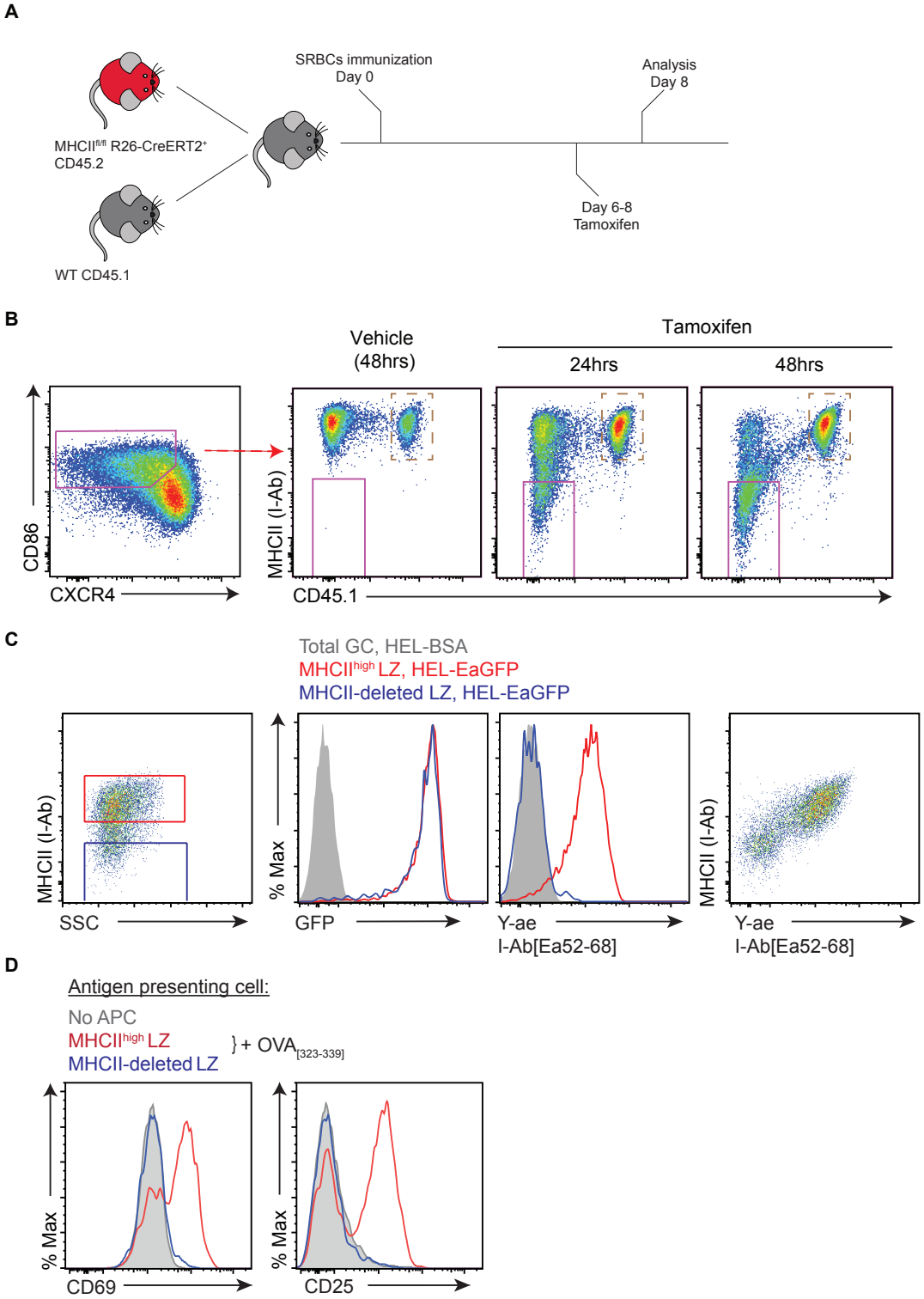

Figure 3.4: Validation of MHCII deletion efficiency.
(A) Schematic diagram of experimental layout. (B) Mixed BM chimeric mice made with mixes of WT CD45.1 and CreERT2^{+} MHCII$^{fl/fl}$ Fucci2 CD45.2 cells were immunised with SRBCs (i.p.). Tamoxifen (or vehicle) was given to mice at indicated time points before spleen harvest on day 8. (Continued in next page)

3. Cyclic re-entry initiation can occur independently of acute cognate T cell interactions

Figure 3.4: Splenic GC B cells (IgD^{low} $CD95^+$ $GL7^+$) were gated. LZ cells were identified (left), and representative plots of MHCII deletion efficiency by LZ cells. Brown dashed gates identify WT cells used in (Fig 3.5). (C) SW_{HEL} *Cd79a*-CreERT2 $MHCII^{fl/fl}$ B cells were adoptively transferred into WT hosts that were subsequently immunised with HEL^{3X}-SRBCs/LPS. Tamoxifen treatments were given 40hrs prior to tissue harvest on day 8. Splenocytes were cultured *ex vivo* for 2hrs with HEL-EaGFP or HEL-BSA (control). SW_{HEL} (CD45.1) LZ GC cells were analysed, with cells were further sub-gated based on their surface MHCII levels (left). Representative plots show GFP florescence and I-Ab[Ea52–68] staining. (D) $CreERT2^+$ $MHCII^{fl/fl}$ mice were immunized with SRBCs and mice received tamoxifen 24hrs before spleen harvest on day 8. $MHCII^{high}$ and MHCII-deleted GC LZ B cells were FACS purified. Naïve CD4 OTII cell were also FACS sorted. LZ B cells were co-cultured with OTII T cells overnight *ex vivo* in supplemented with OTII peptide. Levels of T cell early activation markers on the OTII T cells (CD69 and CD25) were assessed.

3.3.2 Subsets of LZ B cells remain capable of initiating cyclic re-entry after losing their ability to form cognate interactions with T cells

In the last section, we established a system for inducible MHCII deletion from GC B cells by tamoxifen administration and confirmed the high efficiency of deletion both phenotypically and functionally. We next tested whether LZ B cells can still initiate cyclic re-entry when they are not capable of forming cognate interactions with T cells due to the loss of surface MHCII. To allow direct tracking of cell cycle stages in GC B cells, the $MHCII^{fl/fl}$ R26-$CreERT2^+$ mice were further crossed to Fucci2 mice. Then, mixed BM chimeras were made between these CD45.2 $MHCII^{fl/fl}$ R26-$CreERT2^+$ Fucci2 BM cells and CD45.1 WT Fucci2 BM cells. Polyclonal responses were induced in these chimeras by SRBC immunization followed by tamoxifen treatment at indicated time points to induce MHCII deletion and splenic GC responses were analysed on day 8.

Surprisingly, 24 hours after tamoxifen treatment, despite not being able to present cognate antigen to T cells, LZ cells that had lost MHCII expression continued to initiate cyclic re-entry. The continued re-entry into S phase of such cells indicates that cyclic re-entry by LZ cells is not dependent on them receiving cognate help from T cells, at least not acutely (Fig. 3.5, A and B, top panel). 48 hours after MHCII

deletion, the MHCII-deleted cells were still capable of initiating cyclic re-entry at relatively normal frequencies, despite a small decrease (Fig. 3.5, A and B, bottom panel). These MHCII-deleted cells had not interacted with T cells for a significant period of time, while still being in a highly competitive GC environment due to the presence of the remaining WT GC B cells, indicating the existence of T cell independent cyclic re-entry initiation. In fact, there was a small increase in the frequencies of early S phase cells in the MHCII-deleted population compared with WT cells after 24 hours tamoxifen. One possible explanation for the increase is that the CD45.2 LZ MHCII^{high} population after tamoxifen was enriched with some quiescent cell populations possessing more stable MHCII, such as pre-memory cells. Previous studies have shown that MHCII is stabilized on LZ cells due to the high expression level of CD83, which is an antagonist for the ubiquitin ligase MARCH 1 that could target MHCII for degradation (Bannard et al, 2016).

Notably, in contrast to the T cell ablation experiments, where no detectable change was observed for cyclic re-entry initiation or cell cycle progression through later stages 48 hours after DT treatment, a modest but reproducible decrease was detected for early S phase population, followed by a further reduction in the late S-G2-M population, at the same time point post-treatment in the MHCII deletion experiment (Fig. 3.5, A and B, bottom panel). A slightly larger defect was seen at later stages of cell cycle (mVenus^{+}, late S/G2/M), which may reflect that some cells that re-entered the cell cycle failed to complete it, or that the cells that have initiated cell cycle have different kinetics in terms of their transitioning between LZ to DZ states after the loss of MHCII. As already noted, in the T cell ablation setting, T cells were universally depleted and a non-competitive GC environment was created, which could change the way how B cells and some of the regulatory networks in the GC. Second, the MHCII deletion experiment may have a better sensitivity because this experiment was performed in BM chimeras which allowed for internal comparisons for each mouse. Finally, the kinetics of DT-induced apoptosis may be different from the kinetics of tamoxifen induced MHCII deletion, so that

3. Cyclic re-entry initiation can occur independently of acute cognate T cell interactions

LZ B cells have lost interactions with T cells for different periods of time despite the same time interval between treatment and analysis.

While the Fucci2 model has always proven to be a robust and reliable measure of cell cycle stage, it is a single measure of cell cycle progression, so we next wanted to formally exclude the possibility that this phenomenon was specific to the reporter. To this end, we utilized another approach to identify early S phase cells with two nucleotide analogues, BrdU and EdU that was previously described by Gitlin et al (Gitlin et al, 2014). These DNA analogues are incorporated into DNA during replication in S phase, and can be stained for. Mice first received EdU 1.5hours before tissue harvest, which marks all the S phase cells. Then, BrdU was administrated by i.p. injections 30-40mins before tissue harvest. Thus, any cells that initiated cyclic re-entry in the last 40mins before tissue harvest (i.e., in the early S phase) were labelled as EdU^{-} $BrdU^{+}$, and mid-late S phase cells as EdU^{+} $BrdU^{+}$ (Fig. 3.5C). Consistent with the Fucci2 findings, the frequencies of early S phase cells only showed a modest reduction in the MHCII-deleted GC LZ B cell population 48 hours after MHCII deletions, with a similar trend of decrease in the late S phase cells, thereby validating the previous observations (Fig. 3.5D).

Our interpretation of previous experiments that cyclic re-entry initiation is not acutely T cell dependent could be further supported if cyclic re-entry initiation still occurs when most of the tamoxifen has been cleared from the metabolic system, so that MHCII deletion has finished long before our measurements are made. To achieve this, we performed longer MHCII deletion with 4-day and 6-day tamoxifen treatment. Tamoxifen has a half-life of about 6.8 hours *in vivo* (Reid et al, 2014), with these late analyses after treatment, tamoxifen induced MHCII deletion should have finished days before analysis. Therefore, any existing MHCII-deleted cells must have lost their MHCII and had not interacted with T cells for quite some time. Notably, there were still a small number of MHCII-deleted cells remaining in the GC on both days, with 10% of them transitioning from G1 to S phase on day 4 and 5% on day 6 (Fig. 3.6). These results demonstrated that, much in contrary to what

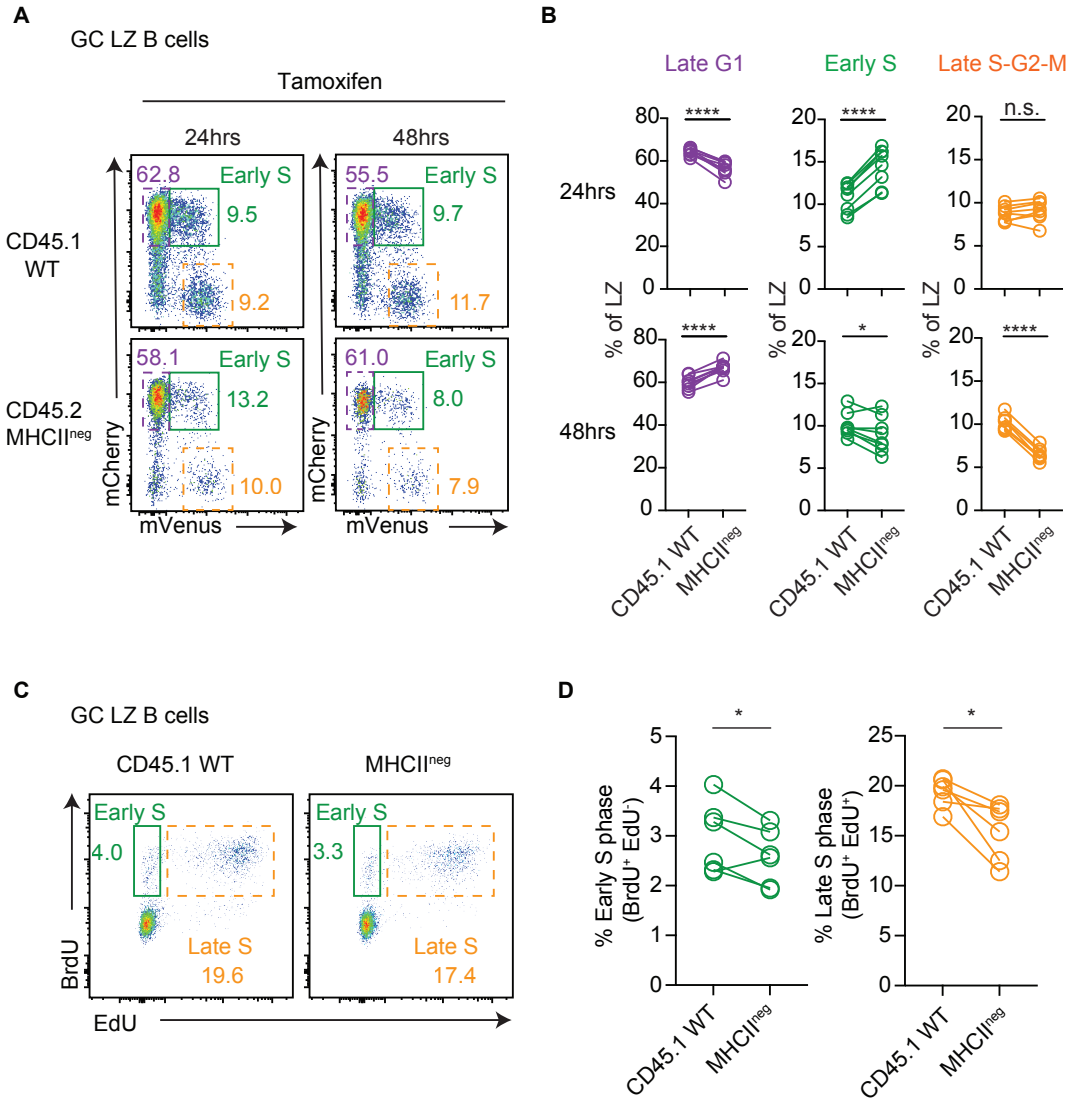

Figure 3.5: GC B cells could still initiate cyclic re-entry after losing machinery to interact with T cells.
(A and B) Mixed BM chimeric mice made with mixes of WT Fucci2 CD45.1 and CreERT2^{+} MHCII$^{fl/fl}$ Fucci2 CD45.2 cells were immunised with SRBCs (i.p.). Mice received tamoxifen (or vehicle) at indicated time points before spleen harvest on day 8. Splenic GC LZ B cells (IgD^{low} CD95^{+} GL7^{+} CXCR4^{low} CD86^{high}) were gated. (A) LZ cells in different cell cycle stages were identified. (B) Frequencies of late G1 (dashed purple), early S (green) and Late S-G2-M (dashed orange) cells were determined and summarized for WT and MHCII-deleted populations. (C - D) Mixed BM chimeric mice made with mixes of WT CD45.1 and CreERT2^{+} MHCII$^{fl/fl}$ Fucci2 CD45.2 cells were immunised with SRBCs (i.p.). Mice received tamoxifen 48hrs before spleen harvest on day 8. (C) Frequencies of Early S (green) and Late S (dashed orange) LZ cells were identified and summarized in D. Results are representative (A, C) or pooled from 2 independent experiments each with 3-4 mice per condition. Lines join populations from individual mice. Analysis, paired student T test, *p < 0.05

3. Cyclic re-entry initiation can occur independently of acute cognate T cell interactions

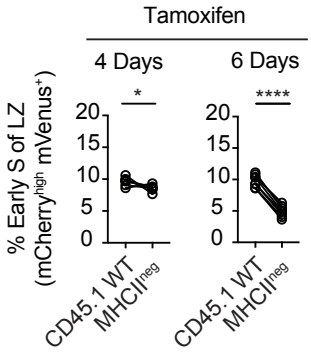

Figure 3.6: Cyclic re-entry in GC LZ B cells 4 days and 6 days after MHCII deletion.
Mixed BM chimeric mice containing WT Fucci2 CD45.1 and CreERT2^{+} MHCII$^{fl/fl}$ Fucci2 CD45.2 cells were immunised with SRBCs (i.p.). Mice received tamoxifen (or vehicle) on day 6 before spleens were harvested on day 10 or 12. Splenic GC LZ B cells (IgD^{low} CD95^{+} GL7^{+} CXCR4^{low} CD86^{high}) were analyzed. Early S phase cells (mCherry^{high} mVenus^{+}) were determined for WT and MHCII-deleted populations. Results are from 2 experiments each containing 4 mice per condition. Analysis, paired two-tailed Student's t test. *p < 0.05, ****p < 0.0001.

the cyclic re-entry model had predicted, acquisition of a threshold level of T cell help is not a pre-requisite for LZ B cells to initiate cyclic re-entry in a given LZ visit.

3.3.3 Validating phenotypes of MHCII-deleted LZ B cells

Given the MHCII-deleted B cells lacked important stimuli from T cells for significant periods of time in the MHCII$^{fl/fl}$ R26-CreERT2^{+} mouse model, various aspects of the phenotypes of these MHCII-deleted early S phase LZ cells in this model need to be validated. The validation includes that MHCII-deletion did not cause undesired loss of GC phenotypes in these GC B cells, the populations we analysed were not DZ B cells contaminating the gate, or that cyclic re-entry initiation was supported by a heterodimer of MHCII complex of two mismatched monomers.

We first wanted to check that the LZ MHCII-deleted cells in our analysis were truly LZ cells and not contaminating DZ cells because some DZ cells have slightly lower MHCII levels. Back-gating the early S phase MHCII-deleted LZ cells and WT

3. Cyclic re-entry initiation can occur independently of acute cognate T cell interactions

LZ cells onto total GC B cells confirmed the similar phenotypic distribution between the two populations with no signs of enrichment of MHCII-deleted populations at the LZ/DZ border region (Fig. 3.7A). Therefore, we can conclude that these MHCII-deleted early S phase cells have bona fide LZ phenotypes. Consistent with this, it is also notable from the Fucci2 MHCII deletion experiments that the early S phase cells expressed LZ-like mCherry levels (reflecting them deriving from a late G1 resting state that is absent from DZs).

Another undesired phenotype we wanted to exclude in the inducible MHCII deletion model is that these MHCII-deleted cells are starting to downregulate genes involved in GC maintenance and are ready to leave GCs. This is because these MHCII-deleted cells had not been able to interact with T cells for a long time, it is possible that they started to lose their GC characteristics. To test if they still possess GC B cell phenotypes, we co-stained well-established GC markers with BrdU/EdU staining in MHCII$^{fl/fl}$ R26-CreERT2^{+}: WT CD45.1 chimeric mice after SRBC immunization and 2-day tamoxifen treatment. The two GC markers we chose were BCL6, which is the gold standard marker for GC B cells, and Ephrin B1, which has also been shown to be a mature GC B cell marker (Kitano et al 2011; Laidlaw et al, 2017). The early S phase MHCII-deleted LZ cells had similar levels of BCL6 and Ephrin B1 when compared with WT LZ cells or total GC B cells, suggesting they were still bona fide GC B cells by the time of analysis (Fig. 3.7B).

One further unwanted possibility that could result in the observation of cyclic re-entry initiation in I-Ab deleted cells was that B cells could present antigens through the unconventional mismatched heterodimers of MHCII complexes to T cells. The MHCII$^{fl/fl}$ locus was derived from 129X1/SvJ mice. The MHCII locus of 129X1/SvJ mice has an *H2-b* haplotype and expresses I-Ab, I-Aa and I-Eb chains from the corresponding *H2-Aa, H2-Ab* and *H2-Eb* genes while the *H2-Ea* gene is inactive, leading to the only functional MHCII complexes being heterodimeric of I-Aa and I-Ab monomers (Hashimoto et al, 2002). The MHCII$^{fl/fl}$ mouse line used in our study was generated by inserting loxP cassettes up and downstream

of exon 1 in the *H2-Ab1* locus. This abolishes the expression of the I-Ab chain in targeted cells, leading to the loss of functional MHCII complexes when crossed to CreERT2 strains followed by tamoxifen treatment. However, there remains an unlikely possibility that these I-Ab knockout B cells can still present antigen derived peptides to T cells through the mismatched I-Aa and I-Eb heterodimer.

To rule out this possibility, cyclic re-entry initiation was measured in a setting where T cells only recognize the peptide in complex with I-Aa/I-Ab MHCII dimers on B cells. We transferred FACS purified SW_{HEL} *Cd79a*-CreERT2^{+} MHCII$^{fl/fl}$ B cells (FACS sorted to ensure no T cells derived from these hosts were not transferred), together with OT-II T cells, into *Tcrb/d*$^{-/-}$ hosts. Recipient mice were then immunized with HEL-OVA in Ribi adjuvant the next day to induce GC responses, and tamoxifen was given on day 6 to induce MHCII deletion, with the responses analyzed on day 8. S phase cells were labelled by 30min BrdU treatment before harvest. The transgenic TCRs in OTII T cells are restricted to recognizing only the $OVA_{223\text{-}239}$ peptide presented on I-Aa/I-Ab MHCII heterodimers, ensuring the I-Ab-deleted cells in this situation did not receive any help from T cells (Barnden et al, 1998). The rate of cyclic re-entry initiation, as measured by the percentage of BrdU^{+} S phase cells in this experiment, showed no change after I-Ab deletions (Fig. 3.7C). Thus, the characterization of the early S phase MHCII-deleted LZ cells confirmed that these cells were truly cycling LZ cells in the GC and that cyclic entry initiation was not detectably supported by T cell help through the interactions of the mismatched MHCII dimers.

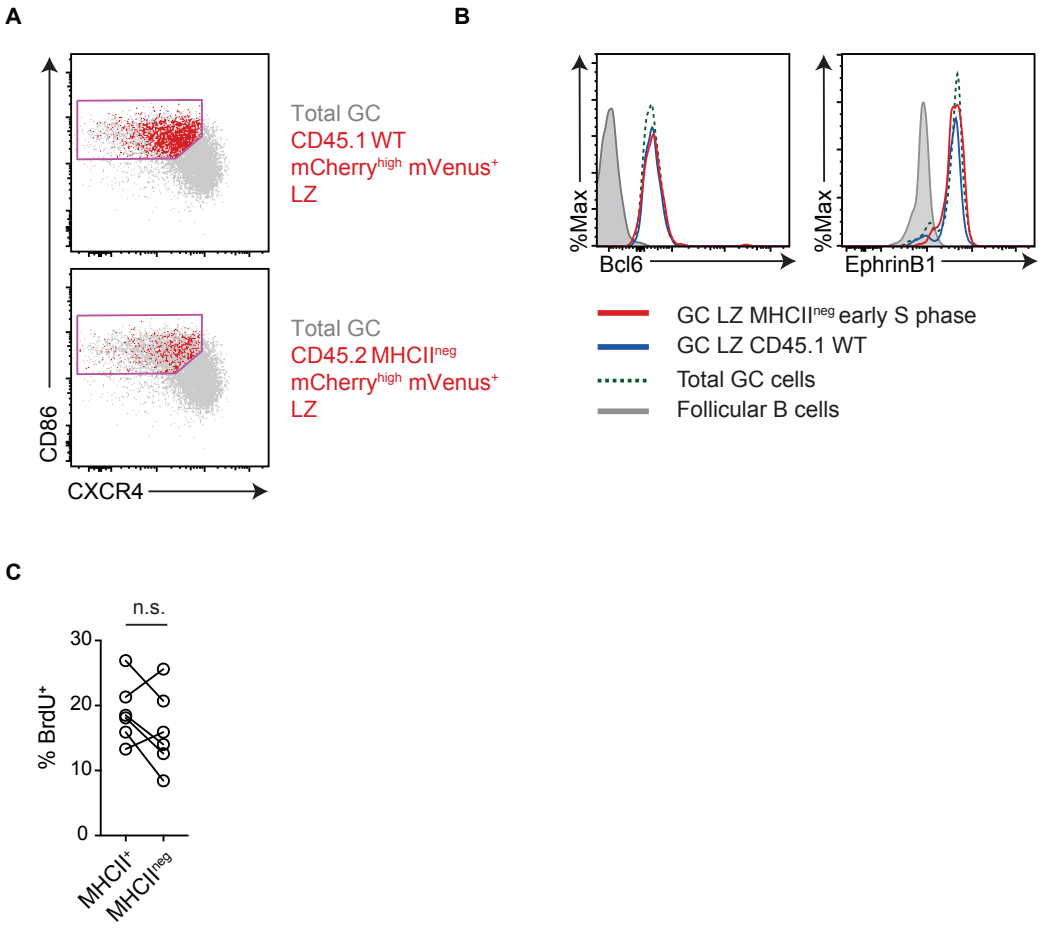

Figure 3.7: Characterizations of MHCII-deleted early S phase LZ cells. (A and B) Mixed BM chimeric mice of WT Fucci2 CD45.1 and CreERT2^{+} MHCII$^{fl/fl}$ Fucci2 CD45.2 cells were immunised with SRBCs (i.p.). Mice received tamoxifen (or vehicle) 48hrs before analysis on day 8. Early S phase WT or MHCII-deleted LZ B cells were backgated onto total GC B cells in (A). (B) Levels of BCL6 and EphrinB1 were compared between different B cell populations. (C) FACS purified SW$_{HEL}$ *Cd79a*-CreERT2 MHCII$^{fl/fl}$ B cells and OTII T cells were co-transferred into sex matched *Tcrb/d*$^{-/-}$ recipients by i.v. injections. These mice were subsequently immunized with HEL-OVA/Ribi and received tamoxifen 43hrs before tissue harvest on day 8. BrdU was administered 30mins before harvest to label S phase cells. Percentages of BrdU+ cells were quantified in MHCII^{+} and MHCII-deleted SW$_{HEL}$ *Cd79a*-CreERT2 MHCII$^{fl/fl}$ GC LZ B cells. Results show representative FACS plots (A and B) or pooled results from 2 experiments each containing 2-4 mice per condition.

3. Cyclic re-entry initiation can occur independently of acute cognate T cell interactions

3.3.4 The decrease in cyclic re-entry initiation after MHCII deletion was not caused by Cre or tamoxifen mediated toxicity

Two-days of MHCII deletion in the MHCII$^{fl/fl}$ R26-CreERT2^{+}: WT CD45.1 chimeric mice led to a noticeable ~20% decrease in the percentage of cyclic re-entry initiating MHCII-deleted LZ cells. We next wanted to further investigate the cause of this reduction, specifically addressing whether it was due to the off-target effects of the Cre recombinase or tamoxifen, and/or it was because these MHCII-deleted cells had lost metabolic reserves and dropped out of GC responses.

Cre recombinase is an efficient and reliable tool for targeted gene manipulation for *in vivo* animal models, however off-target effects from Cre can cause genotoxicity (Kim et al, 2018). At the same time, tamoxifen is a widely used drug for the induction of CreERT2 activity, but it is not an inert drug. It has been reported that tamoxifen can have off-target effects, apart from its primary role as an estrogen receptor modulator (Ma et al, 2015; Finkin et al, 2019). The most relevant off-target effect to our study was that it could enhance c-Myc expression in GCs (Finkin et al, 2019).

To test how Cre toxicity or tamoxifen as a drug is affecting cyclic re-entry initiation, the rate of cyclic re-entry initiation was investigated in the LZ B cells that have active Cre activities and one copy of MHCII gene left, and also in the WT GC B cells with or without tamoxifen treatment. To achieve this, host mice were reconstituted with mixes of CD45.2 MHCII$^{wt/fl}$ R26-CreERT2^{+} BM cells and CD45.1 WT BM cells. Eight weeks after reconstitution, these mice were immunized with SRBCs by i.p. injections and received tamoxifen on day 6. Subsequent 100 mins EdU and 40 mins BrdU treatments were carried out to label cell in different cycle stages before spleen harvest on day 8. There was no evident change in the percentage of early S phase LZ cells (BrdU^{+} EdU^{-}) after tamoxifen treatment in WT population, suggesting tamoxifen alone could not lead to the decrease in LZ S phase entry (Fig. 3.8B). Cyclic re-entry initiation was also not detectably affected

when one copy of the MHCII gene was knocked out in the Cre inducible cells (Fig. 3.8 A and B). This is in contrast to the decrease in the frequencies of the early S phase MHCII-deleted LZ cells we have seen after the same tamoxifen treatment regimen. There have been mixed reports on the level of MHCII protein expression level after knocking out one allele (Yeh et al, 2018). In our model, there was no detectable change in the level of MHCII protein in these MHCII haplo-sufficient cells (Fig. 3.8A). Given the previous observations in Figure 3.5B, these CD45.2 $MHCII^{high}$ R26-$CreERT2^{+}$ LZ cells contained a mixture of quiescent cells with more stabilized MHCII proteins and some cells with more rapid MHCII turnover and cell cycle progression. This mixture of cells may conceal some subtle differences in the changes of cyclic re-entry initiation in the cells that are more active in cell cycle. However, considering the >20% decrease in cyclic re-entry initiation that was observed in MHCII-deleted cells and the ratio of MHCII-deleted cells amongst total CD45.2 $MHCII^{fl/fl}$ R26-$CreERT2^{+}$ at 48 hours tamoxifen treatment, this decrease could not be solely caused by Cre genotoxicity. To conclude, neither Cre mediated genotoxicity nor tamoxifen as a drug could significantly impact the G1-S cell cycle transition in GC LZ B cells. Consequently, the defects in MHCII-deleted cells were likely to be caused by MHCII-deleted cells gradually losing their potential to engage in GC responses.

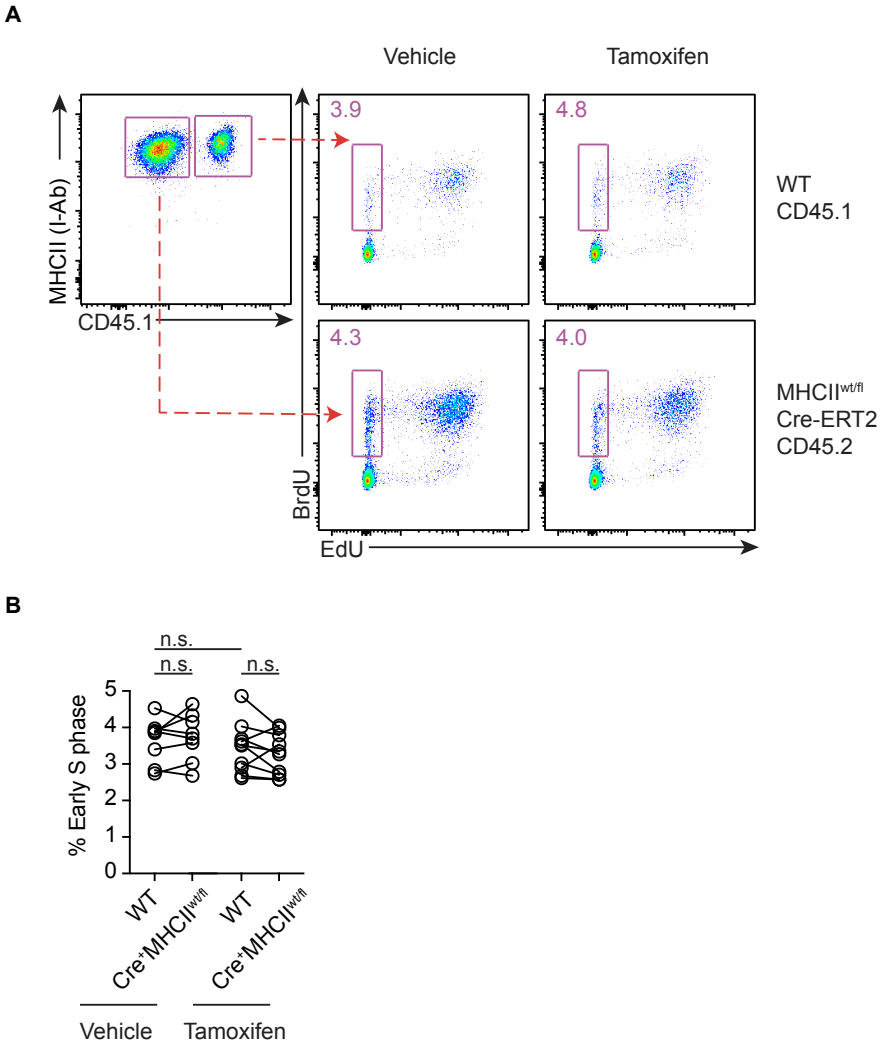

Figure 3.8: Cre or tamoxifen mediated toxicity does not have an evident impact on cyclic re-entry initiation.
Mixed BM chimeric mice with CreERT2^{+} MHCII$^{wt/fl}$ CD45.2 and WT CD45.1 cells were immunized with SRBCs by i.p. injections. These mice received tamoxifen or vehicle on day 6 then EdU and BrdU were injected intraperitoneally 100 mins and 40 mins before spleen harvest on day 8. Splenic GC LZ B cells (IgD$_{low}$ CD95^{+} GL7^{+} CXCR4^{low} CD86^{high}) were analyzed. Early S phase cells (BrdU^{+} EdU^{-}) were identified in both CreERT2^{+} MHCII$^{wt/fl}$ CD45.2 and CD45.1 WT LZ populations after tamoxifen or vehicle treatment (A) and summarized in (B). Results show representative FACS plots (A) or pooled results (B) from 2 experiments each containing 4-6 mice per condition.

3.4 GC B-T interactions are necessary for long term GC participation of B cells

So far, our results showed that LZ B cells do not need to interact with T cells during a particular zonal visit in order to initiate cyclic re-entry, and neither tamoxifen nor Cre-mediated off target effects could negatively impact this process. However, it was well established that T-B interactions are required for long-term GC maintenance and defects in this interaction would lead to GC shrinkage and eventual collapse (Victora et al, 2012).

Consistent with these previously published results, the importance of T cell help in sustaining B cells participation in GC responses was also demonstrated in our model by tracking the frequencies of CD45.2 MHCII-deleted cells in the GC as compared with that of follicular counterparts at various time points after tamoxifen treatment. The MHCII deletion was fast, with the deletion of MHCII completed in 60% of CD45.2 cells in the first 1.5 days post tamoxifen treatment (Fig. 3.9A). Then, MHCII-deleted cells started to be detectably outcompeted from GC responses 2 days post tamoxifen, as shown by the significant reduction of the CD45.2 cells in the GC compared to that of the follicular compartment, followed by greater losses at later time points (Fig. 3.9B). We then investigated if genotoxicity could render cells more susceptible to defects in GC participation, despite them not directly impacting cyclic re-entry initiation. We used control chimeras expressing Cre but without floxed MHCII alleles. 48 hours after tamoxifen, Cre activity alone could lead to a slight but consistent decrease in GC participation (Fig. 3.9C). However, it is not the primary cause of the GC participation defect. Therefore most MHCII-deleted cells probably died from a secondary effect of lacking interactions with T cells and running out of their metabolic reserves. It was difficult to determine the exact time that these MHCII-deleted cells persisted in the GC due to the asynchronous deletion kinetics of MHCII proteins. Considering the GC participation data, it was likely that they would drop out of GC between 2-3 days after MHCII deletion.

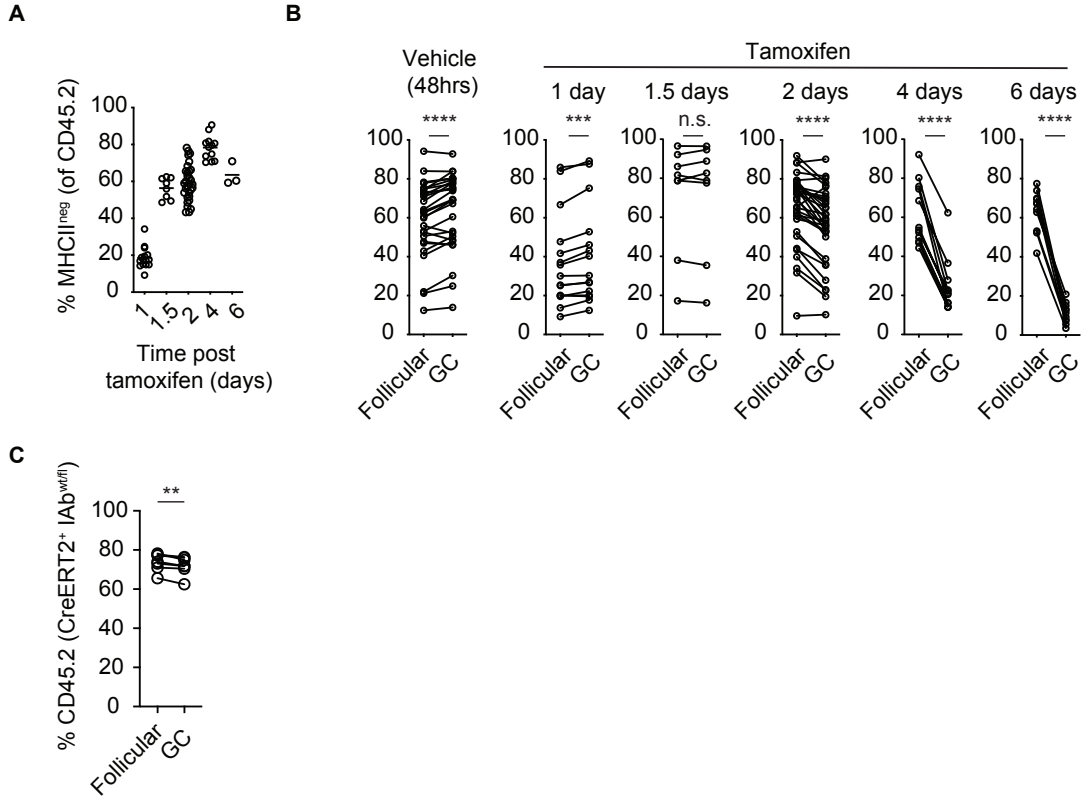

Figure 3.9: GC B cells require T_{FH} cells for long term sustenance .
(A and B) Mixed BM chimeric mice reconstituted with CreERT2^{+} MHCII$^{fl/fl}$ CD45.2 and WT CD45.1 cells were immunized with SRBCs (i.p.). These mice received tamoxifen or vehicle at indicated time points to induce MHCII deletion before tissue harvest on day 8. Splenic GC LZ B cells (IgD^{low} CD95^{+} GL7^{+} CXCR4^{low} CD86^{high}) were analyzed. (A) Frequencies of MHCII-deleted LZ cells were enumerated at various time points post tamoxifen. (B) Percentages of CreERT2^{+} MHCII$^{wt/fl}$ CD45.2 were determined for both follicular and GC compartments at different time points after tamoxifen or vehicle. (C) Day 8 SRBC induced GC responses were analyzed from mixed chimeric mice containing CreERT2+ MHCII$^{wt/fl}$ CD45.2 and WT CD45.1 cells, with 48hr tamoxifen treatment prior to analysis. Frequencies of CD45.2 cells were determined for both follicular and GC compartments. Results were pooled from 2-10 experiments each with 3-5 mice per condition. Analysis, paired two-tail student's T test, **p $<$ 0.001, ***p $<$ 0.001, ***p $<$ 0.0001.

3. Cyclic re-entry initiation can occur independently of acute cognate T cell interactions

3.5 Conclusion

The cyclic re-entry model has explained nicely how stringent positive selection takes place in GCs by only favouring the survival and expansion of the highest affinity GC B cell clones. However, recent emerging experimental evidence revealed the co-existence of B cell clones with varying BCR affinity in GCs and extremely complex mutation trajectories, indicating the permissiveness during the selection process. Prompted by these observations, we decided to re-evaluate this model and examine the key assumptions.

The first assumption we investigated was the presumed acute dependence of T_{FH} cells for cyclic re-entry initiation. We predicted that, given the central importance of B-T interactions in GC positive selection, failing to interact with T cells should lead to these B cells failing to initiate cyclic re-entry. However, as opposed to our prediction, we found neither ablating T cells in established GCs, nor deleting MHCII from a subset of GC B cells, completely prevented LZ cells from transitioning from late G1 into S phase. This demonstrates the cyclic re-entry process could be initiated through T cell independent mechanisms. Concurrently, T cells were still required for long term GC sustenance, with the observation that unhelped cells started to fall out of GC responses as early as two days after MHCII deletion followed by rapid declination in the frequencies of MHCII-deleted cells afterwards.

Our study has its own limitations. Cyclic re-entry starts from S phase re-entry, followed by upregulation of DZ phenotype and physical movement back to DZ. Here, we focused on the transition from G1 to S phase, which is the first and most trackable step during cyclic re-entry. However, limited by the tools, whether these unhelped cells ultimately migrate back to DZ after re-entering S phase to complete cyclic re-entry remains to be proven. But, pending these caveats, our results argue that cyclic re-entry initiation is not acutely sensitive to T cell help, whereas long-term GC maintenance requires functional T-B interactions. The limitations and possible cyclic re-entry mechanisms will be discussed in detail in Chapter 6.

3. Cyclic re-entry initiation can occur independently of acute cognate T cell interactions

Given these findings of the dispensable role of T cells in driving cyclic re-entry but yet the small frequencies of LZ cells initiating this process at any time, we next consider if cyclic re-entry is limited by general competition in germinal centres with B cells competing for resources available such as antigens or cytokines, which we continued to tackle in Chapter 4.

Chapter 4

Cyclic re-entry initiation is not detectably restricted by competition

Contents

In the last chapter, we tested one of the central hypotheses of the cyclic re-entry model for GC B cell positive selection and revealed that cyclic re-entry initiation in the LZ B cells was not acutely dependent on them receiving a threshold level of T cell help in a given LZ visit. Instead, cyclic re-entry initiation was not acutely impaired when the vast majority of the T cells (>90%) were removed from GCs or when MHCII was deleted from the GC B cell surface, suggesting the absence

of T cell participation in this process.

In the seminal studies carried out by Victora et al in 2010, the dynamics of GC B cell's zonal movement were quantified with intravital microscopy and a strong bias of DZ to LZ movement was observed, with about 50% of DZ cells migrating to LZ cells and less than 10% of LZ cells return to the DZ over a period of 6 hours (Victora et al, 2010; Meyer-Hermann et al, 2012). This observation implies there could be a selection bottleneck occurring at LZ to DZ transition, and given it is not restricted by T cell help, the selection could be driven by competition towards other resources in GCs.

One of the next possible candidates to drive cyclic re-entry is antigen-stimulated BCR signalling. In LZs, antigens are deposited on FDCs in the form of immune complexes. B cells endocytose antigens with BCR, and this same process also stimulates downstream BCR signalling. When using Nur77-GFP as a reporter for recent BCR signalling events, a positive correlation between GFP level and c-Myc was observed (Mueller et al, 2015). Although it is likely that cells with strong BCR signalling acquire larger doses of T cell help due to their better presentations of antigens, it remains possible that BCR signalling could contribute to the induction of c-Myc and later cyclic re-entry. Later, anti-BCR stimulation was shown to drive c-Myc expression in a small fraction of GC B cells (Luo et al, 2018). Therefore, it is possible that some LZ B cells had strong BCR stimulation through preferential antigen access which would be sufficient to drive their cyclic re-entry. Other possible stimulants in GCs that could potentially drive the initiation of cell cycle re-entry would be cytokines or other small molecule metabolites. All these stimuli mentioned above are not unlimited in their amount and it is possible that cyclic re-entry still requires B cells to receive some of these stimuli. If this is true, then the selection bottleneck still resides in LZs, but is independent of T cells. As such, in this chapter, we continued to investigate whether cyclic re-entry is a competitive event and the selection bottleneck in the GCs but with the cells competing for T cell-independent inputs.

4.1 Establishing a genetic mouse model to manipulate GC B cell numbers in an unbiased manner

The current cyclic re-entry model predicts that most of the LZ cells are resting in terms of their cell cycle stages, and that they are intensively competing with each other to accumulate stimuli to transition back into the active cell cycle again. Only very few LZ cells could receive a threshold level of stimulation, allowing them to initiate cyclic re-entry, as shown in the schematic illustration in Figure 4.1A (left). If this model is true, when the competition in the LZ is relieved by deleting a large number of the blue GC B cells, the remaining yellow GC B cells should then be capable of accessing more of those stimulants in the GCs regardless of their nature. Consequently, the proportion of the yellow cells that can pass the selection bottleneck is expected to increase (Fig. 4.1A, middle). On the contrary, if cyclic re-entry is not restricted by any form of intra-GC competition, then the percentage of yellow cells initiating cyclic re-entry should remain the same as that in the undisturbed setting even when there are fewer competitors around (Fig. 4.1A, right).

To distinguish between the two potential outcomes, we generated a mouse model that would permit us to experimentally reduce competition without bias for any particular factors, and test if cyclic re-entry initiation rates were affected in the remaining cells. This was achieved by first crossing $AID^{wt/Cre}$ mice to R26-loxp-stp-loxp-DTR mice (Robbiani et al, 2008; Buch et al, 2005). AID (*Aicda*) expression is restricted to GC B cells, thereby limiting Cre activities to these cells, and resulting in the expression of DTR on cell surfaces. As a result, this $AID^{wt/Cre}$ R26-loxp-stp-loxp-DTR mouse model allows specific deletion of GC B cells with DT treatment. Next, mixed BM chimeric mice containing 80% $AID^{wt/Cre}$ R26-loxp-stp-loxp-DTR BM and 20% Fucci2 BM cells were generated to study if the initiation of cyclic re-entry could be enhanced when the competition was relieved in LZs.

4. Cyclic re-entry initiation is not detectably restricted by competition

These mice were immunized with SRBCs to induce polyclonal GC responses and received DT treatments for indicated periods of time before spleen harvest on day 8. In these chimeras, GC B cell ablation was very rapid, possibly completed within the first 8 hours after DT treatment because three-quarters of GC B cells were ablated in this period of time and no further reduction was observed (Fig. 4.1B, right). The deletion was also very efficient and specific, because there were significant decreases in the percentage of DTR^{+} ($Fucci2^{neg}$) GC B cells at both time points after DT treatment (Means, No DT: 5.4% vs 8hrs DT: 0.7% of total $B220^{+}$ cells) while the frequencies of DTR^{neg} cells were not affected (Fig. 4.1B, left and middle).

Given our goal is to universally reduce the same percentage of competition amongst all GCs, we needed to rule out the possibility that some GCs might have been preferentially more affected than others. Because the mice we used are mixed BM chimeras, there may be variations in the mixing ratios within each particular GC due to different frequencies of the two types of cells initially seeding each GC or clonal burst of one type of cells during the GC maturation process. In extreme situations, this could be that some GCs were completely deleted while others remained unaffected. To formally exclude this possibility, GCs were visualized with IHC staining after DT treatment in spleen sections. In cryopreserved spleen sections, the B cell follicles were demarcated with the brown IgD stain and GCs were marked with the blue GL7 stain. The IHC staining revealed that DT treatment led to a general reduction in sizes across all the GCs (Fig. 4.1C). GC areas were also quantified by Image J, and we confirmed there was an overall reduction in the mean (No DT: 31752 um^2 vs DT: 9270 um^2), and the spread of GC sizes, which was consistent with the FACS data, showing similar mixing ratios amongst all GCs (Fig. 4.1D). Therefore, we first confirmed this partial B cell ablation model is highly efficient and specific in reducing GC competition by deleting DTR^{+} B cells.

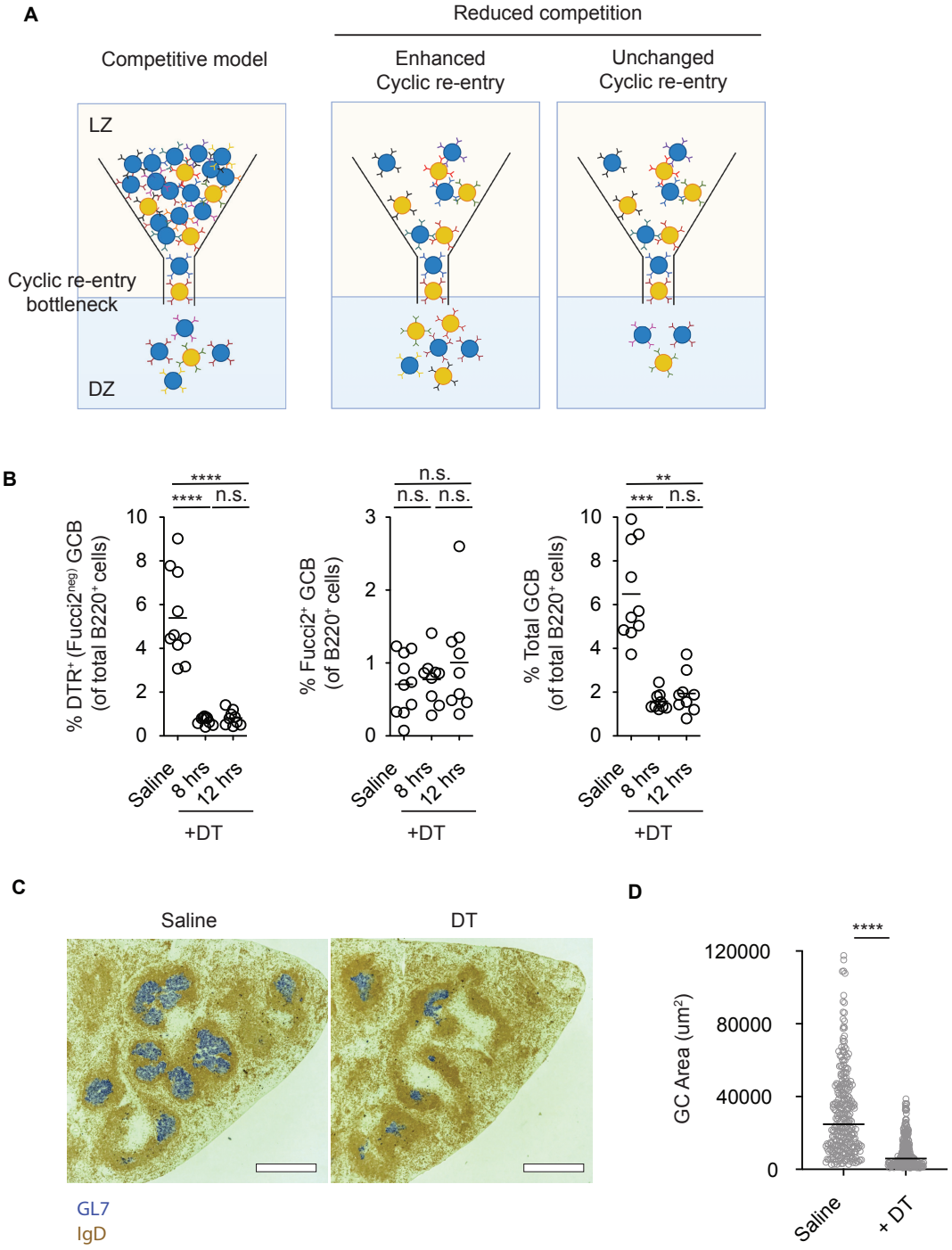

Figure 4.1: Establishment of a system to achieve unbiased depletion of GC B cells.
(A) Schematic illustration of potential outcomes after reducing LZ GC B cell numbers. The current model (left) predicts that LZ cells need to compete intensively to initiate cyclic re-entry. If the competition is relieved by reducing the number of competing LZ B cells (blue), a larger fraction of the remaining cells (yellow) is then expected to pass the cyclic re-entry bottleneck (middle). If cyclic re-entry initiation is independent of competition, then cyclic re-entry rates would remain unaffected (right).

Figure 4.1: (B) Mix BM chimeric mice containing 80% AID-DTR and 20% Fucci2 BM cells were immunized with SRBCs (i.p.). Mice received DT or saline at indicated time points before tissue harvest on day 8. Splenic GC LZ B cells (IgD^{low} $CD95^{+}$ $GL7^{+}$ $CXCR4^{low}$ $CD86^{high}$) were analyzed. (B) Frequencies of DTR^{+} GC B cells (left), $Fucci2^{+}$ GC B cells (middle) and total GC B cells (right) were determined after DT treatment. (C) IHC sections of spleens after DT treatment and GCs were identified by IgD and GL7 stain (scale bar, 550 um) with GC areas quantified and summarized in (D); each point represents a single GC. Results are representative (C) or pooled (B, D) from 3 independent experiments each with 3-4 mice per condition. Analysis, One way ANOVA with Tukey's multiple comparisons (B, left and middle), Kruskal-Wallis with Dunn's multiple comparisons (B, right), Mann-Whitney (D). **p <0.01, ***p < 0.001, ****p < 0.0001.

4.2 T_{FH} cell phenotypes remain relatively unaffected after partial B cell ablation

Now that we had established a system to effectively manipulate GC B cell numbers, with >80% of target population depleted within 8 hours after treatment, another important aspect we needed to assess in this model was the effect of such a significant and abrupt loss of GC B cells on the phenotype and location of the T_{FH} cells. They have long been considered the main driving force for positive selection in the GCs and are of vital importance to GC sustenance. Despite their regulation of GC B cells, B cells have been shown to involve in the long-term maintenance of T_{FH} cells (Baumjohann et al, 2013).

To assess the T_{FH} phenotypes, we continued to analyze the GC responses as outlined in Section 4.1. The expression profile of T_{FH} cell characteristic markers was first examined. We gated the GC T_{FH} as $B220^{-}$ $CD4^{+}$ $TCRb^{+}$ $CD44^{+}$ $CD62L^{low}$ $PD1^{high}$ $CXCR5^{high}$ lymphocytes. GC T_{FH} cells have been reported to be amongst the highest level of PD1 and CXCR5 in the total T_{FH} population and the gates were set accordingly (Fig. 4.2A) (Shulman et al, 2013). Quantification of the T_{FH} cell frequencies as percentages of $CD4^{+}$ T cells showed no evident change at any time point after partial B cell ablation (Fig. 4.2B). As expected, with a 75% decrease in the number of GC B cells, there was an increase in the GC B-T_{FH} ratio, increasing from 5:1 to 2:1, (Fig. 4.2C).

4. Cyclic re-entry initiation is not detectably restricted by competition

However, with such strong ablation leading to massive physical GC shrinkage, it was plausible that some T_{FH} cells retained their phenotypes but had left GCs. To reveal the locations of T_{FH} cells, immunofluorescence (IF) was carried out on cryosections of the same spleens in which T_{FH} cell FACS analyses were performed. The sections were stained with IgD and PD1, which were used to label B cell follicle and T_{FH} cells, respectively. After GCs shrunk 2/3 in their sizes following DT treatment, there was an increase in T_{FH} cell density in the GCs without evident staining of T_{FH} cells in other compartments in the section, reflecting a minimal movement of T_{FH} cells outside of follicles (Fig. 4.2D). However, quantifications of the T_{FH} cells per unit GC area revealed that the increase in T_{FH} cell density in GCs was smaller than what was determined by FACS analysis (Fig. 4.2E, left). This could be partially accounted for by the non-significant small increase in the T_{FH} cells in the follicular mantle region (Fig. 4.2E, middle). It was previously reported that T_{FH} cells were not confined to a particular GC, instead, they were shown to migrate to neighbouring GCs, reflecting the mobility of the T_{FH} cells (Shulman et al, 2013). Similarly, it was possible that T_{FH} cells could traffic between GC and mantle region, and remain accessible to B cells to provide help. Moreover, to formally determine if the T_{FH} cells had migrated out of follicle regions, the total numbers of T_{FH} cells within each follicle were also quantified, and there was a small decrease after DT treatment but should not significantly impact the fidelity of the model (Fig. 4.2E, right).

In conclusion, the $AID^{wt/Cre}$ R26-loxp-stp-loxp-DTR mouse model allows rapid and specific deletion of a tuneable fraction of B cells from each GC, with the last part achieved by mixing with different ratios of WT cells. In addition, this partial B cell ablation resulted in an increased B-T ratio, potentially leading to more frequent B-T interactions, making it a suitable model to study the role of competition in various aspects of GC biology.

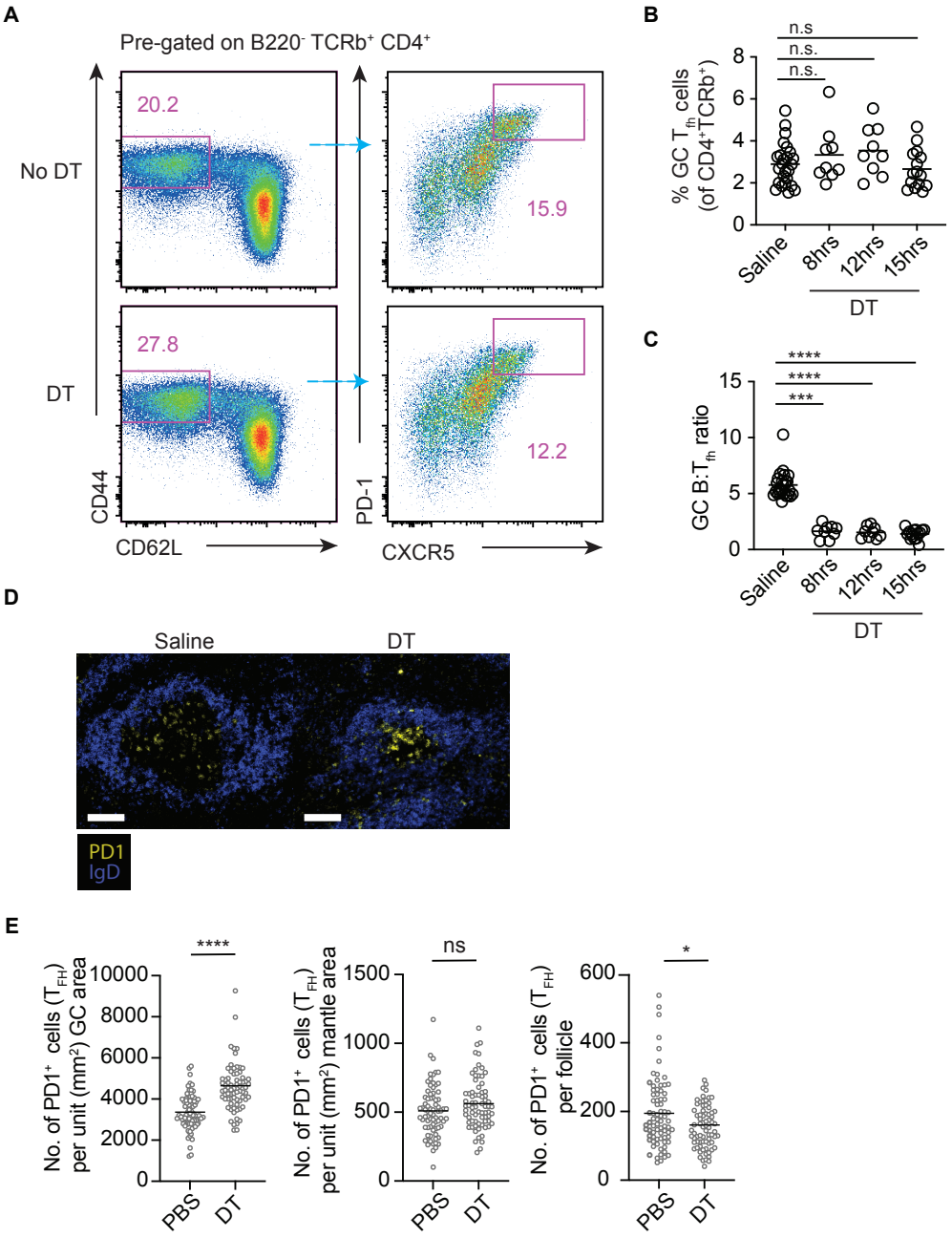

Figure 4.2: Establishment of a system to achieve unbiased depletion of GC B cells.
Mix BM chimeric mice (80% AID-DTR and 20% Fucci2) were immunized with SRBCs. Mice received DT or saline at indicated time points before analysis on day 8. (A) T_{FH} cells were identified as B220$^-$ CD4$^+$ TCRb$^+$ CD44$^+$ CD62L^{low} PD1^{high} CXCR5^{high} and frequencies of T_{FH} cells after various time points of DT treatment were summarized in (B). (C) GC B:T_{FH} ratios were determined for various time points after DT, with the vehicle treatment at 8hrs. (D) Representative spleen IF sections 15hrs after DT treatment to quantify the number of PD1$^+$ cells per unit GC area. Results are representative (A, D) or pooled (B, C, E) from 2-6 independent experiments each with 2-4 mice per condition. Analysis, Kruskal-Wallis one-way ANOVA with multiple comparisons (B, C), Mann-Whitney test (E). *p <0.05, ***p < 0.001, ****p < 0.0001.

4.3 Cyclic re-entry initiation is not restricted by any form of general competition within GCs

In the last two sections, the ablation efficiency and phenotypes of GC B cells and T_{FH} cells were confirmed in the model, so we next investigated if cyclic re-entry initiation was enhanced when there were fewer competitors around. To achieve this, we utilized the same BM chimeras mentioned in the first section that were made with 80% $AID^{wt/Cre}$ R26-loxp-stp-loxp-DTR BM cells and 20% WT CD45.2 Fucci2 cells. These BM chimeras were immunized with SRBCs and received DT or vehicle treatment 12 hours before analysis on day 8. This time point was chosen because the deletion was almost complete in the first 8 hours, and a further 4 hours was added for any changes in the cell cycle progression to become phenotypically obvious. The LZ B cells were identified as $CXCR4^{low}$ $CD86^{high}$ GC B cells, but because in these chimeras, both the WT Fucci and $AID^{wt/Cre}$ R26-loxp-stp-loxp-DTR BM cells were CD45.2, the non-ablatable population in the LZ was identified as the total Fucci2 fluorescent LZ B cells (Fig. 4.3A). Subsequently, cells initiating cyclic re-entry from this population were gated as $mCherry^{high}$ $mVenus^{+}$ (Fig. 4.3B). Surprisingly, the frequencies of early S phase cells in LZ non-ablatable cells did not change even after removing >75% of competing LZ B cells, strongly suggesting that cyclic re-entry initiation was not restricted by intra-GC competition (Fig. 4.3C).

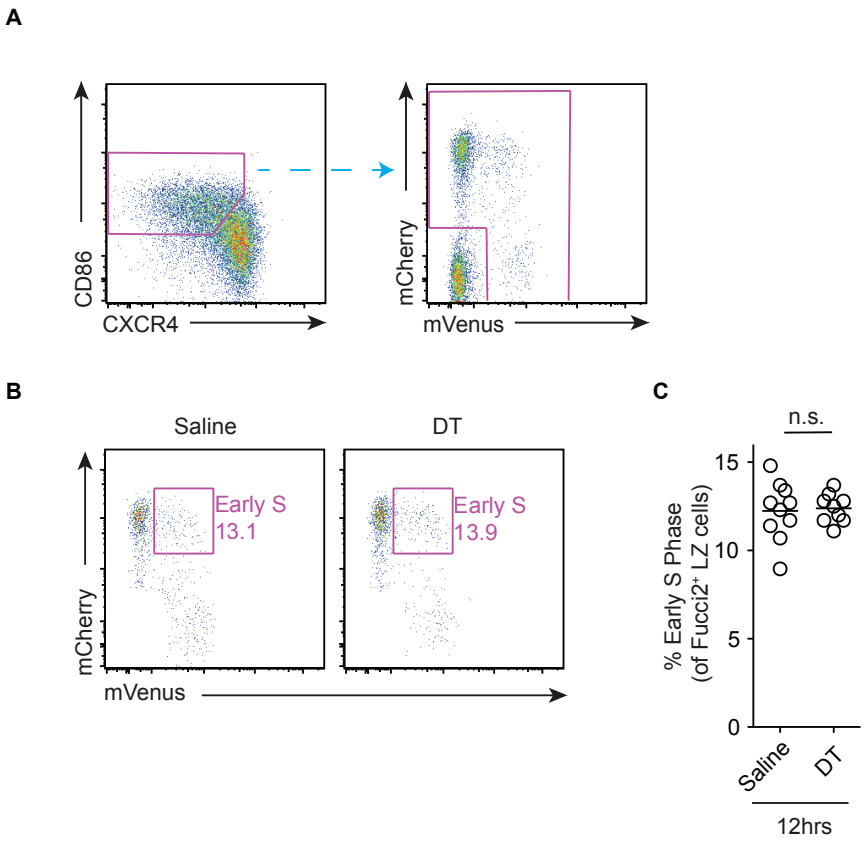

Figure 4.3: Cyclic re-entry is insensitive to the reduction of general competition in the GCs
Mix BM chimeric mice containing 80% AID-DTR and 20% Fucci2 BM cells were immunized with SRBCs (i.p.). Mice received DT or saline at indicated time points before tissue harvest on day 8. Splenic GC B cells (IgD^{low} $CD95^{+}$ $GL7^{+}$) were identified. (A) GC LZ B cells ($CXCR4^{low}$ $CD86^{high}$) and $Fucci2^{+}$ ($mCherry^{+}$ and/or $mVenus^{+}$) cells were identified. (B) Early S phase cells were identified as $mCherry^{high}$ $mVenus^{+}$ GC LZ B cells and frequencies of early S phase cells were enumerated in (C). A and B are representative FACS plots and C is pooled results of 3 experiments, with 3-4 mice examined per group per experiment. Analysis, (C) unpaired two-tailed Student's T test.

To further confirm cyclic re-entry initiation was not restricted by competing LZ B cells, we assessed the G1-S transition with BrdU incorporation as an alternative S phase labelling approach. Similar chimeric mice with 80% $AID^{wt/Cre}$ R26-loxp-stp-loxp-DTR CD45.2 cells and 20% WT CD45.1 cells were utilized for this experiment. These mice received a longer DT treatment of 15 hours on day 7 after SRBC immunization and then received BrdU in the last 30 mins prior to tissue harvest on day 8. Then percentages of S phase cells ($BrdU^{+}$) in both LZ non-deletable

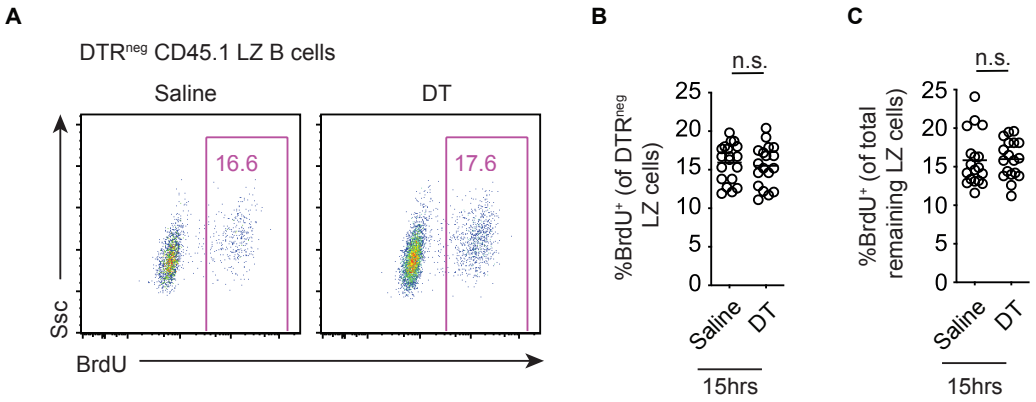

Figure 4.4: Frequencies of LZ S phase cells remain unchanged after partial GC B cell ablation.
Mix BM chimeric mice containing 80% AID-DTR and 20% Fucci2 BM cells were immunized with SRBCs (i.p.). Mice received DT or saline 15hrs and BrdU 30mins before analysis on day 8. Splenic GC B cells (IgD^{low} $CD95^{+}$ $GL7^{+}$) were identified. Frequencies of $BrdU^{+}$ cells were determined for both DTR^{neg} LZ cells (A and B) and total remaining LZ cells (C). Results were representative FACS plots (A) or pooled from 4 experiments each with 4-5 mice per condition. Analysis, (B and C) unpaired two-tailed Student's t test.

population and total remaining LZ cells were identified. Consistent with the previous Fucci2 data, there was no change in the percentage of S phase LZ non-ablatable cells after significant GC B cell ablation (Fig. 4.4A and B). Meanwhile, the same results held up for the total remaining LZ cells (Fig. 4.4C). To summarize, these data suggested that cyclic re-entry initiation was not detectably restricted by any form of general competition in the GC. These results also supported previous conclusions in Chapter 3 that T cells were not limiting for cyclic re-entry initiation from a different angle, because there was an elevated B-T ratio after partial B cell ablation, but this did not lead to a subsequent increased rate of S phase re-entry.

4.4 GC B cells are not detectibly competing for access to antigens

In the last section, cyclic re-entry initiation was shown not to be detectably limited by intra-GC competition for antigen or any other factors. However, access

to antigens may still be a highly competitive process given that sustained antigen availability has been reported to promote the duration of GC responses (Tam et al, 2016; Lee et al, 2022). Although GC B cells do not directly restrict each other's access to antigens, the availability of antigens may still be limiting and B cells can only acquire them through a competition based on their BCR affinity. If antigen availability is indeed limiting in the GC, then we should be expecting more of the cells to encounter antigens and experience BCR stimulation once the competition has been relieved.

To test this hypothesis, a reporter is required to record recent BCR signalling events, which can be used as a surrogate for measuring antigen encounter and uptake. Nur77 has been identified earlier as an orphan receptor and is upregulated rapidly following BCR stimulation (Mueller et al, 2015). The Nur77-GFP transgenic mouse model can therefore be used as a readout for *in vivo* BCR signalling (Zikherman et al, 2012). Then the question now becomes whether there are more of the Nur77-GFP^{+} LZ cells when the competitor cells are depleted from the responses.

Thus, mixed BM chimeras were made with 80% AID$^{wt/Cre}$ R26-loxp-stp-loxp-DTR BM and 20% Nur77-GFP CD45.1 BM cells. These chimeric mice were then rested for 8 weeks before they were immunized with SRBCs. DT was administered 15 hours before analysis on day 8 post-immunization. Consistent with the previous reports that DZ is the site for cell division and LZ is the site for antigen uptake and presentation, there were more Nur77-GFP^{+} cells in LZs, indicating more frequent BCR signalling events occurring in this zone (Fig. 4.5A). However, when the majority of DTR expressing B cells were deleted from GCs, there was no evidence of Nur77-GFP^{+} cells accumulation in LZs, suggesting there is no direct competition for antigens in LZs (Fig. 4.5B).

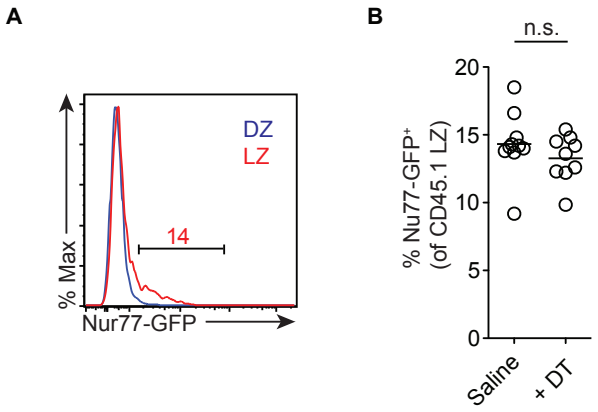

Figure 4.5: There is no evident change in frequencies of Nur77-GFP$^+$ cells following partial GC B cell ablation.
Mix BM chimeric mice containing 80% AID-DTR CD45.2 and 20% Nur77-GFP CD45.1 BM cells were immunized with SRBCs (i.p.). Mice received DT or saline 15hrs before analysis on day 8. (A) Representative FACS plots of Nur77-GFP$^+$ cells identified in both LZs and DZs. (B) Frequencies of LZ Nur77-GFP$^+$ cells were enumerated after DT treatment. Results were representative (A) or pooled (B) from 2 independent experiments each with 4-5 mice per condition. Analysis was done with unpaired two-tailed Student's t test.

4.5 GC B cell proliferation speed is positively associated with BCR affinity.

So far, we have demonstrated cyclic re-entry initiation could occur at relatively normal frequencies despite acute changes in T cell availability, MHCII level and general competition as opposed to what the cyclic re-entry model predicts, that this step should serve as the barrier for positive selection in affinity only allowing the highest affinity cells to pass. This particular assumption in the cyclic re-entry model was proposed based on previous observations that high affinity cells are capable of acquiring more antigens and hence receiving better quality and/or larger quantities of T cell help. However, it is also possible that if cyclic re-entry initiation is restricted by a certain threshold in BCR signalling level, then high affinity cells are still at an advantage because more frequent acquisition of antigens could lead to more chances of BCR stimulation. To address these hypotheses, we first wanted to investigate if high affinity cells are more prevalent in the cyclic

re-entry initiating population in the LZ.

To achieve this, we would need an approach to identify differing BCR affinities on GC B cells. We utilized the SW_{HEL} mouse model, in which B cells express BCR specific for hen egg lysozyme (HEL), due to their carrying a heavy chain variable region "knock-in" and a transgenic HEL specific Igkappa light chain. SW_{HEL} BCRs have a high affinity for HEL but initially limited affinity for HEL^{3X}, a variant of HEL with three point mutations (R21Q, R73E, and D101R) (Phan et al, 2003). However, if immunized with SRBCs conjugated to HEL^{3X}, the SW_{HEL} BCRs could subsequently undergo SHM in GCs to acquire a specific Y53D point mutation to increase affinity for HEL^{3X} by ~80 fold (Phan et al, 2006). High and low-affinity SW_{HEL} cells against HEL^{3X} can be easily distinguished by staining with sub-saturating amounts of fluorescently labelled HEL^{3X} protein.

To establish SW_{HEL} GC responses, we first adoptively transferred ~$1x10^5$ HEL-specific SW_{HEL} B cells into congenic sex-matched WT recipients and then immunized them with HEL^{3X}-SRBCs. The reason only a relatively small number of HEL specific cells were transferred is to mimic the physiological frequency of naïve B cells with particular antigen specificity. As such, only the SW_{HEL} cells could enter responses, and the non-HEL binding cells were outcompeted by endogenous B cells from the host. Given only a small fraction (~10%) of the transferred B cells were HEL binding, we first assessed if we were analyzing the antigen specific SW_{HEL} response as opposed to the response by co-transferred WT B cells responding to epitopes on the SRBC scaffold. We substituted HEL^{3X}-SRBCs with SRBCs alone for immunization, and demonstrated that SRBCs alone could not drive transferred SW_{HEL} cells into GCs (Fig. 4.6, A and B). To further confirm the cells in our analysis are HEL specific SW_{HEL} cells, we have also co-stained GC B cells with HEL-AF488 and HEL^{3X}-AF647, showing both HEL^{3X+} and HEL^{3X-} cells were all HEL binding (Fig. 4.6C).

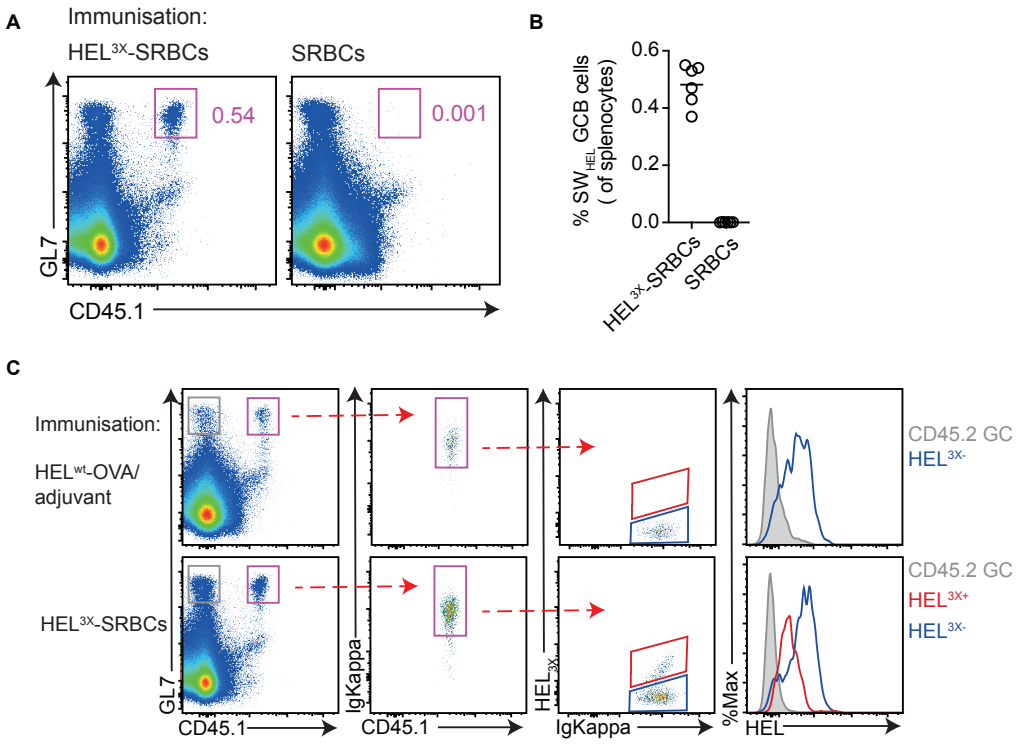

Figure 4.6: All SW_{HEL} GC B cells are responding to HEL^{3X} antigen after HEL^{3X}-SRBC immunisation.
SW_{HEL} CD45.1 B cells were transferred to WT CD45.2 hosts that were subsequently immunised with HEL^{3X}-SRBCs/LPS or SRBCs/LPS (without HEL^{3X}), with analysis of splenic responses on day 8. (A) SW_{HEL} GC B cells (CD45.1, $GL7^{+}$) were gated as percentages of total splenocytes and enumerated in (B), with each dot representing an individual mouse. (C) The same SW_{HEL} adoptive transfer and HEL^{3X}-SRBC immunization regimen, with HEL^{3X} staining control mice also receiving OTII cells and immunization with HEL-OVA/Ribi. Co-staining of HEL-AF488 and HEL^{3X}-AF647 on the SW_{HEL} GC B cells. Results were representative (A, C) or pooled (B) from 2 independent experiments each with 3 mice per condition.

Then, SW_{HEL} mice were crossed to Fucci2 mice to allow tracking of cyclic re-entry patterns of GC B cells with varying affinity. Again, ~10^5 HEL-binding SW_{HEL} Fucci2 B cells were transferred into congenic WT mice by i.v. injections. Mice were immunized i.p. with HEL^{3X}-SRBCs the next day and spleens were harvested on day 8 or 9. We also immunized mice that received SW_{HEL} cells with HEL^{wt}-SRBCs as staining control for HEL^{3X} gating. SW_{HEL} GC LZ B cells (CD45.1, $GL7^{+}$, $CXCR4^{low}$ $CD86^{high}$) were first analysed. Subsequent gatings with different levels of mVenus and mCherry allowed the identification of late G1 and early S phase populations in SW_{HEL} GC LZ B cells. Then, any cells with non-detectable levels of

BCR were excluded from the analysis based on surface Igkappa level. Frequencies of high and low affinity cells were determined in each population by gating on HEL^{3X+} and HEL^{3X-} cells using the gates set with HEL^{wt}-SRBCs immunized GC B cells (Fig. 4.7A). Similar analysis was also carried out in SW_{HEL} GC DZ B cells but with a lower mCherry gate accommodating DZ cells that were transitioning into S phase with a shorter G1 stay (Fig. 4.7B).

Consistent with the hypothesis, HEL^{3X+} cells were more enriched in the early S phase population in the LZ, i.e., the cells that initiated cyclic re-entry, compared with those in the resting late G1 phase. This suggests that higher affinity cells are more likely to initiate cyclic re-entry from LZ. However, the DZ early S phase population showed a similar enrichment of high affinity cells in the early S phase population. Thus, these two pieces of evidence are revealing HEL^{3X+} higher affinity cells are overall in a higher proliferative state so are progressing through the cell cycle faster, and not just being preferentially selected in the LZ (Fig. 4.7C).

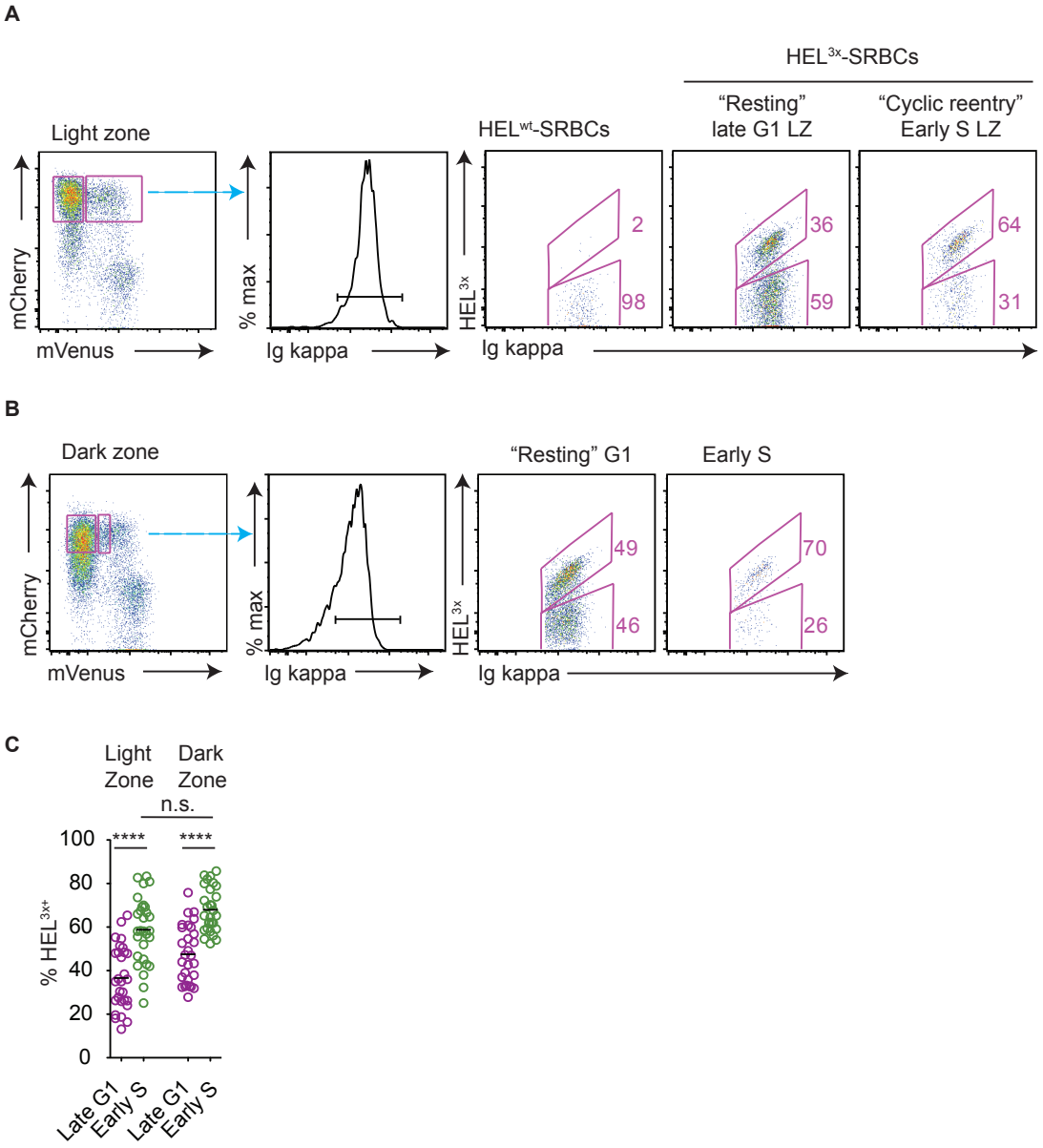

Figure 4.7: Higher affinity cells are proliferating faster in both LZs and DZs. ~1x10^5 SW_{HEL} Fucci2 CD45.1 cells were transferred into congenic CD45.2 sex-matched recipients. Hosts were then immunized with HEL^{3X}-SRBCs/LPS or HEL^{wt}-SRBCs/LPS followed by the subsequent analysis of SW_{HEL} GC responses on day 8 or 9. SW_{HEL} GC B cells (CD45.1, $GL7^+$) were analyzed. (A) SW_{HEL} GC LZ cells (CD45.1, $GL7^+$, $CXCR4^{low}$, $CD86^{high}$) were identified and late G1 and early S phase cells were gated. Igk^+ cells were further gated for each population. Frequencies of HEL^{3X+} and HEL^{3X-} cells were identified for the Igk^+ population for each cell cycle stage. The HEL^{3X} gating was set up by the control mice that were immunized with HEL^{wt}-SRBCs/LPS. (B) Representative plots of the same analysis that was done for DZ ($CXCR4^{high}$ $CD86^{low}$) cells. (C) Summary of results pooled from 7 experiments each with 3-5 mice. Analysis, (C) RM one-way ANOVA with Tukey's comparisons. ****$p < 0.0001$.

4.6 Higher affinity cells reserve the proliferative advantage even after losing interactions with T_{FH} cells

Although cyclic re-entry is not directly associated with B cell's recent acquisition of T cell help, the accumulation of T cell help may still confer advantages to GC B cells for them to be favoured at this step. To test the possibility that T cells are still the major driving force for the enrichment of higher affinity cells initiating cyclic re-entry, a mouse model that allows BCR affinity discrimination and concurrent disruption of T-B interactions was utilized. The mouse model was SW_{HEL} *Cd79a*-CreERT2^{+} MHCII$^{fl/fl}$ mice (Hobeika et al, 2015; Moran et al, 2018). In combination with EdU labelling, this mouse model allows us to track the correlation between BCR affinity, cyclic re-entry and the ability to interact with T cells. A small number (~1x10^{5}) of HEL-specific *Cd79a*-CreERT2^{+} MHCII$^{fl/fl}$ SW_{HEL} B cells were transferred into congenic hosts and then immunized with HEL^{3X}-SRBCs the next day. Mice received tamoxifen 2 days and EdU 30 mins before they were sacrificed, respectively. Notably, there was similar enrichment of HEL^{3X+} cells in S phase population irrespective of whether they were MHCII^{high} or MHCII-deleted in the GC LZs (Fig 4.8). This observation implied that the proliferative advantage that higher affinity cells in the GCs showed in the last section was not sole consequence of their most recent preferential interactions with T cells and may be due to the T cell help they received at earlier stages .

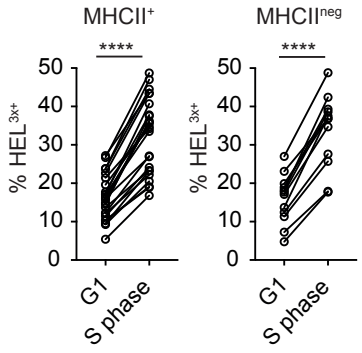

Figure 4.8: HEL^{3X+} LZ cells still preserve proliferative advantage after losing interactions with T^{FH} cells.
~1x10^5 SW$_{HEL}$ *Cd79a*-CreERT2 MHCII$^{fl/fl}$ B cells were transferred into congenic WT mice. The host mice were then immunized with HEL^{3X}-SRBCs/LPS. The HEL^{3X} staining control mice also received the same number of OTII cells and were subsequently immunized with HEL-OVA/Ribi. Experimental mice received tamoxifen to induce MHCII deletion and EdU to label S phase cells, for 42hrs and 30mins before analysis, respectively. SW$_{HEL}$ GC LZ B cells were analyzed. EdU$^-$ and EdU$^+$ cells were identified for both MHCII^{high} and MHCII-deleted SW$_{HEL}$ GC LZ B cells. Frequencies of HEL^{3X+} cells were summarized for each population. Results are pooled from 3 independent experiments each with 2-10 mice/group. Lines join cell populations from single mice. MHCII^{high} populations are combined from mice that received tamoxifen and vehicle. Analysis was performed with paired student T test. ****$p < 0.0001$.

4.7 Conclusion

To summarize, following the observations made in Chapter 3 that cyclic re-entry is not acutely triggered by recent interactions with T cell, in this chapter, we continued to investigate if cyclic re-entry initiation is still a highly competitive process but limited by other resources more generally available in the GCs. In order to tackle this question, a mouse model was first established to allow uniform reduction of the competition in the GCs, and we achieved this by rendering GC B cells susceptible to apoptosis with DT treatment through DTR knockin into the *Aidca* locus. Consequently, when combined with different mixing ratios with WT cells in BM chimeras, targeted fractions of competition in the GC LZ can be relieved.

The completeness, speed and specificity of GC B cell ablation were first confirmed, with the vast majority ($> 80\%$) of DTR$^+$ cells depleted within 8 hours

of DT treatment with no further decrease at a later (12hrs) time point and no evidence of change in the frequencies of DTR^{neg} cells. This observation also suggests that there was no evident expansion of the DTRneg cells to fill out the GC niche when cyclic re-entry initiation was measured, and the intra-GC competition was reduced to the minimum level. However, despite more than 75% competitor cells in the LZ being depleted, there was no evident change in the transition from late G1 into S phase in the remaining non-ablatable cells, as measured in both the Fucci2 model and by BrdU mediated S phase labelling. Therefore, cyclic re-entry initiation was not detectably restricted by any competition.

Then another stimulus to drive cyclic re-entry initiation can be reaching a certain BCR signalling threshold. To dissect the correlation between BCR affinity and cyclic re-entry initiation, we used the SW_{HEL} BCR knockin x Fucci2 model to follow this process in both high and low affinity cells in the GCs. We revealed that there was an enrichment of higher affinity (ie HEL^{3X+}) in the early S phase population in both LZs and DZs. This association indicates that higher affinity cells are overall more proliferative than the low affinity cell counterparts, hence are progressing through cell cycles faster. However, these higher affinity cells could still reserve the proliferative advantage even when T-B interactions were perturbed for 2 days. One possible explanation is that the T cell help they have accumulated could last for more than two days, however, it is also plausible that there are other contributing factors to their superior proliferative status.

Much to the contrary, our results so far have shown that LZ cyclic re-entry initiation is not limited by either T cells or general competition in the GCs, posing the next immediate question of how positive selections are carried out in the GCs? T cells are undoubtedly playing vital roles in this process but how do they achieve this? In the next Chapter, we investigated how T cells could support B cells to different extents and whether GC B cells could initiate cyclic re-entry from different T cell helped states?

Chapter 5

Evidence of competition in light zones for T cell derived "refuelling" cues

Contents

In the previous two chapters, we have investigated the possible restrictions for cyclic re-entry in GC LZs. Contrary to what the cyclic re-entry model predicts, we found that the initiation of cyclic re-entry was not detectably restricted by either the limiting number of T_{FH} cells or any general resources in the GC. This leaves us with the imminent question of how affinity enhancements are conferred if LZ cells do not need to compete in an affinity dependent manner to return to DZ? And, given the central importance of T_{FH} cells in GC development and maintenance, how do T_{FH} cells drive GC positive selection?

The eminent role of T cells in driving GC B cell positive selection has been studied extensively. Blockade of important stimulations that T cells can provide to B cells such as CD40-CD40L, and MHCII-TCR interactions using blocking antibodies leads to reduced GC outputs in terms of antibody production due to shrinkage and even pre-mature dissolution of GCs (Foy et al, 1993; Han et al, 1995; Pae et al, 2021). Then the seminal study carried out by Victora and colleagues in 2010 demonstrated that strong GC B-T_{FH} interactions could result in subsequent preferential and extensive DZ expansion (Victora et al, 2010). Morever, *ex vivo* stimulation of GC B cells with anti-CD40 antibody together with anti-IgM shows synergistic strong induction of c-Myc and IRF4 expression, suggesting the role of T-B interactions in promoting GC B cell growth and selection (Calado et al, 2012; Dominguez-Sola et al, 2012; Luo et al, 2018).

Mechanistically, T cell-B cell interactions could stimulate B cells to be at a metabolically more active state, as shown by the experiment in which T-B interactions were enhanced by augmenting antigen presentation through DEC205. This treatment led to enhanced cell growth as shown by elevated c-Myc expression, larger B cell sizes and upregulations of pS6 in the GC B cells. As discussed previously in Chapter 1, c-Myc is a well-defined proliferation and growth regulator and pS6 is a ribosomal subunit as well as an important contributor to the mTOR pathway,

directly involved in the biogenesis (Calado et al, 2012; Dominguez-Sola et al, 2012; Finkin et al, 2019; Ersching et al, 2017). Moreover, the strength of T cell help could dictate the proliferative potential once the cells are back into DZs, as indicated by the studies where strong T cell help led to overall higher proliferation speed, preferential expansion of the B cells in the DZ possibly due to the induction of cyclin D3, which controls inertial cell cycle progression in DZs (Victora et al, 2010; Gitlin et al, 2015; Finkin et al, 2019; Pae et al, 2021).

In addition to demonstrating that T cell mediated selection preferentially drives LZ cells back into the active cell cycle, these various lines of experimental evidence above are supporting the occurrence of a second process, in which interactions with T cells confer selective advantages to higher affinity cells by feeding into metabolic pathways that could drive more extensive downstream cell proliferation once the cells have returned to the DZs. We termed this second process "T cell mediated refuelling". Conceptually, if cyclic re-entry is not the pass-or-die selection threshold, then LZ B cells that receive different amounts of T cell mediated refuelling are all capable of returning to DZs, with cells that received a larger dose of refuelling potentially undergoing more rounds of cell division and/or progressing through cell cycles faster. Meanwhile, non-refuelled, or minimally refuelled, cells that return to DZ with less metabolic reserves still possess the possibility for affinity enhancements through SHM.

Previous studies have shown that T_{FH} cells are limited in numbers compared with GC B cells and GC B cells can engage in stronger and longer interactions with T_{FH} cells if they are better at presenting antigens than their neighbour competitors (Allen et al, 2007; Shulman et al, 2013). Given that the level of antigen presentation is proportional to the affinity of BCRs, receiving T cell mediated refuelling may be a competitive process depending on the BCR affinity (Batista et al, 2000). Hence, in this Chapter, we studied how BCR affinity and intra-GC competition would impact the acquisition of T cell mediated refuelling.

5.1 Establishing a molecular signature for identifying B cells that have recently received help (or refuelled).

To investigate how T cells instruct positive selections of GC B cells, new biomarkers are needed to identify B cells that have recently interacted with T cells. This is because although c-Myc has long been identified as being induced after strong B-T interactions, there is evidence that it may also be induced to some degree by BCR stimulation alone (Ramezani-Rad, et al, 2020). We therefore explored whether more accurate markers for receiving T cell help exist, with one such candidate being the Basic Leucine Zipper ATF-Like Transcription Factor (BATF). BATF has been shown to be upregulated in a small proportion of LZ cells in a partially CD40L dependent manner and enhanced antigen presentation leads to elevated frequencies of $BATF^{high}$ cells (Inoue et al., 2017). This study suggests that BATF may be a good reporter to identify GC B cells that have received T cell mediated refuelling.

To validate the suitability of BATF, we first examined if BATF expression in GC LZ B cells is strictly T cell dependent. Mixed BM chimeras between R26-CreERT2 x $MHCII^{fl/fl}$ CD45.2 and WT CD45.1 BM cells were utilized again. These BM chimeric mice were immunized with SRBCs to induce polyclonal GC responses and mice received tamoxifen 24 hours before spleen harvest on day 8. $BATF^{high}$ cells were identified in WT GC B cells with IRF4 on the x-axis to facilitate gating (Fig. 5.1A). 24 hours after MHCII deletion, there was almost a complete loss of $BATF^{high}$ cells in the MHCII-deleted population, indicating a high level of BATF expression was induced by B-T interactions (Fig. 5.1B). This observation also confirmed the results in Chapter 3 that 24hrs of tamoxifen treatment was sufficient to functionally terminate T-B interactions. Thus by the time of analysis, any cyclic re-entry events initiated in the MHCII-deleted LZ cells were T cell independent. High levels of BATF expression were primarily restricted to LZ cells, as shown by backgating $BATF^{high}$ population onto total GC B cells, which is consistent with

previous reports and matching the current selection model that LZ is the site for positive selection driven by T cells (Inoue et al, 2017; Victora et al, 2012) (Fig. 5.1C). However, notably, tamoxifen alone could induce BATF expression in GC B cells (Fig. 5.1B). Similar findings have been reported previously that tamoxifen was capable of inducing c-Myc expression (Finkin et al, 2019).

To corroborate the findings from genetic MHCII deletion, we next inspected BATF expression after disturbing GC B-T_{FH} interactions with the anti-CD40L blocking antibody. CD40-CD40L interactions are one of the most important receptor-ligand interactions during B-T interactions and prolonged anti-CD40L treatment results in GC collapse (Han et al, 1995). To achieve this, WT B6 mice were first immunized with SRBCs to allow GC formation, and 24hrs before harvest, anti-CD40L antibodies or vehicle were administered to mice by i.p. injection. Spleens were then harvested on day 8. Consistent with MHCII deletion data, blocking CD40L significantly reduced the number of $BATF^{high}$ cells in GC LZs, further supporting that the BATF level in GC B cells was sensitive to T cell interactions, making it a faithful marker (Fig. 5.1D and E). To note, the size of the decrease in $BATF^{high}$ cells after anti-CD40L treatment was smaller than that of the MHCII deletion. These residual $BATF^{high}$ cells after treatment could possibly be attributed to the incomplete blockade of the antibody, or alternatively indicate that its expression can be supported by T cell dependent, CD40L independent pathways.

c-Myc was not considered the best marker for B-T interactions because of its low-level induction by BCR signalling alone, however, its expression at high levels is still mostly T cell dependent and reports the metabolic and proliferative potential of the cell (Luo et al, 2018; Finkin et al, 2019). Therefore, we would like to test the correlation between high levels of BATF and c-Myc. A correlation would suggest the level of BATF is a good indication for not only recent B-T interactions but also a functional inference of T cell mediated refuelling. As such it could be a better marker than c-Myc for us to study T cell mediated refuelling due to its expression being solely dependent on T cells. We immunized c-Myc-GFP reporter mice with

SRBCs and then co-stained BATF with c-Myc-GFP in GC LZ B cells on day 8. In LZs, most of the cells that had high level BATF expression were also positive for c-Myc-GFP (Fig. 5.1F). To conclude, high levels of BATF can be induced in GC LZ B cells in a T cell dependent manner. Hence, BATF can be used as a marker in later studies to identify cells that had recently been refuelled by T cells. An additional advantage of BATF besides being strictly T cell dependent is that the analysis of BATF level only requires intracellular stain as opposed to c-Myc, where a c-Myc-GFP reporter was needed because the intracellular c-Myc stain did not always give consistent staining patterns in our hands.

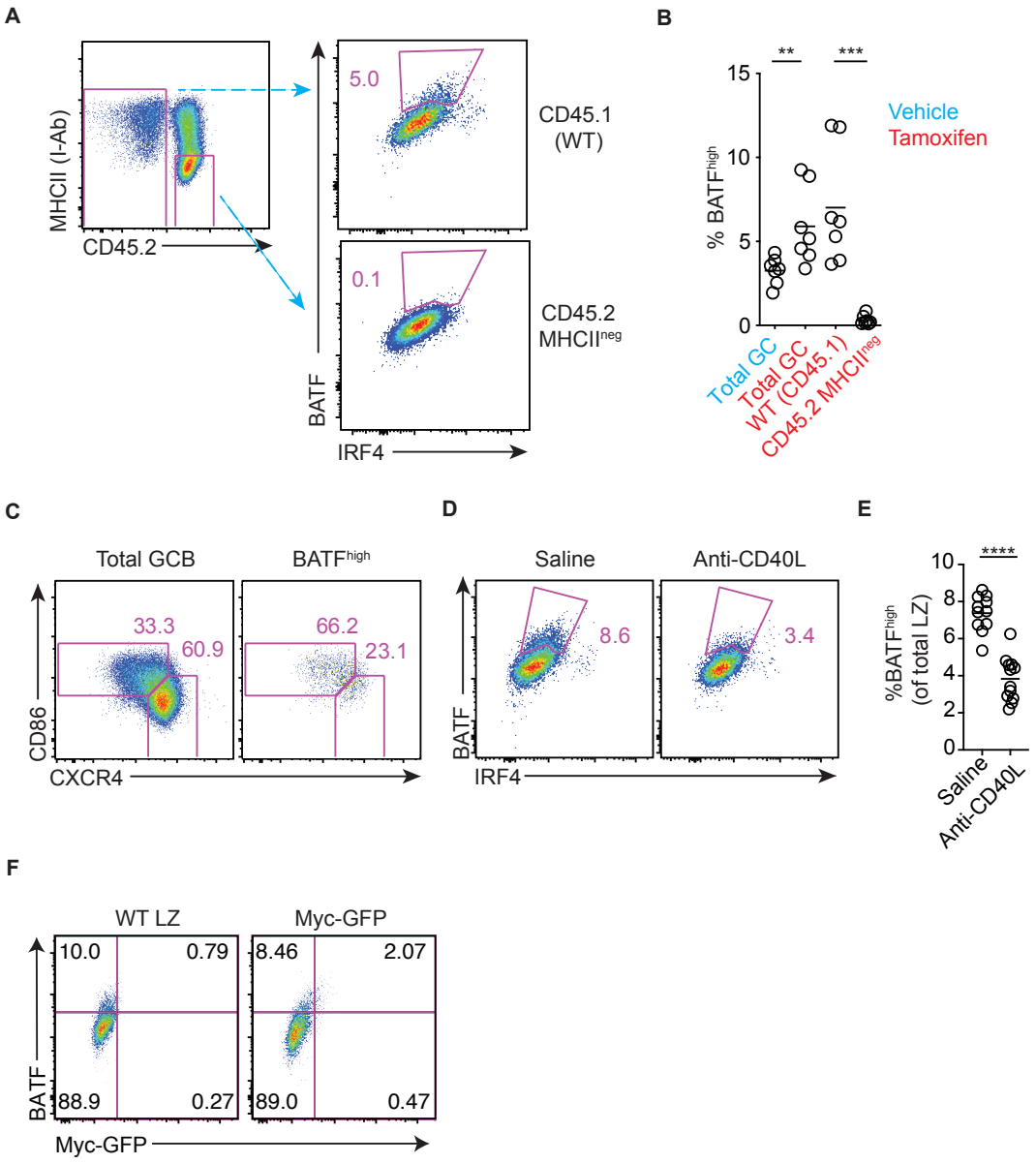

Figure 5.1: BATF as a marker for recent T-B interactions
(A and B) Mixed BM chimeric mice reconstituted with CreERT2^{+} MHCII$^{fl/fl}$ CD45.2 and WT CD45.1 cells were immunized with SRBCs (i.p.). These mice received tamoxifen or vehicle to induce MHCII deletion at the indicated time points before tissue harvest on day 8. Splenic GC LZ B cells (IgD^{low} CD95^{+} GL7^{+} CXCR4^{low} CD86^{high}) were analyzed. (A) Frequencies of BATF^{high} cells were determined in WT and MHCII-deleted populations and summarized in (B). (C and D) WT C57BL/6 mice were immunized with SRBCs and received anti-CD40L antibody or saline 24hrs before spleen harvest. Frequencies of BATF^{high} LZ cells were identified after anti-CD40L or saline treatment in (A) and summarized in (D). (E) Percentages of LZ and DZ cells were identified in both total GC B cells and BATF^{high} GC B cells. (F) Polyclonal GC responses following 8d SRBC immunization were analyzed in c-Myc$^{GFP/GFP}$ and WT mice. The correlation between c-Myc-GFP and BATF was shown in c-Myc$^{GFP/GFP}$ LZ B cells, with WT LZ B cells used as controls for c-Myc-GFP gate setup. Results were representative plots (A, C, D, F) or pooled (B, E) from 2-4 experiments each with 3-4 mice per condition. Lines were joining populations from the same mouse. Analysis, two-tailed paired student T test, **p < 0.01, ***p < 0.001, ****p < 0.0001.

5.2 Higher affinity cells are more likely to receive T cell mediated refuelling

Now that we have identified a biomarker for recent T-B interactions, the first question to be asked is whether GC B cells receive T cell mediated refuelling in an affinity dependent manner. This hypothesis is postulated based on the observations that cells with enhanced antigen presentation in LZs display a selective and proliferative advantage once they return to DZs (Victora et al, 2010). The level of pMHCII presentation is directly proportional to the amount of antigen that could be acquired by the BCRs from the FDC so is correlated to the BCR affinity (Batista et al, 2000). As such, it is plausible that B cells are receiving these T cell mediated fuelling factors in an affinity dependent manner. Then, higher affinity should be more likely to receive more T cell mediated refuelling, to be shown by higher frequencies of $BATF^{high}$ cells in this population.

To test this hypothesis, we utilized the SW_{HEL} system again, because this system allows for the concurrent identification of high and low affinity cells, as well as the percentages of $BATF^{high}$ cells in each population, all by direct FACS staining. About $1x10^5$ SW_{HEL} cells were first adoptively transferred into sex-matched congenic recipient mice. Then, host mice were immunized with HEL^{3X} conjugated SRBCs the next day to establish GC responses, with analysis on day 8. SW_{HEL} GC LZ B cells were gated as CD45.1, $GL7^+$ Igk^+, $CXCR4^{low}$, and $CD86^{high}$. Subsequent $BATF^{high}$ and $BATF^{low}$ populations were identified among LZ B cells. Next, high and low affinity cells towards HEL^{3X} were identified in both refuelled ($BATF^{high}$) and non-refuelled ($BATF^{low}$) LZ B cells (Fig. 5.2A). There was a significant enrichment of HEL^{3X+} (ie the higher affinity) cells in the $BATF^{high}$ population, consistent with the current hypothesis that higher affinity cells are more likely to acquire T cell mediated refuelling (Fig. 5.2B).

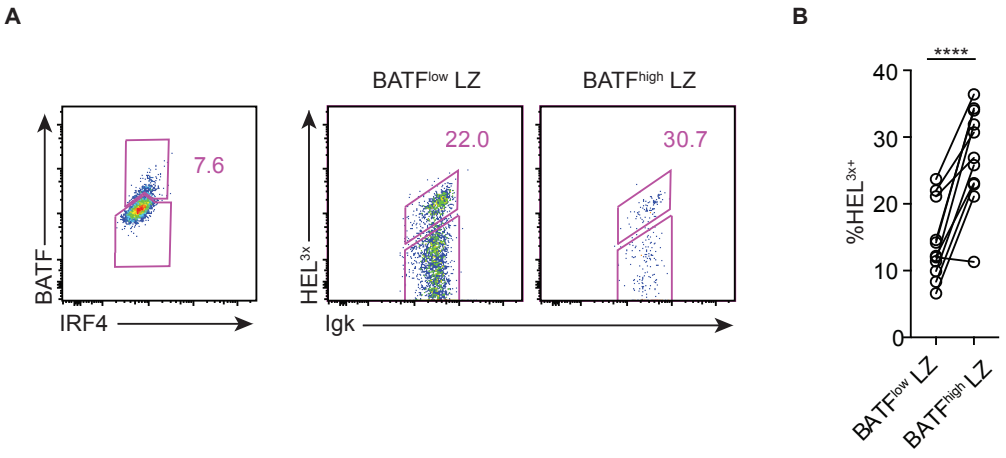

Figure 5.2: Higher affinity cells are more likely to receive T cell mediated refuelling
1x10^5 SW_{HEL} B cells were adoptive transferred to congenic WT recipients. The host mice were immunized with HEL^{3X}-SRBCs by i.p. injections the next day. SW_{HEL} GC responses were analyzed on day 8 or 9. SW_{HEL} GC B cells (CD45.1, $GL7^+$) were identified. (A) $BATF^{high}$ and $BATF^{low}$ populations were gated in SW_{HEL} GC LZ. Frequencies of high affinity (HEL^{3X+}) cells were determined for both populations and enumerated in (B). Lines joining populations from the same mouse. The representative FACS plot in A and results in B were summarized from 4 experiments each with 4 mice. Analysis, paired two-tailed Student T test. ****$p < 0.0001$.

5.3 Acquisition of T cell mediated refuelling is restricted by competition amongst GC B cells

Having established a correlation between affinity and receiving of T cell mediated refuelling, we next asked how refuelling is conferred to B cells. Given our previous observation in Chapter 4 the high B-T ratio (~5:1 without any perturbation) in the GC, T cells are always limiting in numbers, suggesting competition between LZ B cells may be required to engage in any interactions with T cells (Fig. 4.2C). Also, in section 5.1, in WT splenic cells, less than 10% cells were detected as $BATF^{high}$, implying competition is restricting the frequencies of LZ cells that could receive T cell mediated refuelling (Fig. 5.1B). Therefore, we are next investigating if receiving T cell mediated refuelling is a highly competitive process amongst GC LZ B cells.

Initially, we considered studying the impact of intra-GC competition on

receiving T cell mediated refuelling by deleting MHCII from a subset of GC B cells, using the R26-CreERT2^{+} MHCII$^{fl/fl}$ CD45.2: WT CD45.1 BM chimera model. The goal then would be to explore after deleting MHCII from a fraction of GC B cells, whether the remaining competitors could show an advantage at interacting with T cells in a largely normal GC environment with a physiological level of pMHCII and no exogenous augmentation of presentation. However, as reported in the previous section, tamoxifen treatment alone could induce BATF expression, which hindered our effort to use this model (Fig. 5.1B). So we return to the partial B cell ablation model to reduce the competition in GCs by removing a pre-determined fraction of GC B cells.

To achieve partial GC B cell ablation, BM chimeras reconstituted with 80% AID$^{wt/Cre}$ R26-loxp-stp-loxp-DTR BM and 20% WT BM cells were immunized with SRBCs. DT was administrated 15hrs before spleen harvest to induce DTR^{+} GC B cell death. Mice were sacrificed and spleens were harvested on day8. The deletion efficiency was confirmed by flow cytometric analysis, with GC B cells identified as (B220^{+}, IgD^{-}, CD95^{+}, and GL7^{+}). 15 hours after DT treatment, there was almost a three-quarter decrease in the percentage of GC B cells and $>$ 85% deletion of DTR^{+} GC B cells, meanwhile, the deletion was very specific, with no effect in DTR^{-} GC B cells (Fig. 5.3A).

After relieving the competition in the GCs, the frequencies of BATF^{high} cells in the non-ablatable CD45.1 LZ B cells showed an increase, from 10.6% to 14.4% (comparing +/- DT treatment) (Fig. 5.3B and C). A similar increase was also observed in the total remaining LZ cells, when the remaining DTR^{+} cells were included in the analysis (Fig. 5.3D). These data support that acquisition of T cell mediated refuelling is a competitive process. However, in this experiment, a relatively large fraction of GC B cells (>75%) were depleted from GC responses and only resulted in a relatively small increase in the percentage of BATF^{high} cells (~30% increase). One possible explanation is that the competition between B cells was not so very stringent, such the phenotype only became obvious when there

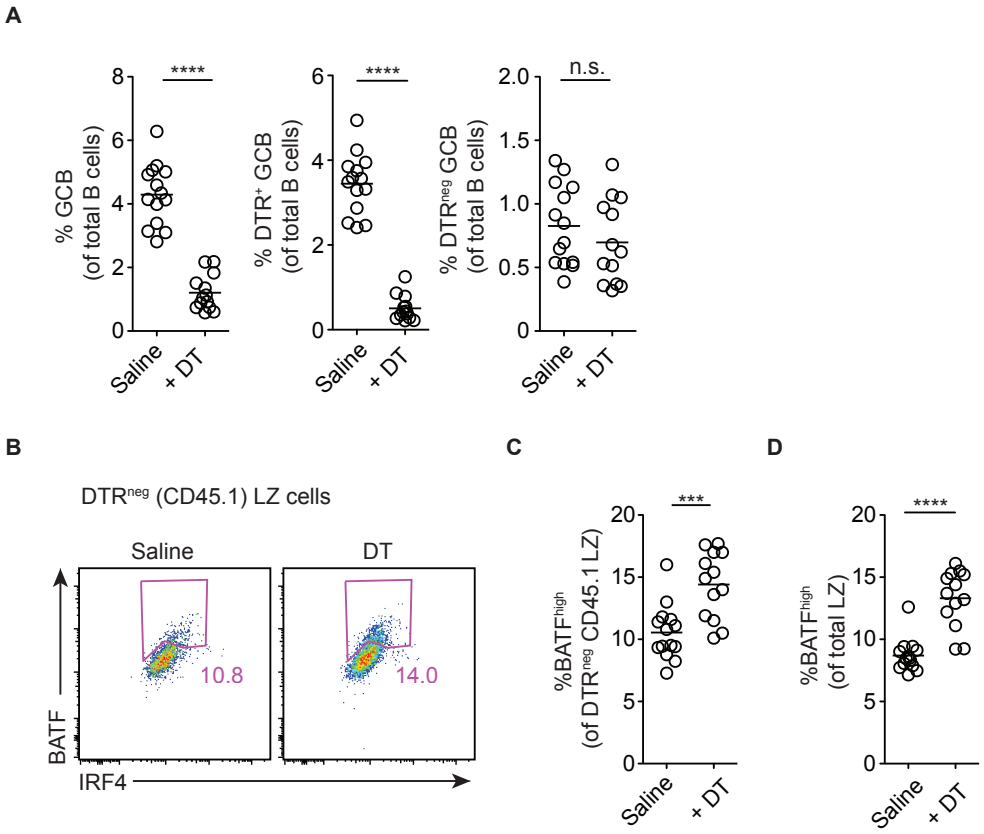

Figure 5.3: B cells upregulate BATF in a competition dependent manner
Mix BM chimeric mice containing 80% AID-DTR CD45.2 and 20% CD45.1 BM cells were immunized with SRBCs (i.p.). Mice received DT or saline 15hrs before tissue harvest on day 8. Splenic GC B cells (IgD^{low} $CD95^{+}$ $GL7^{+}$) were analyzed. (A) Frequencies of total GC B cells, DTR^{+} and DTR^{neg} GC B cells were quantitated. (B) Frequencies of $BATF^{high}$ population were identified in DTR^{neg} LZ B cells after DT or saline treatment and summarized in (C). (D) Percentages of $BATF^{high}$ cells were enumerated for total LZ cells after treatment. Representative plots (B) or pooled (A, C, D) from 4 experiments each with 3-4 mice per condition. Analysis, Mann-Whitney U test, ***p < 0.001, ****p < 0.0001.

was a large fraction of the competition relieved. If this is true, one might expect no change or a smaller increase would be observed when a smaller portion of GC B cells is deleted from the competition.

To test this possibility, a smaller fraction of GC competition between B cells was relieved followed by the quantification of the percentage of LZ cells displaying a refuelled signature. We made mixed BM chimeras less biased towards the WT cells, with 50% $AID^{wt/Cre}$ R26-loxp-stp-loxp-DTR BM and 50% WT BM cells. Eight

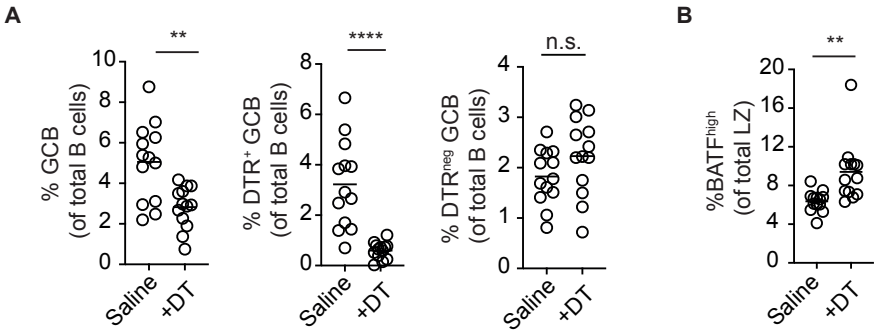

Figure 5.4: BATF is regulated by more than competition between GC B cells Mix BM chimeric mice containing 55% AID-DTR and 45% CD45.1 WT BM cells were immunized with SRBCs (i.p.). Mice received DT or saline 15hrs before tissue harvest on day 8. Splenic GC B cells (IgD^{low} $CD95^{+}$ $GL7^{+}$) were analyzed. (A) Frequencies of total GC B cells, DTR^{+} and DTR^{neg} GC B cells were quantitated. (B) Frequencies of $BATF^{high}$ population were enumerated as percentages of total remaining LZ cells after DT or saline treatment. Results were pooled from 3 experiments each with 3-4 mice per condition. Analysis, Mann-Whitney U test, $^{**}p < 0.01$, $^{****}p < 0.0001$.

weeks after their BM reconstitution, these mice were immunized with SRBCs, and they again then received DT treatment 15hrs before analysis on day 8. Consistent with expectations, the overall GC contraction was approximately 50%, with the DTR^{+} cells efficiently depleted from GC responses and frequencies of DTR^{-} cells remaining unaffected (Fig. 5.4A). Surprisingly, the frequencies of $BATF^{high}$ cells amongst total LZ population still increased when there was less competition relieved, and the size of the increase was similar to when 75% competition was removed, possibly reflecting competition between B cells may not be the only limiting factor determining whether a B cell could receive T cell support (Fig. 5.4B). As such, additional factors beyond simply competition between B cells for T cells may determine whether or not help is received.

5.4 Intrinsic ability to acquire antigens of B cells is also limiting the amount of T cell mediated refuelling the B cells received

So far in this Chapter, we used BATF as a marker for recent T-B interactions and showed that in contrast to cyclic re-entry, which was independent of acute interactions with T cells, LZ B cells needed to compete with each other with to receive T cell mediated refuelling in an affinity dependent manner. However, the finding that relieving competition only caused relatively modest increases in the frequencies of $BATF^{high}$ cells led us to consider whether the situation may be even more complicated than a cell's chances of successfully receiving help is restricted only by inter-GC B cell competition. Next, we set to explore what other factors might also be limiting for productive interactions with T cells.

The quantity and quality of T cell support that a B cell receives are thought to be provided in proportion to the amount of pMHCII that B cells present (Victora et al, 2012). While the amount of antigen presented by a given B cell correlates with its BCR affinity, which determines the ability for antigen uptake, antigen presentation could also be dependent on the intrinsic ability of BCRs to uptake antigen at the levels available to them. Theoretically, higher frequencies of LZ B cells could receive T cell mediated refuelling if more antigen is introduced into the system at times where their capability to take up antigens is limiting.

To test this possibility, we supplemented GCs with an extra dose of immunogen and assessed the frequencies of $BATF^{high}$ cells in GC LZ populations. WT C57BL/6 mice were immunized with SRBCs to induce polyclonal GC responses. On day 7, we supplemented the GCs with more antigens by re-injecting the same amount of SRBCs as the original immunization dose. These mice also received BrdU by i.p. injections 30mins before tissue harvest on day 8. Strikingly, after the extra dosage of antigen injection, the percentage of LZ cells that were $BATF^{high}$ cells already showed a significant two-fold increase (Fig. 5.5 A and B). In this experiment, we

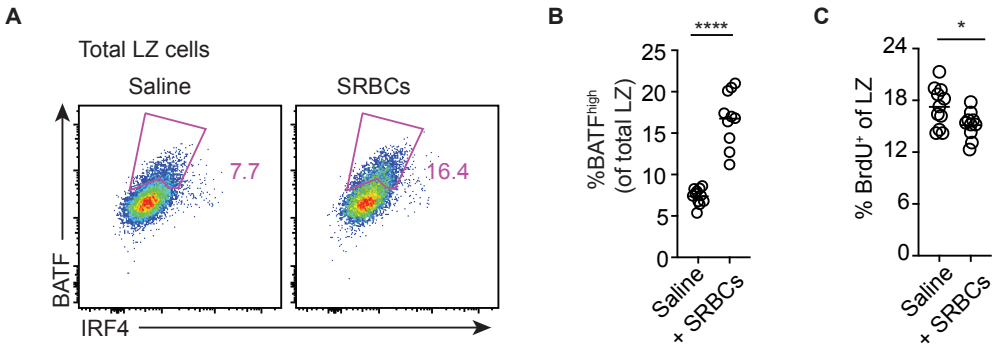

Figure 5.5: Augmenting antigen availability in GCs leads to increases in the frequency of BATF^{high} cells in LZs, but not cyclic re-entry
WT mice were immunized with SRBCs (i.p.) and then received the same dose of SRBCs again 1d before analysis. BrdU was injected i.p. 30mins before tissue harvest, to label S phase cells. Spleens were harvested on day 8. (A) Percentages of BATF^{high} cells in LZs were quantified after SRBC or saline treatment and summarized in (B). (C) Frequencies of S phase cells (BrdU^{+}) were determined in both conditions. Results are representative (A) or pooled (B, C) from three independent experiments each with 3-4 mice per condition. Analysis, Mann-Whitney U test, *p $<$ 0.05, ****p $<$ 0.0001.

boosted the system with only more antigens, and yet still maintained a physiological level of pMHCII presentation. As such, the intrinsic ability of a B cell to acquire antigen is also imposing limits on the amount of T cell support it could receive. In contrast, there was no increase in the S phase (BrdU^{+}) LZ cells after the extra dose of antigens (Fig. 5.5C). This observation indicates that increasing B cell refuelling does not necessarily directly lead to an increase in LZ S phase entry, or cyclic re-entry initiation, again suggesting that these are two independently regulated processes.

5.5 LZ cells engaged in cyclic re-entry initiation represent a heterogeneous population in terms of their fueling status

In contrast to what the cyclic re-entry model predicts, in the last section our data proved that receiving T cell mediated refuelling was not a pre-requisition for LZ B cells to initiate cyclic re-entry. If this is correct, and the G1 to S transition in the LZ does not serve as the stringent selection barrier, then we should expect to

find cells at different states of refuelling within populations initiating cyclic re-entry. To test this hypothesis, BATF was co-stained with BrdU and EdU, allowing us to distinguish whether LZ cells are uniform or indeed different in terms of their fuelling status at the point of re-entering cell cycle. WT C57BL/6 mice were immunized with SRBCs and received EdU and BrdU by i.p. injections on day 8, 100mins and 40mins before tissue harvest, respectively.

GC LZ B cells were pre-gated ($B220^+$, IgD^-, $CD95^+$, $GL7^+$, $CD86^{high}$ and $CXCR4^{low}$) and further sub-gated into different cell cycle stages based on EdU and BrdU incorporation. G1 cells were gated as EdU^- $BrdU^-$ (shown with purple dashed gate), and early S phase cells were identified as EdU^- $BrdU^+$ (solid green gate) (Fig. 5.6A). When $BATF^{high}$ cells were identified in each population, only between 10-20% of cells displayed a refuelled signature in the cyclic re-entry population in a non-perturbed setting, with the vast majority of the cells initiating cyclic re-entry in an unrefuelled state (Fig. 5.6B). To note, there was an enrichment of $BATF^{high}$ cells in the cyclic re-entry population, which was consistent with previous reports that refuelled cells are in a superior metabolic and higher proliferative state due to their higher expression levels of c-Myc and mTORC pathways regulators (Finkin et al, 2019; Ersching et al, 2017). To conclude, the cyclic re-entry population was heterogeneous in terms of their refuelled state and only small fractions of these cells had after recent interactions with T cells.

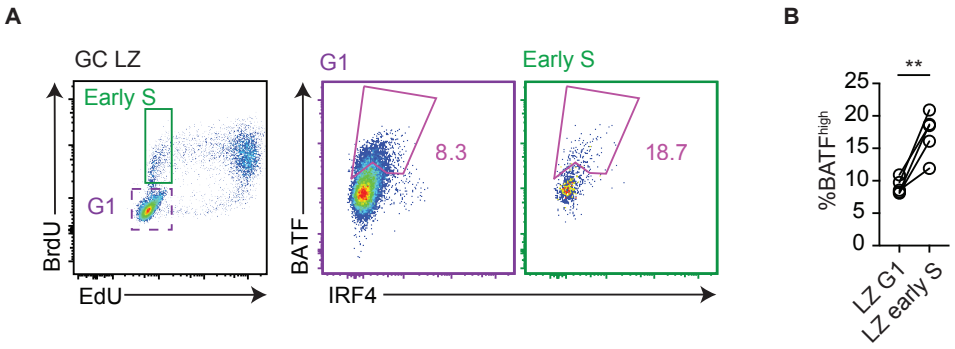

Figure 5.6: Majority cells in the cyclic re-entry population are unrefuelled. WT mice were immunized with SRBCs (i.p.) and received EdU 100mins and BrdU 40mins before spleen harvest on day 8. Splenic GC LZ B cells were gated as $B220^{+}$, IgD^{-}, $CD95^{+}$, $GL7^{+}$, $CD86^{high}$ and $CXCR4^{low}$. (A) Representative plots of $BATF^{high}$ population among early S ($BrdU^{+}$, EdU^{-}) and G1 ($BrdU^{-}$, EdU^{-}) LZ cells. (B) Frequencies of $BATF^{high}$ cells in each population. Results were pooled from two experiments each with 2-3 mice. Lines were joining populations from the same mouse. Analysis was performed with two-tailed paired student T test, $^{**}p < 0.01$.

5.6 Single cell RNA sequencing reveals heterogeneity in LZ GC B cells

5.6.1 Validating the transcriptomic signatures of sorted GC B cells

In the last section, we observed that the cyclic re-entry initiating populations in LZs are heterogeneous in terms of their refuelling status, as only a small fraction of cells (10-20%) displayed a signature of recent T-B interactions as determined by BATF stain. As informative as it is, BATF is a single marker for recent T-B interactions. It has been reported that despite GCs being divided only into LZs and DZs based on phenotypic characteristics, there is a high level of heterogeneity within each zone of cells on the transcriptomic level (Kennedy et al, 2020). Therefore, in order to more comprehensively characterize and explore the heterogeneity within the LZ cells initiating cyclic re-entry, analysis on the single cell transcriptomic level was needed to reveal any subtle differences. To achieve this, we subjected GC LZ B cells in different cell cycle stages to single cell RNA sequencing analysis.

5. Evidence of competition in light zones for T cell derived "refuelling" cues

We utilized CreERT2^{+} MHCII$^{fl/fl}$ Fucci2 mice to combine the identification of cell cycle stages together with MHCII manipulation in GC LZ cells. These mice were immunized with SRBCs and received tamoxifen to induce MHCII deletion 24hrs prior to analysis. The GC responses were analyzed on day 8. Then, single cell index sorting was performed on GC LZ B cells (B220^{+}, IgD^{-}, CD95^{+}, GL7^{+}, CD86^{high} and CXCR4^{low}) in either resting late G1 phase (mCherry^{high} mVenus^{-}) or early S phase (mCherry^{high} mVenus^{+}) in both MHCII^{high} and MHCII-deleted populations. Meanwhile, small populations of DZ cells were also sorted as controls for gene expression comparisons. "Indexing" records the information regarding surface marker (protein) levels which can provide additional information supplementary to the transcriptomic data. Then, these cells were subjected to single cell RNA sequencing with plate based SmartSeq2 sequencing technique. The processing and filtering of raw sequencing data was described in Methods. After gene count matrices were generated, downstream analysis was performed in Seurat.

Before we further focused on individual populations and made any deeper analysis, the zonal transcriptomic characteristics were first examined in each population to verify the fidelity of the sorting and data processing process. Lists of genes that have been confirmed for differential high levels of expression in LZ or DZ B cells were utilized. These genes have been identified in previous studies where LZs or DZs were microscopically marked by photoconversion and then sorted for bulk RNA sequencing (Victora, et al, 2012). To calculate the cumulative expression levels of a list of genes in individual cells, the module score function in Seurat was applied. This function allows the calculation of the average expression levels of a defined cluster of genes on a single cell level. This score was subsequently plotted for each sorted population to visualize their transcriptomic features. In our experiment, the sorted LZ cells displayed higher levels of LZ signature genes, while DZ cells are enriched with the gene list for DZ cells, confirming the fidelity of our data analysis (Fig. 5.7A and B).

5. Evidence of competition in light zones for T cell derived "refuelling" cues

To complement the BATF staining experiments, we further verified the expression patterns of T cell dependent/promoted genes in the MHCII^{high} and MHCII-deleted LZ cells. This list T cell dependent genes that we used was identified in the study in which GC B cells were loaded with a significant amount of peptide antigens by targeting DEC205. The transcriptomes of these cells were analyzed by bulk RNA sequencing and T cell dependent genes were identified by their differential high levels of expression when compared with non-overloading GC B cells (Victora, et al, 2010). We applied this gene list to the module score function to calculate the integrated expression of these genes in each population and observed that these gene signatures were preferentially enriched in the MHCII^{high} LZ population, in both resting and cyclic re-entry state, as compared with MHCII-deleted cells (Fig. 5.7C). A similar analysis was also performed with a list of FoxO1 dependent genes (Dominguez-Sola, et al, 2015). Given that FoxO1 is activated in DZ cells and controls DZ phenotypic programme, these genes were expected to have a higher level of expression in these cells as compared with LZ populations. Consistent with this, the average integrated score of these genes was higher in DZ cells as compared with the rest of the four sorted LZ populations (Fig. 5.7D). In conclusion, the observations from our single cell RNA data analysis were consistent with the phenotypes of the sorted cells, and could accurately reflect the transcriptomic status of the cells, making them suitable for further analysis to reveal any differences amongst individual populations.

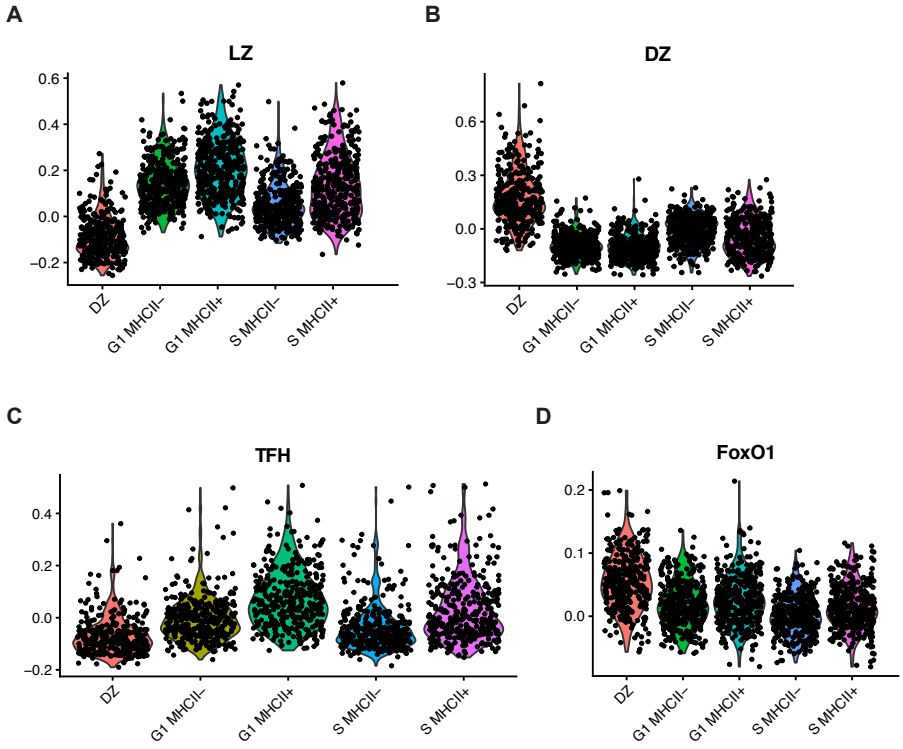

Figure 5.7: Validation of signature gene expression in single cell sorted. R26-CreERT2^{+} MHCII$^{fl/fl}$ Fucci2 mice were immunized with SRBCs (i.p). These mice were treated with tamoxifen on day 7 following immunization, and spleens harvested on day 8. Splenic GC LZ B cells (B220^{+}, IgD^{-}, CD95^{+}, GL7^{+}, CD86^{high} and CXCR4^{low}) were analyzed. (A) Module scores of LZ signature genes on a per cell basis in each sorted population. (B) Module scores of DZ signature genes of each individual cell in each sorted population. (C) Module scores of T cell dependent genes and (D) FoxO1 dependent genes. Each dot represents a single cell. Results were pooled from two experiments each with 2 mice per condition.

5.6.2 LZ cyclic re-entry population shows a high level of transcriptomic heterogeneity

Having established a suitable data set to study the heterogeneity in the cyclic re-entry population, we next subjected the S phase MHCII^{high} cells to non-supervised clustering with uniform manifold approximation and projection (UMAP). Four clusters were identified, clearly showing there was a high level of heterogeneity within this population. Interestingly, there was only one cluster (Cluster 1) characterized by the signature genes of T-B interactions, including BATF, c-Myc, and NFkB etc (Fig. 5.8), indicating T cell mediated refuelling. This data corroborated with

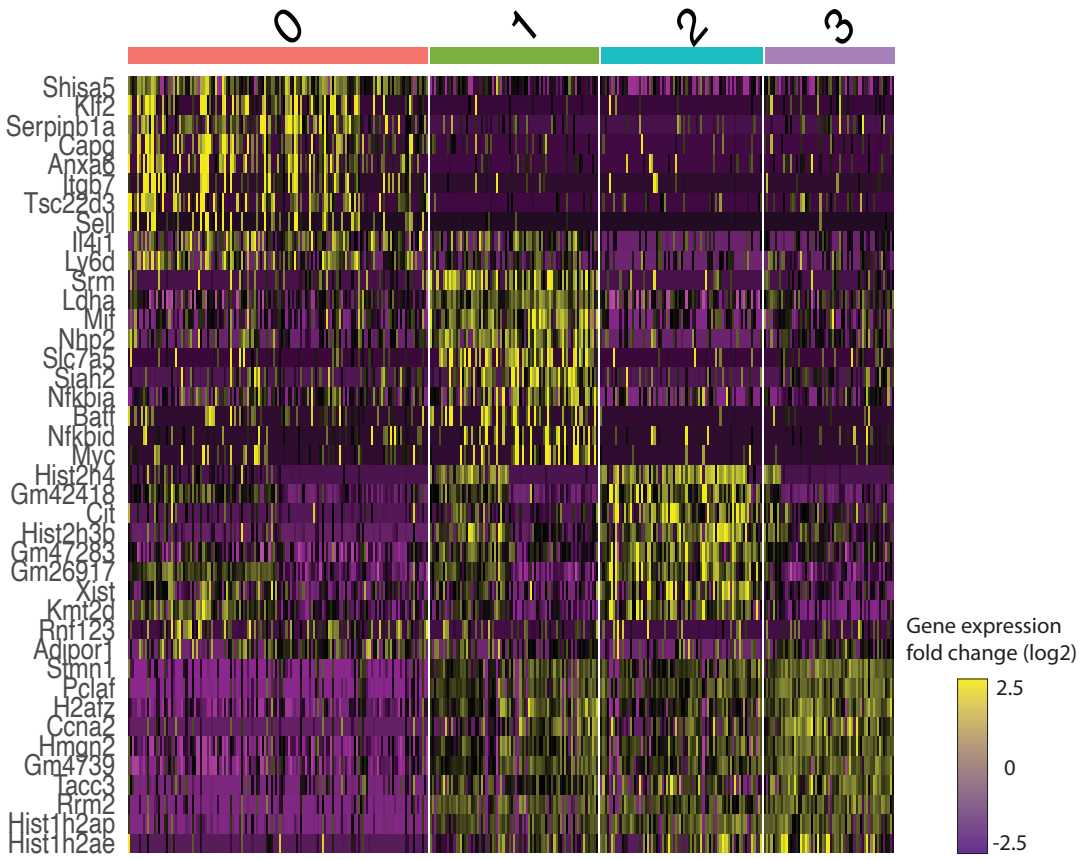

Figure 5.8: LZ cyclic re-entry population shows a high level of heterogeneity on the transcriptomic level.
R26-CreERT2^{+} MHCII$^{fl/fl}$ Fucci2 mice were immunized with SRBCs (i.p). These mice were treated with tamoxifen on day 7 following immunization, and spleens harvested on day 8. Splenic GC LZ MHCII^{high} early S phase B cells (B220^{+}, IgD^{-}, CD95^{+}, GL7^{+}, CD86^{high} and CXCR4^{low} mCherry^{high} mVenus^{+}) were single cell sorted and subjected to single cell RNA sequencing. Heatmap of top ten most variable genes from each cluster.

the flow cytometry data suggesting that recent strong T-B interaction was not the threshold for cyclic re-entry initiation and indeed only a small fraction of cyclic re-entry cells had engaged in strong recent interactions with T cells.

5.7 Cyclic re-entry is not detectably dependent on intracellular c-Myc levels

5.7.1 Optimal c-Myc expression depends on stimulation from both T cell and Btk signalling pathways

c-Myc is a well-defined positive selection marker in GC B cells, which has been first identified to be expressed in a small fraction of GC LZ B cells, marking their superior metabolic conditions over their competitors and suggesting these cells have been positively selected for cyclic re-entry (Calado et al, 2012; Dominguez-Sola et al, 2012; Victora et al, 2022). c-Myc is central to many aspects of cell growth and proliferation, and has been reported to correlate with GC B cells' potential for growth and clonal expansion in DZs (Finkin et al, 2019). Having made the observations that cyclic re-entry initiation was independent of T cells, and possibly did not act as the major barrier for positive selection in the GCs, we now consider if this process relies upon optimal (or detectable) expression of c-Myc.

To study the contribution of c-Myc to cyclic re-entry, a direct reporter for intracellular protein level was needed. To this end, we used a c-Myc-GFP reporter mouse model (Huang, 2008). These mice have a GFP gene introduced in frame into the N terminal of c-Myc gene locus, resulting in a c-Myc-GFP fusion protein. This fusion protein has the same turnover rate/degradation kinetics as the endogenous c-Myc protein (albeit with GFP possibly leading to subtle impacts on turnover rate), making it better suited than a pure transcriptional reporter. Although this strain may suffer in sensitivity due to the relatively slow maturation kinetics of GFP relative to c-Myc protein half-life, it has been proven as a valuable tool for assessing GC biology. This c-Myc reporter also allows direct assessment of c-Myc level in the cell by flow cytometry, bearing the advantage of not requiring intracellular c-Myc staining, which was more difficult than some other transcription factors such as BATF.

5. Evidence of competition in light zones for T cell derived "refuelling" cues

Previous studies have reported that optimal c-Myc expression requires both anti-CD40 and anti-BCR stimulation (Luo et al, 2018). Therefore, to perturb c-Myc level in GC B cells, we utilized MHCII genetic deletion to disrupt the ability of GC B cells to interact with T cells together with a Btk inhibitor, Ibrutinib, to terminate downstream Btk signalling. We first crossed the c-Myc-GFP reporter mice to R26-CreERT2^{+} MHCII$^{fl/fl}$ mice to generate R26-CreERT2^{+} MHCII$^{fl/fl}$ c-Myc$^{GFP/+}$ mice. Then, mixed BM chimeras were generated using cells from these R26-CreERT2^{+} MHCII$^{fl/fl}$ c-Myc$^{GFP/+}$ CD45.2 BM cells together with c-Myc$^{GFP/+}$ CD45.1 BM cells. The recipient mice were rested for 8 weeks and then immunized with SRBCs. Tamoxifen was given by i.p. injections on day 7 to induce MHCII deletion. Finally, two doses of Ibrutinib, 3hrs apart, were given to some mouse cohorts before spleen harvest on day 8.

Following MHCII deletion, there were significant decreases in the frequencies of c-Myc-GFP^{+} cells in LZ MHCII-deleted cells compared with LZ WT cells (Fig. 5.9 A and B). Moreover, the level of c-Myc-GFP intensity per c-Myc-GFP^{+} cell (MFI) also reduced significantly after MHCII deletion (Fig. 5.9 A and C). These results were consistent with the notion that the strength of T cell help could instruct the level of c-Myc expressed in GC B cells (Finkin et al, 2019).

Btk inhibition alone (in LZ WT cells) did not affect the frequencies of c-Myc-GFP^{+} cells or the intensity of c-Myc-GFP per cell (Fig. 5.9A). However, notably, in the MHCII-deleted LZ cells, there was a low but consistent level of residual c-Myc-GFP expression, and this was sensitive to Ibrutinib treatment (Means, Vehicle: 2.34% vs Ibrutinib: 0.39%), supporting previous observations where BCR signalling alone could stimulate c-Myc expression (Fig. 5.9 A and B) (Ramezani-Rad et al, 2020). It was difficult to make a similar comparison to determine the intensity of c-Myc-GFP per residual cell after Ibrutinib treatment in the MHCII-deleted cells, because there were too few positive cells left, meaning that MFI determinations would not be accurate. Given the sensitivity of flow cytometry could not detect every single molecule of c-Myc-GFP, I do note that

it remains possible that some of the c-Myc-GFP$^-$ cells still retained a very low level of c-Myc that is under the detection threshold.

In summary, high levels of c-Myc expression are dependent on B cells interacting with T cells, however, BCR signalling (inferred, but not directly proven, by Btk dependence) alone could maintain low levels of c-Myc when T cell support was absent. A possible explanation would be that low levels of c-Myc are induced and sustained by BCR signalling, but that this signal is only amplified when T cell help is also received.

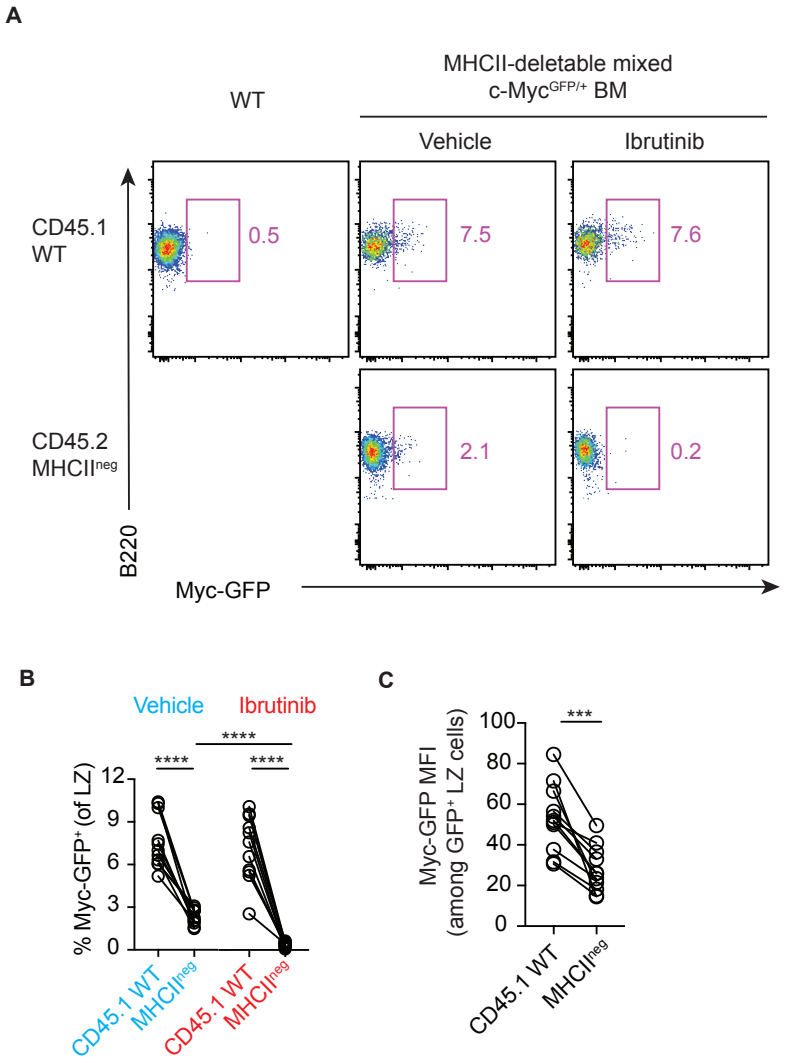

Figure 5.9: Low level of c-Myc is sustained by Btk signalling and amplified by T cell help in LZ B cells.
Mixed BM chimeric mice containing 60% R26-CreERT2^{+} MHCII$^{fl/fl}$ c-Myc$^{GFP/+}$ CD45.2 and 40% WT c-Myc$^{GFP/+}$ CD45.1 BM cells were immunized with SRBCs (i.p.). Tamoxifen was given on day 7 (i.p.). Mice then received two doses of Ibrutinib or vehicle, 6hrs and 3hrs before analysis on day 8. Splenic GC LZ B cells (IgD^{-}, CD95^{+}, GL7^{+}, CD86^{high} and CXCR4^{low}) were analyzed. (A) Representative plots of c-Myc-GFP^{+} population identified in both WT and MHCII deleted LZ cells following tamoxifen in combination with Ibrutinib or vehicle treatment. The gating for c-Myc-GFP was set with GC LZ B cells from SRBC immunized WT C57BL/6 mice. (B) Frequencies of c-Myc-GFP^{+} cells were summarized for each population after different treatments. (C) MFI of c-Myc-GFP^{+} population. MFI of c-Myc-GFP^{-} (WT) population was subtracted from the c-Myc-GFP^{+} population to allow sample pooling across experiments. Results were representative plots (A) or pooled (B, C) from 3 experiments each with 3-4 mice per condition. Lines were joining populations from the same mouse. Analysis, two-tailed paired student T test within treatment group (B) and C, and two-tailed non-paired student T test in MHCII^{neg} population between Vehicle and Ibrutinib (B), ***p $<$ 0.001, ****p $<$ 0.0001.

5.7.2 Cyclic re-entry could still occur when there is no detectable level of c-Myc

Next, we considered whether the tamoxifen and Ibrutinib double treatment, that block both T-B interaction and Btk signalling, would interfere with normal LZ cell cyclic re-entry initiation. These two treatments diminished c-Myc-GFP expression to an undetectable level in LZ B cells, so the dependency of c-Myc in the initiation of cyclic re-entry initiation can also be inferred by these experiments. The same BM chimeras were used, and the same immunisation and treatment regimens applied, as in section 5.7.1. In addition, in order to identify LZ cells in different cell cycle stages, these mice received BrdU and EdU, 100 mins and 40 mins before harvest, respectively.

GC LZ B cells were identified as ($B220^+$, IgD^-, $CD95^+$, $GL7^+$, $CD86^{high}$ and $CXCR4^{low}$) and further sub-gated into MHCII-deleted and WT cells using I-Ab and congenic CD45.1 stain. Then, cells in different cell cycle stages were separated based on EdU and BrdU incorporation in each population. G1 cells were gated as EdU^- $BrdU^-$, and early S phase cells were identified as EdU^- $BrdU^+$ (Fig. 5.6A). Consistent with previous findings (Chapter 3), there was no reduction in the percentage of early S phase cells 24hrs after MHCII deletion (Fig. 5.10A). Moreover, LZ B cells were still capable of initiating cyclic re-entry when they had both lost MHCII and their Btk signalling cascade blocked with Ibrutinib treatment (Fig. 5.10A). The tamoxifen and Ibrutinib double treatment had led to an undetectable level of c-Myc expression in the cells, suggesting these cells transitioned into early S phase with a minimal level of, or no, c-Myc induction (Fig. 5.9A and 5.10A). The percentages of early S phase cells in fact increased in both populations (WT and MHCII-deleted) after Ibrutinib treatment, which was caused by the reduction in the LZ sizes, with Ibrutinib treatment led to LZ contractions, leading to almost 1/3 decrease (Means, Vehicle: 33% vs Ibrutinib: 20%), which recapitulated the previously reported phenotypes of genetic Syk deletion (Fig. 5.10B) (Luo et al, 2018).

In summary, the combination of MHCII deletion and Btk signalling blockade did not stop cyclic re-entry initiation from LZ cells, indicating that cyclic re-entry could be independent of both T cells and BCR signalling and that high levels of c-Myc were not necessary for this process. Given the central importance of T cell driven c-Myc expression during positive selection, its irrelevance to cyclic re-entry is implying T cell mediated positive selection junction did not take place at the point of cyclic re-entry initiation in the LZ. However, while it is fair to make these conclusions based on our findings, we do recognize the important caveat that one cannot be certain of the "absoluteness" of pharmacological blocks and so we do not mean to claim this proves BCR signalling as not playing a role in triggering cyclic re-entry. For this, genetic deletion of critical non-redundant BCR signalling components such as Syk or Btk will be required.

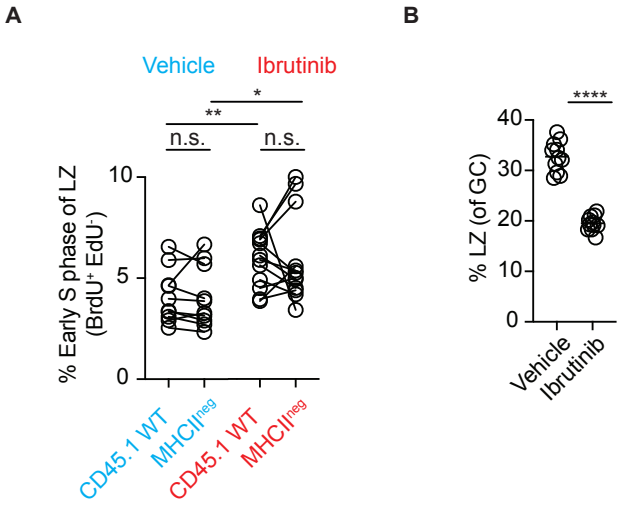

Figure 5.10: Frequencies of LZ early S phase cells remained unchanged after MHCII deletion and Btk signalling inhibition.
Mix BM chimeric mice containing 60% R26-CreERT2^{+} MHCII$^{fl/fl}$ c-Myc$^{GFP/+}$ CD45.2 and 40% WT c-Myc$^{GFP/+}$ CD45.1 BM cells were immunized with SRBCs (i.p.). Tamoxifen was given to mice on day 7 by i.p. injections. Mice then received two doses of Ibrutinib or vehicle, 6hrs and 3hrs before analysis on day 8. Finally, mice were injected with EdU and BrdU, 100mins and 40mins, respectively, before spleen harvest on day 8, respectively. Splenic GC LZ B cells (IgD^{-}, CD95^{+}, GL7^{+}, CD86^{high} and CXCR4^{low}) were analyzed. (A) Frequencies of early S phase cells (BrdU^{+}, EdU^{-}) amongst LZ cells were enumerated. (B) Frequencies of LZ cells after each treatment. Results were pooled from 3 experiments each with 3-4 mice per condition. Lines were joining populations from the same mouse. Analysis, two-tailed paired student T test, *p $<$ 0.05, **p $<$ 0.01, ****p $<$ 0.0001.

5.7.3 Low levels of c-Myc can be sustained in MHCII-deleted LZ B cells 6days after tamoxifen

Our previous observation of low-level T cell independent c-Myc expression was made with 24hrs of MHCII deletion. While unlikely, it was technically possible that the small population of residual c-Myc-GFP^{+} cells in the MHCII-deleted population were not truly MHCII independent but rather arose due to the complicated kinetics of MHCII loss that the cells, with T cell help received after cells entered LZs but prior to them losing MHCII and triggering cyclic re-entry. We believed this highly unlikely due to the relatively short time periods that GC B cells spend in LZs, and because MHCII is preferentially stabilized in that zone as a consequence of LZ cells down-regulating the E3 ubiquitin ligase March1 and increasing its antagonist

CD83, however, this was an important point and so justified additional assessments (Bannard et al, 2016). To exclude this possibility, we made a similar analysis but with a longer rest period given following tamoxifen treatment to ensure the completion of MHCII deletion.

We utilized the BM chimeras made with R26-CreERT2^{+} MHCII$^{fl/fl}$ c-Myc$^{GFP/+}$ CD45.2 and WT c-Myc$^{GFP/+}$ CD45.1 BM cells and treated mice with tamoxifen on day 7 after SRBC immunization. Then, GC responses were analysed on day 13, 6 days after tamoxifen treatment.

Given the half life of tamoxifen *in vivo* is about 6.8 hours and most is cleared from the circulating system within three days, the MHCII deletion should have finished three days before analysis. Consistent with 24hrs time point data, a small population of c-Myc-GFP^{+} cells in MHCII-deleted LZ cells remained 6 days after tamoxifen, with a decrease in the intensity of c-Myc-GFP expression again observed (Fig. 5.11 A and B). Hence, the existence of low level c-Myc-GFP expression was independent of T-B interactions.

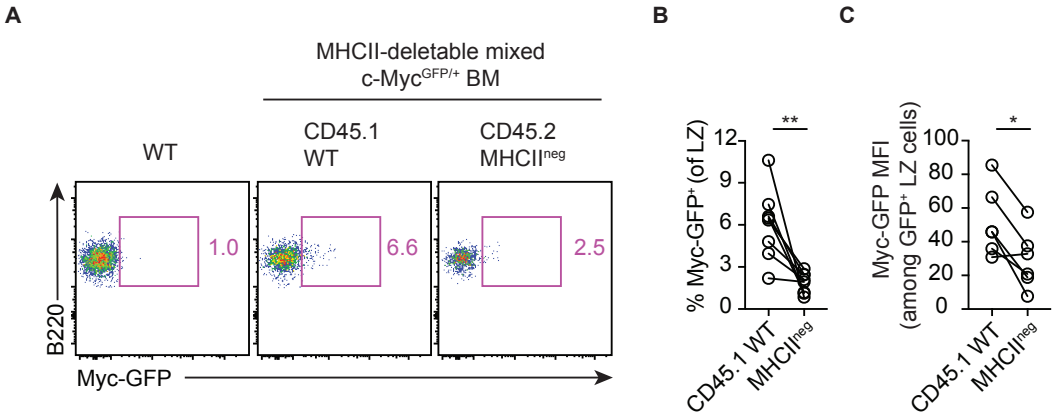

Figure 5.11: Residual low levels of c-Myc-GFP can be sustained 6days after MHCII deletion
Mix BM chimeric mice containing 60% R26-CreERT2^{+} MHCII$^{fl/fl}$ c-Myc$^{GFP/+}$ CD45.2 and 40% WT c-Myc$^{GFP/+}$ CD45.1 BM cells were immunized with SRBCs (i.p.). Tamoxifen was given to mice on day 7 by i.p. injections. Analysis of GC responses was carried out on day 13. (A) Representative FACS plots of c-Myc-GFP^{+} population in either WT or MHCII-deleted LZ GC B cells (IgD^{-}, CD95^{+}, GL7^{+}, CD86^{high} and CXCR4^{low}) and frequencies of c-Myc-GFP^{+} cells were summarized in (B). (C) MFI of c-Myc-GFP^{+} population after subtracting the MFI from c-Myc-GFP^{-} (WT) population. Results were pooled from two experiments each with 3-4 mice per condition. Lines were joining populations from the same mouse. Analysis, two-tailed paired student T test, *$p < 0.05$, **$p < 0.01$

5.8 Conclusion

In Chapter 3 and Chapter 4, we showed that some of the assumptions in the original cyclic re-entry model were not correct. Recent interactions with T cells were not a pre-requisite for cyclic re-entry initiation in the LZ, and the whole process was seemingly independent of any intra-acute GC B cell competition. We, therefore, continued to study how T cell mediated affinity enhancements were conferred to LZ B cells in this chapter, and what were the requirements for LZ B cells to receive T cell mediated refuelling.

We first identified BATF upregulation as a molecular marker for B cells that had engaged in recent interactions with T cells and confirmed its high level expression correlated with c-Myc levels. Next, we investigated whether the amount of T cell mediated refuelling B cells receive was dependent on the BCR affinity. We

utilized a BCR knock-in mouse model SW_{HEL} to allow us to distinguish high and low affinity GC B cells through staining with fluorescently labelled HEL^{3X} protein. We found that higher affinity cells (HEL^{3X+}) were more likely to be refuelled. In addition to affinity, competition between B cells and the intrinsic ability of B cells to acquire antigens also restricted the amount of refuelling that B cells could receive. Hence, B cells were competing for the pro-fitness factors from T cells in an affinity dependent manner.

Notably, in our continuous effort to study the heterogeneity within the cyclic re-entry population, we found that although early S phase LZ populations (i.e., those triggering cyclic re-entry) were enriched for $BATF^{high}$ cells, they still only consisted of 10-20% of the population, presumably reflecting cells could initiate cyclic re-entry regardless of their "refuelled" state. Similar observations were made using single cell RNA sequencing analysis, where we sequenced early S phase LZ cells and found that after unsupervised clustering, only a small cluster of cells displayed cluster signatures enriched with genes involved in refuelling, including c-Myc, NF-kB and BATF. However, despite our effort to look for potential contributors in driving cyclic re-entry initiation by performing differential gene analysis between different populations, the majority of the genes identified in this analysis were cell cycle related. Additional analysis is required to understand what might be the trigger for cyclic re-entry initiation, and what factors might be limiting (or sustained) in terms of metabolic reserves. In terms of the former, one possibility is that Cyclin D3 protein is not entirely lost in all cells. Lastly, we showed that consistent with previous reports, optimal c-Myc expression requires stimulation from both T cell and BCR, however cyclic re-entry initiation occur at a relatively normal rate even when cells were unable to induce c-Myc to a detectable level as a consequence of combined MHCII deletion and Btk inhibitor treatment. This could also be suggesting the lack of involvement of BCR signalling in driving cyclic re-entry. However, given the blockade by small molecule inhibitors may be incomplete, this observation needs to be confirmed with genetic perturbation of components in the BCR signalling pathway.

5. Evidence of competition in light zones for T cell derived "refuelling" cues

When considered together with results from previous chapters, our data points to a more permissive selection model for GC B cells, where instead of competing for direct re-entry into DZ, B cells compete for differential metabolic refuelling from T cells based on the amount of peptide MHCII complexes they present, which will generally correlate with their BCR affinities. Our revised model could potentially contribute to explaining the high level of clonal diversity present in GCs even at relatively late stages of responses (Tas et al, 2016; Kuroaka et al, 2016). We argue that this model goes some way to explaining how GCs balance the needs to promote clonal diversity while simultaneously driving affinity enhancements. This model will be discussed in more detail in Chapter 6.

Chapter 6

Discussion

Contents

Antibody affinity maturation is driven by mutating B cells undergoing iterative rounds of clonal selection in GCs. The clonal selection event itself has long been considered a stringent process in which GC B cells have needed to compete for a "threshold" selection signal – which, for the last ~12 years, has generally been considered to be provided by T cells. Only a very small fraction of LZ cells (estimated ~10-30%) could succeed in this process of initiating cyclic re-entry, with the remaining cells dying in the LZ (Victora et al, 2010). Given that the amount of pMHCII complexes B cells can present is proportional to the affinity

of their BCRs, it has been speculated that only the highest affinity cells in each round of selection could survive this process (Batista et al, 2000; Victora et al, 2012). However, according to the experimental evidence emerging in the last few years, GCs retain surprising amounts of clonal diversity and appear somewhat permissive in terms of the BCR affinities that they can co-support (Tas et al, 2016; Kuraoka et al, 2016). This may have evolved to ensure antibody responses are sufficiently broad and to accommodate more complex maturation pathways, which cannot be easily explained by the cyclic re-entry model. Therefore, in my thesis, we tested critical assumptions in this (cyclic re-entry) model. We found that LZ GC B cells that were incapable of interacting with T cells due to acute loss of MHCII, as well as B cells within GCs lacking T_{FH} cells, could still initiate cyclic re-entry. This G1 to early S phase transition was also not detectably restricted by competition for other resources in the GC, according to experiments in which we deleted competing GC B cells in an unbiased manner. In contrast, our findings showed that LZ cells needed to compete to receive T_{FH} cell mediated refuelling in an affinity dependent manner. Consistent with S phase transition not being the selection barrier, LZ cells initiated this process from differentially refuelled states. In the following section, I aim to outline a working model for clonal selection that we believe to be consistent with these findings.

6.1 A more permissive positive selection helps nurture clonal diversities in GCs

The goal of GC selection is to preferentially expand high affinity B cells targeting both immunodominant and subdominant epitopes. Sometimes it is difficult to achieve this because the pathogens try to hide their critical pathogenic epitopes through heavy glycosylation, molecular mimicry to the host or enhanced rate of mutations to escape from recognition by the existing antibodies. Antibody responses should therefore not only or excessively favour “easy” targets, and to maximise the coverage on the pathogens, complex mutation trajectories are

sometimes indispensable to nurturing antibodies against key epitopes that require a large number of mutations to achieve high binding affinity. As such, the increase in overall antibody affinity that occurs as a result of selection in GCs should not come at the expense of diversity.

For more than a decade, the cyclic re-entry model has predicted that LZ GC B cells must reach an affinity-based selection threshold amount of help from T_{FH} cells if they are to trigger the cyclic re-entry process, and only LZ cells successfully reaching this threshold can survive (Fig. 6.1A). One conceptual concern with such a model is that, if accurate, then most or all LZ cells undergoing cyclic re-entry would subsequently show similar division capacities when they return to DZs. This is because considering the extent of DZ expansion is directly proportional to the amount of T cell help received in LZs, if cyclic re-entry is indeed triggered by threshold-level of T cell help, most of cyclic re-entry cells may initiate this process after having received similar doses (Victora et al, 2010; Pae et al, 2021). However, it was recently demonstrated that DZ cells could divide a different number of times, triggered and regulated by the c-Myc level that was induced in LZs proportional to the amount of T cell help received, proposing the existence of a dynamic range of T cell help can be provided (Calado et al, 2012; Dominguez-Sola et al, 2012; Gitlin et al, 2014; Gitlin et al, 2015; Finkin et al, 2019). Also if the cyclic re-entry model is correct, then one might predict that GCs would become dominated by only very few clones. However, high levels of clonal diversity were demonstrated in two studies in 2016 that tracked GC responses following immunization with complex antigens. These studies confirmed that the overall antibody affinity increased over time. However, they also demonstrated that GCs could co-support cells crossing a range of affinities even at quite late GC stages (both between and within clonal lineages), seemingly contradicting the original selection model that only considers antibody affinity as the only selecting criteria (Kuraoka et al, 2016; Tas et al, 2016).

It is difficult to see how the cyclic re-entry model for selection can explain these observations. Here we propose a revised model where cyclic re-entry initiation

and T cell mediated refuelling are two processes regulated independently, with the latter determining the proliferation potential in the DZ and future performance (Fig. 6.1B). A key difference in this model is that it is largely non-binary. Combined with recently published studies, our data points towards a more merciful two-step positive selection in the GCs. In DZs, GC B cells undergo SHM and risk generating premature stop codons or frameshifts that lead to the expression of non-functional BCRs. Previously, positive selection was thought to have two roles, one being negatively selecting B cells with non-functional BCRs and the second being selecting the highest affinity clones. As such, a high threshold is required to ensure none of these "non-useful" cells could be selected. However, it was recently reported that DZ B cells usually exchange their BCRs within the DZ after each round of SHM, and cells that failed to express a functional BCR mostly did not make it to the LZ stage – instead undergoing apoptosis while still in DZs (Stewart et al, 2018; Mayer et al, 2017). Consequently, some of the burdens for positive selection in LZs have been taken away so that when cells reach that zone, they can be metabolically refuelled depending on the amount of pMHCII complexes presented, which is proportional to the affinity of their new BCRs. This non-binary selection model could allow the co-evolvement of high and low affinity B cells in the GCs – or at least help explain how low affinity clones may avoid being very quickly eliminated. The separation of cyclic re-entry promoting and refuelling cues means cells have the opportunity to return to DZs having been refuelled just a little or to a much greater extent. In silico simulation that was carried out in consideration of our findings supports the separation of cyclic re-entry and later DZ division potential allowing a more diverse response (Meyer-Hermann, 2021).

The model that we propose, and that our findings support, is similar in many aspects to one put forward by Victora and Nussenzweig in a review published around the same time as our study. In that "birth limited" model, the selection barrier lies in the proliferative potential of a particular B cell in the DZ but not necessarily a pass-or-die barrier in the LZ determined by the strength of T cell help (Fig. 6.2B). The review contrasted this with a "death limited" model without

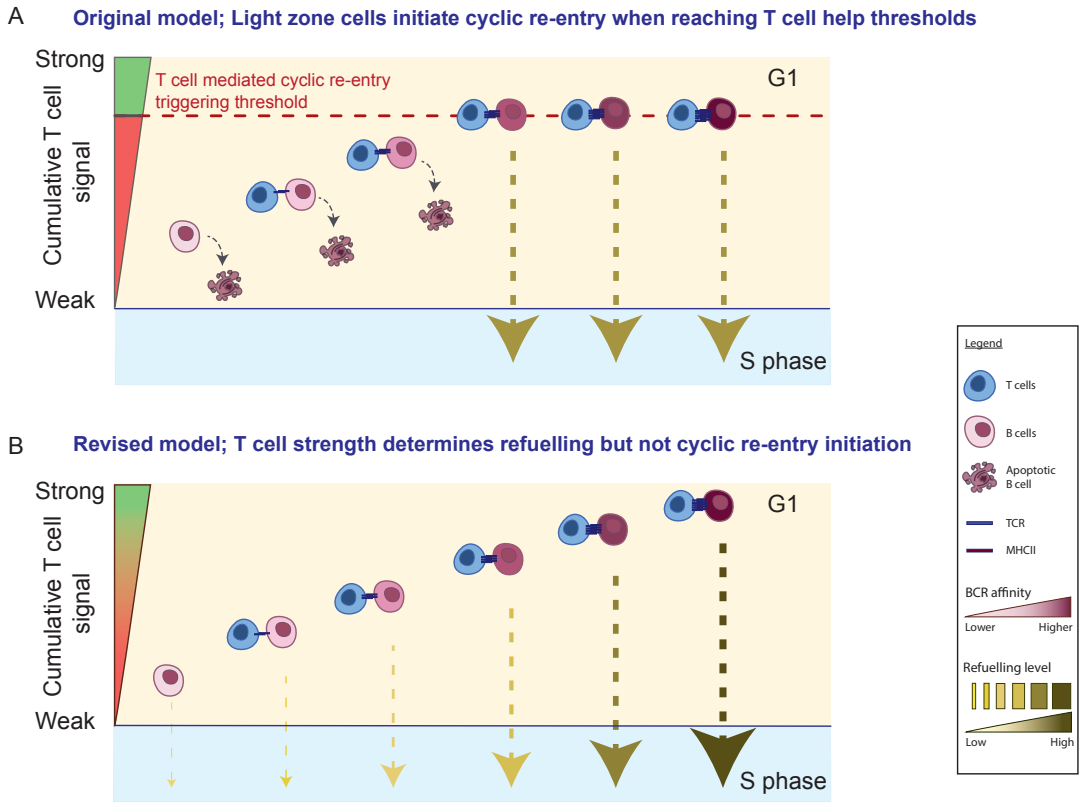

Figure 6.1: Our revised model for how GC positive selection occurs.
GC is the place for affinity maturation by cells diversifying their BCR genes in DZs followed by a subsequent selection process in LZs. In LZs, cells are in quiescent late G1 phase and take up antigens from FDCs, and attempt to engage T_{FH} interactions through antigen presentations. The are multiple possible mechanisms for the selection process. (A) The cyclic re-entry dictates that only cells that receive a threshold level of T cell help are selected to initiate cyclic re-entry. The rest of the cells that fail to receive sufficient help die of neglect. As such, only the highest affinity cells are selected. (B) Our data proposes a revised model, in which undergoing cyclic re-entry and receiving T cell mediately refuelling are two processes regulated independently. At the same time, the strength of T cell mediated refuelling determines the expansion capacity when cells are back in DZs. As such, both high and low affinity cells can initiate cyclic re-entry, just each with different levels of refuelling.

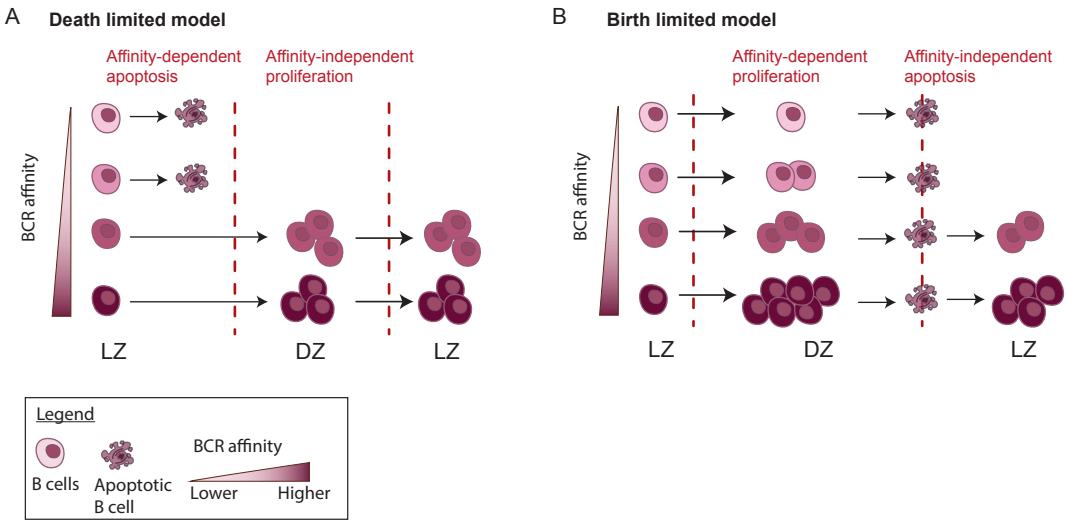

Figure 6.2: Birth and death limited selection models in GCs.
(A) Death limited model predicts that the positive selection occurs by selecting higher affinity cells for the avoidance of their death in the LZ, and only these selected cells can return to DZs and undergo subsequent cell divisions. While the low affinity cells are eliminated from GCs because they do not receive enough T cell help and die in LZs. (B) In the birth limited model, different affinity cells can co-exist and they can all return to DZs. The proliferation capacity they bear in DZs is dependent on the accumulative strength of T cell help they received in previous LZ visits. (Adapted from Victora and Nussenzweig, 2022)

favouring one over the other; in this latter setting clonal selection takes place by cells actively competing for resources to be selected, and cells failing this process die of apoptosis (Fig. 6.2A). These two models are not mutually exclusive. The initial stage of the responses may be more limited by the death limited selection. During the steady state, the birth limited selection may contribute more to expanding the more fit clones. In addition, we propose that GC cells that "exhausted" their ability to undergo T cell independent cyclic re-entry may be capable of being rescued if they then receive T cell support. This might explain why cyclic re-entry initiation rates decreased slightly at later time points post MHCII deletion.

Our revised model could better explain the development of complex antibodies. B cells with "knockin" BCRs unspecific for immunizing antigens showed the capability to enter GCs and affinity maturation over a long time of chronic immunizations showing that, at least in certain experimental settings, extremely low affinity antibodies can be retained for affinity maturation (Silver et al, 2018). The development of broadly neutralizing antibodies to HIV has also strongly suggested similar principles. Broadly neutralizing antibodies can be identified with low frequencies in people infected with HIV, however, these antibodies take years to affinity mature (Mikell et al, 2011; McCoy et al, 2013). Moreover, on average these antibodies carry three times more SHMs compared with normal antibodies and could require more than 100 mutations to achieve full neutralizing potential (Tiller et al, 2007; Walker et al, 2011). The germline precursors start with close to the non-detectable level of affinity and require significant time in the GCs to accumulate all these necessary mutations. These antibodies can only be developed in a relatively permissive environment, as our model has proposed, that lower affinity antibodies can be developed by retaining them with low strength of T cell help to allow the accumulation of all the necessary mutations.

One potential mechanism for these low affinity cells to accumulate more T cell help is by conferring them more dwell time in the LZ each time that they visit. When we combined the Fucci system with the BrdU pulse chase experiment, we found that lower affinity cells, on average, spent more time in the LZ before they initiated cyclic re-entry, indicating that the length of LZ stay could be different between individual LZ cells, permitting them to accumulate antigens and refuelling before initiating cyclic re-entry (Long et al, 2022). Lower affinity cells hence could have a longer resting time in the LZs, increasing their probability of gathering refuelling, potentially supporting the survival of these cells in GCs to sustain clonal diversity.

Finally, despite T cell interactions being vital during affinity discrimination and conferring selective advantage to high affinity cells, the availability of T cell help in the LZs may not be the sole limiting factor determining if refuelling is provided.

The intrinsic ability of B cells to acquire antigens may also be a contributing factor. This is because by supplementing the system with more antigens alone, there was a significant increase in the number of refuelled LZ cells, and there was no change in the amount of help or the level of competition. LZ cells that acquire a large amount of antigens through either affinity enhancing mutations or stochasticity may break off from the constraint and expand quickly, possibly seeding clonal bursts. The latter may be one additional possible mechanism supporting the complex affinity maturation pathways, in which some low affinity cells can periodically receive sufficient refuelling to survive in GCs.

To summarize, our findings provide new conceptual explanations for the diversity sustenance in GCs by replacing the stringent cyclic re-entry selection barrier with a more permissive selection process which depends on the affinity-based T cell-mediated refuelling. But at the same time, our model proposes new questions, and one of them is then what are the possible pathways in LZ B cells to be refuelled by T cells that can influence their future performance.

6.2 Refuelling potentially feeds into pathways regulating B cell metabolism and DZ maintenance

Multiple pathways have been shown to be involved in T cell mediated refuelling, mainly focussing on the ones controlling cell growth, cell proliferation, DZ phenotype induction and maintenance. Most notably would be the NF-kB pathways. In GCs B cells, BCR signalling appears to be re-wired, with its activation selectively inducing AKT phosphorylation without inducing activation of NF-kB pathways (in contrast to naïve B cells) (Luo et al, 2018). On the other side, signalling through CD40 can induce optimal NF-kB activity, as demonstrated by the nuclear translocation of c-Rel and RelA (Luo et al, 2018). NF-kB pathway is one of the central signalling pathways in immune cells and regulates many aspects of the cell proliferation and

growth (Kaileh et al, 2012). In GC B cells, it has been shown to be important for GC maintenance (Pohl et al, 2002). One of its targets would be c-Myc. c-Myc is a key cell cycle/metabolic regulator and has been shown to promote a higher proliferative state in the GC B cells in a dose dependent manner in response to the amount of T cell help the LZ B cell receives (Finkin et al, 2019).

A related pathway that is induced in GC B cells by T cell help is mTORC1, as shown by the pS6 staining (Ersching et al, 2017). S6 is a component of ribosomes so its phosphorylation directly correlates with rates of protein translation. Stimulation of these pathways potentially leads to the upregulation of cyclin D3, which controls the rate of cell cycle progression in DZs (Pae et al, 2021). However, these are all upstream regulators for cell metabolism, in future studies more direct measurements of the rate of protein synthesis as readouts for metabolic status can be made with puromycin analogue OPP (O-propargyl-puromycin) mediated protein labelling. OPP can be efficiently incorporated into newly synthesized proteins during translation *in vitro* and *in vivo* and can be detected by click chemistry so that the level of its incorporation can be assessed by flow cytometry (Signer et al, 2014). It will therefore be interesting to test if T cell refuelling feeds into the biogenesis of target cells using OPP labelling and the MHCII deletable chimeric mouse model. In this experiment, the level of *in vivo* OPP incorporation will be assessed in both WT and MHCII-deleted LZ B cells to assess the impact of T cell help on the LZ B cell metabolism.

Another important aspect that affects cell performance after cyclic re-entry initiation is their potential for DZ maintenance. Interactions with T cells lead to the upregulation of BATF, which is important in sustaining DZ phenotypes (Inoue et al, 2017). Although BATF is downregulated quickly after B cells move away from T cells, most LZ cells have higher than basal BATF levels when compared to $Batf^{-/-}$ controls (even after anti-CD40L block), suggesting these cells have reserves when they return to DZs (Inoue et al, 2017). Our data did not demonstrate the level of BATF induction is directly proportional to the BCR affinity, but higher

affinity cells still showed higher level of BATF in general, potentially promoting the length of their stay in DZs.

In summary, the refuelling resources that GC B cells are receiving from T_{FH} cells are stimulations that potentially upregulate metabolism activities for proliferation and DZ maintenance, both of which provide the cells with advantages in DZ performance.

6.3 How cyclic re-entry and DZ phenotype induction processes are correlated

The first step of cyclic re-entry is the transition from the resting late G1 state into early S phase again. Subsequently, these cells need to upregulate the DZ program related genes to prepare them for physical movement back into DZs. The DZ phenotype is mainly controlled by FoxO1, and one of its essential targets is CXCR4 (Dominguez-Sola et al, 2015; Sander 2015). FoxO1 activity is repressed by BCR signalling pathways, with AKT phosphorylating and inactivating FoxO1 by their nuclear exclusion. In the LZ, antigen encountering stimulates BCR and activates AKT, thereby inhibiting FoxO1 activity from allowing cells to adopt LZ phenotypes. The identification of the colocalization of c-Myc and nuclear FoxO1 in LZ B cells implied that positive selection de-represses FoxO1, preparing cells for DZ movement (Finkin et al, 2019).

However, now that cyclic re-entry initiation is independent of recent T-B interactions, how would LZ B cells make the decision to upregulate DZ phenotypes? One possible contributing factor is the CbI induced auto degradation of Syk, which activates FoxO1 by dephosphorylating Akt kinases (Davidzohn et al, 2020). However, in the same study, the relatively normal-sized DZs in Syk mutants resisting ubiquitination and degradation suggest the involvement of more components in this process. Meanwhile, when FoxO1 was defective or when Syk kinases were hyperactive, the cells started to have LZ-like phenotypes while they were still

proliferating like DZ cells (Dominguez-Sola et al, 2015; Sander 2015). And when cells were defective in CXCR4, they were still able to proliferate and accumulate SHMs, albeit at lower frequencies. These studies are suggesting that the proliferation and DZ program maintenance could be two independent parallel processes controlled by the same upstream pathways. Or there is an unlikely possibility that cyclins/other cell cycle related regulators are feeding into FoxO1 pathways. In summary, we can at best speculate about the regulation of FoxO1 to be independent of proliferation in GC B cells. Moreover, given we assessed only the cyclic re-entry initiation step, the translocation of FoxO1, upregulation of DZ phenotypes and actual physical movement of the unhelped cells back into DZs remains to be proven.

6.4 Cyclic re-entry is potentially driven by tonic BCR signalling or inertia

Our study revealed that cyclic re-entry was not detectibly restricted by any form of competition and did not acutely require T cell derived signals. Consequently an important question remains unanswered: what cues drive cyclic re-entry, if not T cells or competition for antigens? Here we propose two potential candidates.

The first possibility is that a low "threshold" level of BCR signalling triggers the cyclic re-entry process – essentially the intrinsic ability of the B cell to sense the antigen. Teleologically, this would mean that the cyclic re-entry initiation step involves B cells testing that they remain specific, but it would not meaningfully select for affinity. BCR signalling alone was previously shown to be sufficient to induce c-Myc to a low level *ex vivo*, and in our hands, it appeared sufficient to sustain detectable c-Myc levels *in vivo* when T cell refuelling was absent (Ramezani-Rad et al, 2020). Other studies have shown that BCR-dependent signals can induce early-stage plasma cell differentiation independent of T cell inputs (Krautler et al, 2017). Hence, it is possible that BCR signalling was sufficient to sustain the minimal level of c-Myc-related growth signalling pathways to drive cyclic re-entry.

However, our current experimental evidence was inconclusive in terms of supporting this hypothesis. When we treated mice with the Btk inhibitor Ibrutinib, combined with MHCII deletion, c-Myc expression was reduced to an undetectable level, yet no reduction in cyclic re-entry initiation was observed. Also, we failed to observe an enhanced rate of LZ S phase entry when we augmented BCR engagement by delivering a boost of antigen the day before analysis. These findings might suggest cyclic re-entry to occur independently of c-Myc expression, and in a BCR independent fashion. However, we certainly do not mean at this stage to infer that these results are conclusive and additional experimentation is needed. One particular caveat in our experiments is that we cannot be sure that the Ibrutinib-mediated BCR signalling block is absolute.

A definitive test for the role of BCR signaling in the cyclic re-entry process requires additional tools. To this end, we are now generating S1PR2-CreERT2 $Syk^{fl/fl}$ mice to inducibly block Btk signalling genetically. The requirement for cognate BCR signalling in driving cyclic re-entry can potentially be tested with mouse models whose BCR specificity can be switched by Cre recombinase activities (Oberdoerffer et al, 2003; Maruyama et al, 2000). These B cells can be driven into GC responses with immunogen recognized by the knockin BCRs in the correct orientation before Cre activities. Then tamoxifen treatment can induce the excision of the BCRs immunized against while turning on the expression of a BCR with irrelevant specificity. If these cells are still able to initiate cyclic re-entry, this would then suggest the stimulation of BCRs by the antigens is unnecessary for cyclic re-entry initiation but rather the presence of integrative BCRs is sufficient for this process. However, a potential confounding issue with both these approaches remains the relatively crude temporal kinetics provided by tamoxifen-inducible Cre, and therefore additional approaches involving degron-based or similar systems may be needed.

If GC B cells are ultimately found to initiate cyclic re-entry independently of BCR signalling, then this would suggest that the process may be driven by cell intrinsic properties that were set into play during earlier events, a form of

"inertia" (the second candidate). We observed that higher affinity cells were overall in a more proliferative state than their lower affinity neighbours, resulting in them progressing through the cell cycle faster in both LZs and DZs. Therefore, cells that receive more refuelling during previous LZ visits may retain more metabolic and proliferation-supporting reserves by the time they finish DZ proliferation and return to LZ again, potentially helping them to initiate cyclic re-entry even without particular inputs. The molecular mechanism by which this might occur is not clear, however we can speculate. Cyclin D3 has recently been identified to be necessary for controlling the G1 to S checkpoint in DZs but not LZs (Pae et al, 2021). Consistent with this, cyclin D3 protein appeared more abundant in DZs than LZs by western blot – however bands were present for both zones. It remained possible that the lowly expressed residual level of cyclin D3 may be sufficient to drive one further round of cyclic re-entry in LZs. Moreover, despite total inhibition of cyclin activity stopping G1 to S phase transition in both LZs and DZs, depletion of either cyclin D2 or cyclin D3 alone significantly impacted this process in LZs (Pae et al, 2021). As such, it seems plausible if not likely that some amount of redundancy exists between the 3 cyclin D members, and that the retention of some cyclin D3 by certain LZ cells is sufficient to push them back into cell cycle even if it is not always required.

Our findings also raised the question of whether cyclic re-entry initiation is acutely dependent upon c-Myc induction. Being a central regulator for GC positive selection and cell cycle progression, it has been proposed that c-Myc is upregulated in the selected cells before their transition from resting state into active cell cycle again (Calado et al, 2012; Dominguez-Sola et al, 2012, Victora et al, 2022). However, in our experiments seemingly c-Myc was not required for cyclic re-entry because dual treatment of MHCII deletion and Btk signalling blockade resulted in almost complete loss of c-Myc-GFP^{+} cells and yet the cyclic re-entry was not affected, indicating many cells were initiating cyclic re-entry from c-Myc negative state. However, there are a few alternative possibilities that could explain the absence of c-Myc upregulation in the cyclic re-entry LZ cells. One possibility is that we are using c-Myc-GFP reporter mice; limited by the resolution of flow cytometry and GFP

reporter, it is difficult to confirm whether the cells are absolutely negative for c-Myc or some of them still have an undetectable level of c-Myc that was sufficient to initiate cyclic re-entry. Another possibility is that c-Myc was not sustained, but it has fed into downstream targets, and those pathways can still drive cyclic re-entry initiation.

Given the loss of c-Myc leads to ultimate GC dissolution, in order to tease apart the roles of c-Myc in sustaining GC participation and cyclic re-entry, we are considering the acute inhibition of c-Myc activities. Cre recombinase is not most suitable for this purpose because it has asynchronous activities, making it difficult to determine the kinetics of c-Myc loss. c-Myc inhibitors may be used instead despite the caveat that the inhibition may not be complete (Madden et al, 2021). Or alternatively, we are now developing an auxin inducible degron system operator mouse line, with which c-Myc can be tagged with degron and targeted for very rapid degradation by the administration of auxin (Natsume et al, 2016).

In conclusion, so far we have demonstrated that provisionally neither BCR signalling nor c-Myc induction was required for cyclic re-entry initiation and we are now in the process of generating mouse models to provide more definitive answers to these questions.

6.5 Fate decision process in GCs

Another important question that arises from our study is how the fate decision process is carried out in GC LZ cells. LZ cells can potentially bear three fates; differentiate into plasma cells, become memory B cells or undergo cyclic re-entry and return to DZs for further SHM and proliferation. Cells unselected into any of these fates ultimately die of metabolic failures. There are several models currently deciphering potential mechanisms.

One possible model is that the fate decision process is instructed by the cumulative strength of the stimuli that LZ cells have received. Previous studies

suggested that T_{FH} cell help strength can dictate the choice between plasma cell or cyclic re-entry (Ise et al, 2018). The strongest T cells help directly upregulates IRF4 in LZ B cells, which is central to plasma cell differentiation and pre-determines the fate of plasma cells (Inoue et al, 2020). While slightly less strong T cell help induces the upregulation of c-Myc, which is the signature for cyclic re-entry GC B cell fate (Calado et al, 2012; Dominguez-Sola et al, 2012; Finkin et al, 2019). In this model, memory B cells are considered to arise from the quiescent population as demonstrated in multiple studies where the precursors are enriched in the cells with the longest residing time in the GC (Suan et al, 2017; Wang et al, 2017). The memory cell differentiation in GCs has been proposed to be associated with a sub-optimal level of T cell help, resulting in them being low in mTOR activities (Inoue et al, 2020; Laidlaw et al, 2020). Other fate decision models include the asymmetric fate model, where GC B cells undergo asymmetric cell divisions, due to their cell polarization when interacting with T_{FH} cells, resulting in the daughter cells inheriting different amounts of transcription factors. And the level of inherited amount of IRF4 and c-Myc resulted in cells differentiation into plasma cells or cycling GC B cells (Laidlaw et al, 2020). But in contrast, *in vitro* studies and simulations suggested symmetric cell division in B cells (Thomas et al, 2019; Duffy et al, 2012).

However, our revised model for cyclic re-entry, in which cells are capable of initiating cyclic re-entry from different refuelled states, indicates that the decision to undergo this process is not through acute active selection (at least in a competitive manner, or from T cells), posing the question of how the fate decision process is determined in GCs? If cyclic re-entry initiation is driven by tonic BCR signalling, then the decision to choose any of the three fates requires integrative inputs from the BCR signalling and the strength of T_{FH} cell help. Or, if the cyclic re-entry is driven by inertia, then the fate decision process may depend on the metabolic reserve the cells are left with – here it is the sum between what they retain by the time they return to LZs together with the strength of T_{FH} cell help they receive again during a given LZ visit. If cells are rich in metabolic reserves, initiating cyclic re-entry may be their default fate in the LZ, unless they receive more/stronger stimuli by which

they then could be biased towards the plasma cell fate. When cells return to the LZ but are low in the reserves, they may not immediately initiate another round of cyclic re-entry, but rather extend their length of stay in the LZ to gather more refuelling or another possible fate for them is to differentiate into memory B cells.

Another possible mechanism for this fate decision process is an integrative fate decision model. Previous studies support that there is a high level of heterogeneity in the epigenetic and transcriptomic levels in the LZ cells, which may explain why individual cells respond differently to external cues (Young et al, 2021; Radtke et al, 2019). It is possible that cells are already pre-sensitized to different fates based on their signalling history upon returning to LZs, but the ultimate cell fate can still be influenced by the stimuli they receive before differentiation. In summary, the question of how terminal fate decisions are made in GCs has been investigated for several decades. Our work does not directly address this issue, but our findings do provide additional insights that are impossible to ignore in relation to this question. It is clear that there is still much still to learn.

6.6 Caveats in our studies

A major limitation of our study is that we are using late G1 to early S phase transition in the LZ cells to measure cyclic re-entry initiation; the subsequent movement of the unhelped LZ cells back to DZs remains to be proven. Intravital microscopy would provide the most definitive answer to this question by directly tracking the movement of early S phase MHCII-deleted cells back to DZs *in vivo*. A direct reporter for MHCII would then be required to visualize the surface MHCII level to identify these cells *in vivo*. However, given that the resolution in the microscopy is not down to a single fluorescent protein level, it is difficult to be certain that no visible signal reflects complete MHCII deletion. One way around this might be to combine imaging approaches with antibody-mediated MHCII blocking – although very careful controls will be needed. To address this question

from a slightly different angle, FoxO1 nuclear translocation may be assessed in the MHCII-deleted LZ cells. FoxO1 controls the induction of DZ phenotypes; hence its nuclear import would be a more direct indication of the induction of DZ programs (Dominguez-Sola et al, 2015; Sander et al, 2015). This experiment is technically challenging because the early S phase MHCII-deleted LZ cells are a relatively rare population; the fluorescent features of a large number of GC B cells need to be analyzed. ImageStream supports the combination of flow cytometric and photometric analysis in a high throughput manner (Zuba-Surma et al, 2007). However, the channels on Imagestream are more limited than other high-end flow cytometry analyzers. It already requires a minimum of five fluorophores to identify GC B cells, thus making subsequent identification of MHCII level and FoxO1 staining very challenging. However, this is an approach we aim to follow.

Another important unanswered question is why the rate of cyclic re-entry initiation decreased at the later time points after MHCII deletions? Considering the asynchronous Cre activity that complicated the MHCII turnover, the most trivial explanation would be that some of these cells lost MHCII after interacting with T_{FH} cells and receiving the stimulation for cyclic re-entry initiation. However, this is a very unlikely possibility. First, the general resident time of LZ cells is insufficient for this whole series of events to play out in one LZ visit. It roughly takes about 8hrs for the DZ cells to exit the cell cycle, downregulate CXCR4 and migrate back to LZs (Stewart et al, 2018). Using EdU and BrdU combined with Fucci to track when the early S phase LZ cells were last in the active cell cycle, we observed that more than 50% of GC LZ B cells initiate cyclic re-entry within 12hrs of their last mitotic event (Long et al, 2022). As a consequence, this would leave new entrants with only 4 hours in the LZ before they re-enter S phase. Considering that LZ cells have very stable MHCII, these observations strongly argue that cells would not have sufficient time to acquire antigens, process and present cognate peptides on MHCII, interact with T cells, initiate cyclic re-entry and then lose MHCII expression due to Cre activities (Bannard et al, 2016). Second, we used BATF as a marker for recent T-B interactions and showed that 24hrs after MHCII deletion, the frequencies of

$BATF^{high}$ cells dropped significantly, showing cells had lost functional interactions with T cells by the time of cyclic re-entry analysis. Thirdly, at later time points after tamoxifen (4days and 6days), when tamoxifen should be cleared from the system hence MHCII deletions should have been completed for some time, the MHCII deleted cells were still able to transition into the early S phase, strongly supporting that T cells were not required for cyclic re-entry initiation.

Despite cyclic re-entry seeming to be initiated independently of any stimulation from T cells or the GC niche environment, the frequencies of early S phase LZ MHCII-deleted cells dropped after 48hrs tamoxifen, and later stage cell cycle transition was also affected. This observation differed from the T cell ablation experiment, where no apparent defects in cyclic re-entry initiation were observed. The discrepancies between the two experiments could be due to the differences between the two experimental settings; in the T cell ablation experiment, the intra-GC competition was removed completely, but in the $MHCII^{fl/fl}$: WT BM chimeras, the MHCII-deleted cells co-existed with the WT cells in GCs, which could amplify their defects in the competition. Furthermore, the regulatory environment could have been changed when all T_{FH} cells were depleted at once, which could rewire some of the regulatory networks in GCs. Another possibility is that this frequency drop reflected secondary effects after LZ B cells lost contact with T cells. Because we started to see the decline of early S phase MHCII-deleted cells from 48hrs, where the cells could have lost MHCII and then still cycled between DZs and LZs for a few rounds in the meantime, relying on the reserves they previously accumulated before MHCII deletion. As touched on in an earlier section, it is possible that some of these cells failed to re-enter cell cycle because they ran out of their metabolic reserves.

Despite these caveats, our study has significance in clearly demonstrating the cyclic re-entry initiation step is not dependent on T cell/competition-based selection, revising the current model and providing a conceptual explanation of how GC responses are capable of promoting affinity maturation but not at the expense of clonal diversity.

6.7 Additional future directions; other sources of permissiveness in the GC positive selection process

Our revised model helps explain how less competitive B cells avoid immediate deletion when they enter LZs and provides a framework for how they can be refuelled in proportion to their BCR affinity. However, additional sources of permissiveness probably exist in GCs. This assertion is supported by the observation that BATF^{high} refuelled populations are enriched but not uniform for high affinity cells in our experimental systems. This raises the possibility that competition itself may be noisy, and that this too may contribute to supporting clonal diversity. We propose there are two possible stages at which this noisiness or permissiveness may occur – and we plan to test them in future studies. The first is during the antigen acquisition stage. While it is quite clear that higher affinity B cells will on average acquire more antigen than lower affinity cells, it seems likely that this rule will not be absolute and that low affinity cells may sometime mascaraed as high affinity as a result of stochastic encounters with large immune complexes. Such cells would be capable of presenting more pMHCII to T cells than is typical for cells of their affinity, and as such they would receive a high level of T cell mediated refuelling that is enough to sustain their continued participation in the GCs. Alternatively, permissiveness or noise may occur at the point of T-B interactions during the refuelling process. Conventionally the amount of T cell mediated refuelling the B cells accumulatively receive is proportional to the affinity of BCRs. However, it is plausible that T cells may sometimes "misread" this and provide support to B cells expressing modest amounts of pMHCII, or lower affinity B cells may sometimes run into particularly "generous" (highly activated) T cells or from the local environment (Quast et al, 2022).

If the first hypothesis is correct, then periodically low affinity cells can be identified in the population with highest level of antigen presentation (highest

pMHCII level). To test this, LZ B cells with highest pMHCII expression can be single cell sorted and have their BCR cloned into expression vectors. Then low affinity binders are expected to be found in these cells. In contrast, to test the second hypothesis, GC B cells can be sorted based on their BATF level, which reports their refuelling status, followed by *in vitro* expression of the antibodies from the sorted cells. If the second hypothesis is true, then low affinity antibodies should be identified in the population with high level BATF expression.

6.8 Summary

In summary, in my thesis, I have tested key assumptions in the cyclic re-entry model, starting from the requirement of LZ B cells competing for T_{FH} cells derived stimuli to transition from late G1 to early S phase. Much to our surprise, we found T cells were dispensable for this process as cyclic re-entry could still be initiated in GCs lacking T_{FH} cells as well as by LZ B cells that lacked MHCII expression. Furthermore, LZ B cells also did not appear to need to compete for any other resources to pass this key transition. However, we found that higher affinity cells were overall in a higher proliferative state, with them transitioning faster in cell cycle stages in both LZs and DZs. Then using BATF as the molecular marker for recent T-B interactions, we demonstrated that receiving T cell refuelling is an affinity based competitive process.

Our observations support a positive selection model based on the proliferative potential of the GC B cells, but not necessarily the amount of T cell help it gathered in a particular LZ visit. According to our data, LZ cells receiving different amounts of refuelling can return to DZs but do so in different metabolic states. This less binary selection model helps to explain how some antibodies with close to non-detectable levels of affinity can be affinity-matured via complex SHM trajectories in the GCs concurrently with high affinity ones. Moreover, a selection model that does not consider affinity as the only selection criteria allow GCs to improve the

overall antibody affinity over the course of the responses while maintaining relatively high diversity to develop antibodies with complex maturation pathways and allow good coverage of epitopes to prevent escape mutations as well as to prepare for future encountering of similar pathogens.

Bibliography

Abe, T., Sakaue-Sawano, A., Kiyonari, H., Shioi, G., Inoue, K., Horiuchi, T., Nakao, K., Miyawaki, A., Aizawa, S., and Fujimori, T. (2013). Visualization of cell cycle in mouse embryos with Fucci2 reporter directed by Rosa26 promoter. Development 140, 237-246. 10.1242/dev.084111.

Akkaya, M., Kwak, K., and Pierce, S.K. (2020). B cell memory: building two walls of protection against pathogens. Nat Rev Immunol 20, 229-238. 10.1038/s41577-019-0244-2.

Allen, C.D. (2015). Germinal center quality control: death by Fas. Immunity 42, 783-785. 10.1016/j.immuni.2015.05.005.

Allen, C.D., Ansel, K.M., Low, C., Lesley, R., Tamamura, H., Fujii, N., and Cyster, J.G. (2004). Germinal center dark and light zone organization is mediated by CXCR4 and CXCR5. Nat Immunol 5, 943-952. 10.1038/ni1100.

Allen, C.D., Okada, T., Tang, H.L., and Cyster, J.G. (2007). Imaging of germinal center selection events during affinity maturation. Science 315, 528-531. 10.1126/science.1136736.

Amarante-Mendes, G.P., Adjemian, S., Branco, L.M., Zanetti, L.C., Weinlich, R., and Bortoluci, K.R. (2018). Pattern Recognition Receptors and the Host Cell Death Molecular Machinery. Front Immunol 9, 2379. 10.3389/fimmu.2018.02379.

Ansel, K.M., McHeyzer-Williams, L.J., Ngo, V.N., McHeyzer-Williams, M.G., and Cyster, J.G. (1999). In vivo-activated CD4 T cells upregulate CXC chemokine receptor 5 and reprogram their response to lymphoid chemokines. J Exp Med 190, 1123-1134. 10.1084/jem.190.8.1123.

Bannard, O., Horton, R.M., Allen, C.D., An, J., Nagasawa, T., and Cyster, J.G. (2013). Germinal center centroblasts transition to a centrocyte phenotype according to a timed program and depend on the dark zone for effective selection. Immunity 39, 912-924. 10.1016/j.immuni.2013.08.038.

Bannard, O., McGowan, S.J., Ersching, J., Ishido, S., Victora, G.D., Shin, J.S., and Cyster, J.G. (2016). Ubiquitin-mediated fluctuations in MHC class II facilitate efficient germinal center B cell responses. J Exp Med 213, 993-1009. 10.1084/jem.20151682.

Barnden, M.J., Allison, J., Heath, W.R., and Carbone, F.R. (1998). Defective TCR expression in transgenic mice constructed using cDNA-based alpha- and beta-chain genes under the control of heterologous regulatory elements. Immunol Cell Biol 76, 34-40. 10.1046/j.1440-1711.1998.00709.x.

Basso, K., and Dalla-Favera, R. (2010). BCL6: master regulator of the germinal center reaction and key oncogene in B cell lymphomagenesis. Adv Immunol 105,

193-210. 10.1016/S0065-2776(10)05007-8.

Basu, U., Chaudhuri, J., Alpert, C., Dutt, S., Ranganath, S., Li, G., Schrum, J.P., Manis, J.P., and Alt, F.W. (2005). The AID antibody diversification enzyme is regulated by protein kinase A phosphorylation. Nature 438, 508-511. 10.1038/nature04255.

Batista, F.D., and Neuberger, M.S. (2000). B cells extract and present immobilized antigen: implications for affinity discrimination. EMBO J 19, 513-520. 10.1093/emboj/19.4.513.

Baumgarth, N. (2011). The double life of a B-1 cell: self-reactivity selects for protective effector functions. Nat Rev Immunol 11, 34-46. 10.1038/nri2901.

Baumjohann, D., Preite, S., Reboldi, A., Ronchi, F., Ansel, K.M., Lanzavecchia, A., and Sallusto, F. (2013). Persistent antigen and germinal center B cells sustain T follicular helper cell responses and phenotype. Immunity 38, 596-605. 10.1016/j.immuni.2012.11.020.

Benson, M.J., Elgueta, R., Schpero, W., Molloy, M., Zhang, W., Usherwood, E., and Noelle, R.J. (2009). Distinction of the memory B cell response to cognate antigen versus bystander inflammatory signals. J Exp Med 206, 2013-2025. 10.1084/jem.20090667.

Blink, E.J., Light, A., Kallies, A., Nutt, S.L., Hodgkin, P.D., and Tarlinton, D.M. (2005). Early appearance of germinal center-derived memory B cells and plasma cells in blood after primary immunization. J Exp Med 201, 545-554. 10.1084/jem.20042060.

Briney, B., Inderbitzin, A., Joyce, C., and Burton, D.R. (2019). Commonality despite exceptional diversity in the baseline human antibody repertoire. Nature 566, 393-397. 10.1038/s41586-019-0879-y.

Buch, T., Heppner, F.L., Tertilt, C., Heinen, T.J., Kremer, M., Wunderlich, F.T., Jung, S., and Waisman, A. (2005). A Cre-inducible diphtheria toxin receptor mediates cell lineage ablation after toxin administration. Nat Methods 2, 419-426. 10.1038/nmeth762.

Calado, D.P., Sasaki, Y., Godinho, S.A., Pellerin, A., Kochert, K., Sleckman, B.P., de Alboran, I.M., Janz, M., Rodig, S., and Rajewsky, K. (2012). The cell-cycle regulator c-Myc is essential for the formation and maintenance of germinal centers. Nat Immunol 13, 1092-1100. 10.1038/ni.2418.

Cao, Y., Wang, J., Jian, F., Xiao, T., Song, W., Yisimayi, A., Huang, W., Li, Q., Wang, P., An, R., et al. (2022). Omicron escapes the majority of existing SARS-CoV-2 neutralizing antibodies. Nature 602, 657-663. 10.1038/s41586-021-04385-3.

Caron, G., Le Gallou, S., Lamy, T., Tarte, K., and Fest, T. (2009). CXCR4 expression functionally discriminates centroblasts versus centrocytes within human germinal center B cells. J Immunol 182, 7595-7602. 10.4049/jimmunol.0804272.

Carrasco, Y.R., and Batista, F.D. (2007). B cells acquire particulate antigen in a macrophage-rich area at the boundary between the follicle and the subcapsular sinus of the lymph node. Immunity 27, 160-171. 10.1016/j.immuni.2007.06.007.

Chan, T.D., Gatto, D., Wood, K., Camidge, T., Basten, A., and Brink, R. (2009). Antigen affinity controls rapid T-dependent antibody production by driving the expansion rather than the differentiation or extrafollicular migration of early plasmablasts. J Immunol 183, 3139-3149. 10.4049/jimmunol.0901690.

Chan, T.D., Gatto, D., Wood, K., Camidge, T., Basten, A., and Brink, R. (2009). Antigen affinity controls rapid T-dependent antibody production by driving the expansion rather than the differentiation or extrafollicular migration of early plasmablasts. J Immunol 183, 3139-3149. 10.4049/jimmunol.0901690.

Chaudhuri, J., Tian, M., Khuong, C., Chua, K., Pinaud, E., and Alt, F.W. (2003). Transcription-targeted DNA deamination by the AID antibody diversification enzyme. Nature 422, 726-730. 10.1038/nature01574.

Chou, C., Verbaro, D.J., Tonc, E., Holmgren, M., Cella, M., Colonna, M., Bhattacharya, D., and Egawa, T. (2016). The Transcription Factor AP4 Mediates Resolution of Chronic Viral Infection through Amplification of Germinal Center B Cell Responses. Immunity 45, 570-582. 10.1016/j.immuni.2016.07.023.

Chung, Y., Tanaka, S., Chu, F., Nurieva, R.I., Martinez, G.J., Rawal, S., Wang, Y.H., Lim, H., Reynolds, J.M., Zhou, X.H., et al. (2011). Follicular regulatory T cells expressing Foxp3 and Bcl-6 suppress germinal center reactions. Nat Med 17, 983-988. 10.1038/nm.2426.

Cirelli, K.M., Carnathan, D.G., Nogal, B., Martin, J.T., Rodriguez, O.L., Upadhyay, A.A., Enemuo, C.A., Gebru, E.H., Choe, Y., Viviano, F., et al. (2019). Slow Delivery Immunization Enhances HIV Neutralizing Antibody and Germinal Center Responses via Modulation of Immunodominance. Cell 177, 1153-1171 e1128. 10.1016/j.cell.2019.04.012.

Cirelli, K.M., and Crotty, S. (2017). Germinal center enhancement by extended antigen availability. Curr Opin Immunol 47, 64-69. 10.1016/j.coi.2017.06.008.

Clement, R.L., Daccache, J., Mohammed, M.T., Diallo, A., Blazar, B.R., Kuchroo, V.K., Lovitch, S.B., Sharpe, A.H., and Sage, P.T. (2019). Follicular regulatory T cells control humoral and allergic immunity by restraining early B cell responses. Nat Immunol 20, 1360-1371. 10.1038/s41590-019-0472-4.

Crotty, S. (2011). Follicular helper CD4 T cells (TFH). Annu Rev Immunol 29, 621-663. 10.1146/annurev-immunol-031210-101400. Crotty, S. (2014). T follicular helper cell differentiation, function, and roles in disease. Immunity 41, 529-542. 10.1016/j.immuni.2014.10.004.

Cunningham, A.F., Serre, K., Toellner, K.M., Khan, M., Alexander, J., Brombacher, F., and MacLennan, I.C.M. (2004). Pinpointing IL-4-independent acquisition and IL-4-influenced maintenance of Th2 activity by CD4 T cells. Eur J Immunol 34, 686-694. 10.1002/eji.200324510.

Cyster, J.G., and Allen, C.D.C. (2019). B Cell Responses: Cell Interaction Dynamics and Decisions. Cell 177, 524-540. 10.1016/j.cell.2019.03.016.

Davidzohn, N., Biram, A., Stoler-Barak, L., Grenov, A., Dassa, B., and Shulman, Z. (2020). Syk degradation restrains plasma cell formation and promotes zonal transitions in germinal centers. J Exp Med 217. 10.1084/jem.20191043.

De Silva, N.S., and Klein, U. (2015). Dynamics of B cells in germinal centres. Nat Rev Immunol 15, 137-148. 10.1038/nri3804.

Depoil, D., Fleire, S., Treanor, B.L., Weber, M., Harwood, N.E., Marchbank, K.L., Tybulewicz, V.L., and Batista, F.D. (2008). CD19 is essential for B cell activation by promoting B cell receptor-antigen microcluster formation in response to membrane-bound ligand. Nat Immunol 9, 63-72. 10.1038/ni1547.

Dogan, I., Bertocci, B., Vilmont, V., Delbos, F., Megret, J., Storck, S., Reynaud, C.A., and Weill, J.C. (2009). Multiple layers of B cell memory with different effector functions. Nat Immunol 10, 1292-1299. 10.1038/ni.1814.

Dominguez-Sola, D., Kung, J., Holmes, A.B., Wells, V.A., Mo, T., Basso, K., and Dalla-Favera, R. (2015). The FOXO1 Transcription Factor Instructs the Germinal Center Dark Zone Program. Immunity 43, 1064-1074. 10.1016/j.immuni.2015.10.015.

Dominguez-Sola, D., Victora, G.D., Ying, C.Y., Phan, R.T., Saito, M., Nussenzweig, M.C., and Dalla-Favera, R. (2012). The proto-oncogene MYC is required for selection in the germinal center and cyclic reentry. Nat Immunol 13, 1083-1091. 10.1038/ni.2428.

Draghi, N.A., and Denzin, L.K. (2010). H2-O, a MHC class II-like protein, sets a threshold for B-cell entry into germinal centers. Proc Natl Acad Sci U S A 107, 16607-16612. 10.1073/pnas.1004664107.

Duffy, K.R., Wellard, C.J., Markham, J.F., Zhou, J.H., Holmberg, R., Hawkins, E.D., Hasbold, J., Dowling, M.R., and Hodgkin, P.D. (2012). Activation-induced B cell fates are selected by intracellular stochastic competition. Science 335, 338-341. 10.1126/science.1213230.

Ersching, J., Efeyan, A., Mesin, L., Jacobsen, J.T., Pasqual, G., Grabiner, B.C., Dominguez-Sola, D., Sabatini, D.M., and Victora, G.D. (2017). Germinal Center Selection and Affinity Maturation Require Dynamic Regulation of mTORC1 Kinase. Immunity 46, 1045-1058 e1046. 10.1016/j.immuni.2017.06.005.

Finkin, S., Hartweger, H., Oliveira, T.Y., Kara, E.E., and Nussenzweig, M.C. (2019). Protein Amounts of the MYC Transcription Factor Determine Germinal Center B Cell Division Capacity. Immunity 51, 324-336 e325. 10.1016/j.immuni.2019.06.013.

Foy, T.M., Shepherd, D.M., Durie, F.H., Aruffo, A., Ledbetter, J.A., and Noelle, R.J. (1993). In vivo CD40-gp39 interactions are essential for thymus-dependent humoral immunity. II. Prolonged suppression of the humoral immune response by an antibody to the ligand for CD40, gp39. J Exp Med 178, 1567-1575. 10.1084/jem.178.5.1567.

Franchi, L., Warner, N., Viani, K., and Nunez, G. (2009). Function of Nod-like receptors in microbial recognition and host defense. Immunol Rev 227, 106-128. 10.1111/j.1600-065X.2008.00734.x.

Garin, A., Meyer-Hermann, M., Contie, M., Figge, M.T., Buatois, V., Gunzer, M., Toellner, K.M., Elson, G., and Kosco-Vilbois, M.H. (2010). Toll-like receptor 4 signaling by follicular dendritic cells is pivotal for germinal center onset and affinity maturation. Immunity 33, 84-95. 10.1016/j.immuni.2010.07.005.

Garside, P., Ingulli, E., Merica, R.R., Johnson, J.G., Noelle, R.J., and Jenkins, M.K.

(1998). Visualization of specific B and T lymphocyte interactions in the lymph node. Science 281, 96-99. 10.1126/science.281.5373.96.

Gatto, D., Paus, D., Basten, A., Mackay, C.R., and Brink, R. (2009). Guidance of B cells by the orphan G protein-coupled receptor EBI2 shapes humoral immune responses. Immunity 31, 259-269. 10.1016/j.immuni.2009.06.016.

Gitlin, A.D., Mayer, C.T., Oliveira, T.Y., Shulman, Z., Jones, M.J., Koren, A., and Nussenzweig, M.C. (2015). HUMORAL IMMUNITY. T cell help controls the speed of the cell cycle in germinal center B cells. Science 349, 643-646. 10.1126/science.aac4919.

Gitlin, A.D., Shulman, Z., and Nussenzweig, M.C. (2014). Clonal selection in the germinal centre by regulated proliferation and hypermutation. Nature 509, 637-640. 10.1038/nature13300. Gnanaprakasam, J.N., and Wang, R. (2017). MYC in Regulating Immunity: Metabolism and Beyond. Genes (Basel) 8. 10.3390/genes8030088.

Gomes de Castro, M.A., Wildhagen, H., Sograte-Idrissi, S., Hitzing, C., Binder, M., Trepel, M., Engels, N., and Opazo, F. (2019). Differential organization of tonic and chronic B cell antigen receptors in the plasma membrane. Nat Commun 10, 820. 10.1038/s41467-019-08677-1.

Gonzalez, S.F., Lukacs-Kornek, V., Kuligowski, M.P., Pitcher, L.A., Degn, S.E., Kim, Y.A., Cloninger, M.J., Martinez-Pomares, L., Gordon, S., Turley, S.J., and Carroll, M.C. (2010). Capture of influenza by medullary dendritic cells via SIGN-R1 is essential for humoral immunity in draining lymph nodes. Nat Immunol 11, 427-434. 10.1038/ni.1856.

Gonzalez-Figueroa, P., Roco, J.A., Papa, I., Nunez Villacis, L., Stanley, M., Linterman, M.A., Dent, A., Canete, P.F., and Vinuesa, C.G. (2021). Follicular regulatory T cells produce neuritin to regulate B cells. Cell 184, 1775-1789 e1719. 10.1016/j.cell.2021.02.027.

Grandien, A., Fucs, R., Nobrega, A., Andersson, J., and Coutinho, A. (1994). Negative selection of multireactive B cell clones in normal adult mice. Eur J Immunol 24, 1345-1352. 10.1002/eji.1830240616.

Green, J.A., and Cyster, J.G. (2012). S1PR2 links germinal center confinement and growth regulation. Immunol Rev 247, 36-51. 10.1111/j.1600-065X.2012.01114.x.

Green, J.A., Suzuki, K., Cho, B., Willison, L.D., Palmer, D., Allen, C.D., Schmidt, T.H., Xu, Y., Proia, R.L., Coughlin, S.R., and Cyster, J.G. (2011). The sphingosine 1-phosphate receptor S1P(2) maintains the homeostasis of germinal center B cells and promotes niche confinement. Nat Immunol 12, 672-680. 10.1038/ni.2047.

Gregoire, C., Spinelli, L., Villazala-Merino, S., Gil, L., Holgado, M.P., Moussa, M., Dong, C., Zarubica, A., Fallet, M., Navarro, J.M., et al. (2022). Viral infection engenders bona fide and bystander subsets of lung-resident memory B cells through a permissive mechanism. Immunity 55, 1216-1233 e1219. 10.1016/j.immuni.2022.06.002.

Han, S., Hathcock, K., Zheng, B., Kepler, T.B., Hodes, R., and Kelsoe, G. (1995). Cellular interaction in germinal centers. Roles of CD40 ligand and B7-2 in established germinal centers. J Immunol 155, 556-567.

Hanna, M.G., Jr. (1964). An Autoradiographic and Histologic Study of Spleen White Pulp Germinal Centers during Early Intervals of the Primary Immune Response. Ornl-3595. ORINS Rep US At Energy Comm 34, 1-102.

Hashimoto, K., Joshi, S.K., and Koni, P.A. (2002). A conditional null allele of the major histocompatibility IA-beta chain gene. Genesis 32, 152-153. 10.1002/gene.10056.

Hauser, A.E., Junt, T., Mempel, T.R., Sneddon, M.W., Kleinstein, S.H., Henrickson, S.E., von Andrian, U.H., Shlomchik, M.J., and Haberman, A.M. (2007). Definition of germinal-center B cell migration in vivo reveals predominant intrazonal circulation patterns. Immunity 26, 655-667. 10.1016/j.immuni.2007.04.008.

Hauser, A.E., Kerfoot, S.M., and Haberman, A.M. (2010). Cellular choreography in the germinal center: new visions from in vivo imaging. Semin Immunopathol 32, 239-255. 10.1007/s00281-010-0214-z.

Haynes, N.M., Allen, C.D., Lesley, R., Ansel, K.M., Killeen, N., and Cyster, J.G. (2007). Role of CXCR5 and CCR7 in follicular Th cell positioning and appearance of a programmed cell death gene-1high germinal center-associated subpopulation. J Immunol 179, 5099-5108. 10.4049/jimmunol.179.8.5099.

Heesters, B.A., Chatterjee, P., Kim, Y.A., Gonzalez, S.F., Kuligowski, M.P., Kirchhausen, T., and Carroll, M.C. (2013). Endocytosis and recycling of immune complexes by follicular dendritic cells enhances B cell antigen binding and activation. Immunity 38, 1164-1175. 10.1016/j.immuni.2013.02.023.

Heinzel, S., Binh Giang, T., Kan, A., Marchingo, J.M., Lye, B.K., Corcoran, L.M., and Hodgkin, P.D. (2017). A Myc-dependent division timer complements a cell-death timer to regulate T cell and B cell responses. Nat Immunol 18, 96-103. 10.1038/ni.3598.

Hobeika, E., Levit-Zerdoun, E., Anastasopoulou, V., Pohlmeyer, R., Altmeier, S., Alsadeq, A., Dobenecker, M.W., Pelanda, R., and Reth, M. (2015). CD19 and BAFF-R can signal to promote B-cell survival in the absence of Syk. EMBO J 34, 925-939. 10.15252/embj.201489732.

Inoue, T., Shinnakasu, R., Ise, W., Kawai, C., Egawa, T., and Kurosaki, T. (2017). The transcription factor Foxo1 controls germinal center B cell proliferation in response to T cell help. J Exp Med 214, 1181-1198. 10.1084/jem.20161263.

Inoue, T., Shinnakasu, R., Kawai, C., Ise, W., Kawakami, E., Sax, N., Oki, T., Kitamura, T., Yamashita, K., Fukuyama, H., and Kurosaki, T. (2021). Exit from germinal center to become quiescent memory B cells depends on metabolic reprograming and provision of a survival signal. J Exp Med 218. 10.1084/jem.20200866.

Ise, W., Fujii, K., Shiroguchi, K., Ito, A., Kometani, K., Takeda, K., Kawakami, E., Yamashita, K., Suzuki, K., Okada, T., and Kurosaki, T. (2018). T Follicular Helper Cell-Germinal Center B Cell Interaction Strength Regulates Entry into Plasma Cell or Recycling Germinal Center Cell Fate. Immunity 48, 702-715 e704. 10.1016/j.immuni.2018.03.027.

Ise, W., and Kurosaki, T. (2019). Plasma cell differentiation during the germinal center reaction. Immunol Rev 288, 64-74. 10.1111/imr.12751.

Ito, S., Nagaoka, H., Shinkura, R., Begum, N., Muramatsu, M., Nakata, M., and Honjo, T. (2004). Activation-induced cytidine deaminase shuttles between nucleus and cytoplasm like apolipoprotein B mRNA editing catalytic polypeptide 1. Proc Natl Acad Sci U S A 101, 1975-1980. 10.1073/pnas.0307335101.

Itohara, S., Mombaerts, P., Lafaille, J., Iacomini, J., Nelson, A., Clarke, A.R., Hooper, M.L., Farr, A., and Tonegawa, S. (1993). T cell receptor delta gene mutant mice: independent generation of alpha beta T cells and programmed rearrangements of gamma delta TCR genes. Cell 72, 337-348. 10.1016/0092-8674(93)90112-4.

Jacob, J., and Kelsoe, G. (1992). In situ studies of the primary immune response to (4-hydroxy-3-nitrophenyl)acetyl. II. A common clonal origin for periarteriolar lymphoid sheath-associated foci and germinal centers. J Exp Med 176, 679-687. 10.1084/jem.176.3.679.

Jacob, J., Kelsoe, G., Rajewsky, K., and Weiss, U. (1991). Intraclonal generation of antibody mutants in germinal centres. Nature 354, 389-392. 10.1038/354389a0.

Jacobsen, J.T., Hu, W., TB, R.C., Solem, S., Galante, A., Lin, Z., Allon, S.J., Mesin, L., Bilate, A.M., Schiepers, A., et al. (2021). Expression of Foxp3 by T follicular helper cells in end-stage germinal centers. Science 373. 10.1126/science.abe5146.

Jain, A., and Pasare, C. (2017). Innate Control of Adaptive Immunity: Beyond the Three-Signal Paradigm. J Immunol 198, 3791-3800. 10.4049/jimmunol.1602000.

Ju, B., Zhang, Q., Ge, J., Wang, R., Sun, J., Ge, X., Yu, J., Shan, S., Zhou, B., Song, S., et al. (2020). Human neutralizing antibodies elicited by SARS-CoV-2 infection. Nature 584, 115-119. 10.1038/s41586-020-2380-z.

Junt, T., Moseman, E.A., Iannacone, M., Massberg, S., Lang, P.A., Boes, M., Fink, K., Henrickson, S.E., Shayakhmetov, D.M., Di Paolo, N.C., et al. (2007). Subcapsular sinus macrophages in lymph nodes clear lymph-borne viruses and present them to antiviral B cells. Nature 450, 110-114. 10.1038/nature06287.

Kaileh, M., and Sen, R. (2012). NF-kappaB function in B lymphocytes. Immunol Rev 246, 254-271. 10.1111/j.1600-065X.2012.01106.x.

Kawasaki, T., and Kawai, T. (2014). Toll-like receptor signaling pathways. Front Immunol 5, 461. 10.3389/fimmu.2014.00461.

Kennedy, D.E., Okoreeh, M.K., Maienschein-Cline, M., Ai, J., Veselits, M., McLean, K.C., Dhungana, Y., Wang, H., Peng, J., Chi, H., et al. (2020). Novel specialized cell state and spatial compartments within the germinal center. Nat Immunol 21, 660-670. 10.1038/s41590-020-0660-2.

Kepler, T.B., and Perelson, A.S. (1993). Somatic hypermutation in B cells: an optimal control treatment. J Theor Biol 164, 37-64. 10.1006/jtbi.1993.1139.

Kepler, T.B., and Perelson, A.S. (1993). Cyclic re-entry of germinal center B cells and the efficiency of affinity maturation. Immunol Today 14, 412-415. 10.1016/0167-5699(93)90145-B.

Khalil, A.M., Cambier, J.C., and Shlomchik, M.J. (2012). B cell receptor signal

transduction in the GC is short-circuited by high phosphatase activity. Science 336, 1178-1181. 10.1126/science.1213368.

Kim, H., Kim, M., Im, S.K., and Fang, S. (2018). Mouse Cre-LoxP system: general principles to determine tissue-specific roles of target genes. Lab Anim Res 34, 147-159. 10.5625/lar.2018.34.4.147.

Kitano, M., Moriyama, S., Ando, Y., Hikida, M., Mori, Y., Kurosaki, T., and Okada, T. (2011). Bcl6 protein expression shapes pre-germinal center B cell dynamics and follicular helper T cell heterogeneity. Immunity 34, 961-972. 10.1016/j.immuni.2011.03.025.

Klasener, K., Maity, P.C., Hobeika, E., Yang, J., and Reth, M. (2014). B cell activation involves nanoscale receptor reorganizations and inside-out signaling by Syk. Elife 3, e02069. 10.7554/eLife.02069.

Klein, U., Casola, S., Cattoretti, G., Shen, Q., Lia, M., Mo, T., Ludwig, T., Rajewsky, K., and Dalla-Favera, R. (2006). Transcription factor IRF4 controls plasma cell differentiation and class-switch recombination. Nat Immunol 7, 773-782. 10.1038/ni1357.

Klein, U., Tu, Y., Stolovitzky, G.A., Keller, J.L., Haddad, J., Jr., Miljkovic, V., Cattoretti, G., Califano, A., and Dalla-Favera, R. (2003). Transcriptional analysis of the B cell germinal center reaction. Proc Natl Acad Sci U S A 100, 2639-2644. 10.1073/pnas.0437996100.

Kleinstein, S.H., Louzoun, Y., and Shlomchik, M.J. (2003). Estimating hypermutation rates from clonal tree data. J Immunol 171, 4639-4649. 10.4049/jimmunol.171.9.4639.

Koncz, G., and Hueber, A.O. (2012). The Fas/CD95 Receptor Regulates the Death of Autoreactive B Cells and the Selection of Antigen-Specific B Cells. Front Immunol 3, 207. 10.3389/fimmu.2012.00207.

Krautler, N.J., Suan, D., Butt, D., Bourne, K., Hermes, J.R., Chan, T.D., Sundling, C., Kaplan, W., Schofield, P., Jackson, J., et al. (2017). Differentiation of germinal center B cells into plasma cells is initiated by high-affinity antigen and completed by Tfh cells. J Exp Med 214, 1259-1267. 10.1084/jem.20161533.

Kuppers, R., Zhao, M., Hansmann, M.L., and Rajewsky, K. (1993). Tracing B cell development in human germinal centres by molecular analysis of single cells picked from histological sections. EMBO J 12, 4955-4967. 10.1002/j.1460-2075.1993.tb06189.x.

Kuraoka, M., Holl, T.M., Liao, D., Womble, M., Cain, D.W., Reynolds, A.E., and Kelsoe, G. (2011). Activation-induced cytidine deaminase mediates central tolerance in B cells. Proc Natl Acad Sci U S A 108, 11560-11565. 10.1073/pnas.1102571108.

Kuraoka, M., Schmidt, A.G., Nojima, T., Feng, F., Watanabe, A., Kitamura, D., Harrison, S.C., Kepler, T.B., and Kelsoe, G. (2016). Complex Antigens Drive Permissive Clonal Selection in Germinal Centers. Immunity 44, 542-552. 10.1016/j.immuni.2016.02.010.

Kwon, H., Thierry-Mieg, D., Thierry-Mieg, J., Kim, H.P., Oh, J., Tunyaplin, C., Carotta, S., Donovan, C.E., Goldman, M.L., Tailor, P., et al. (2009). Analysis

of interleukin-21-induced Prdm1 gene regulation reveals functional cooperation of STAT3 and IRF4 transcription factors. Immunity 31, 941-952. 10.1016/j.immuni.2009.10.008.

Laidlaw, B.J., and Cyster, J.G. (2021). Transcriptional regulation of memory B cell differentiation. Nat Rev Immunol 21, 209-220. 10.1038/s41577-020-00446-2.

Laidlaw, B.J., Duan, L., Xu, Y., Vazquez, S.E., and Cyster, J.G. (2020). The transcription factor Hhex cooperates with the corepressor Tle3 to promote memory B cell development. Nat Immunol 21, 1082-1093. 10.1038/s41590-020-0713-6.

Lee, J.H., Sutton, H.J., Cottrell, C.A., Phung, I., Ozorowski, G., Sewall, L.M., Nedellec, R., Nakao, C., Silva, M., Richey, S.T., et al. (2022). Long-primed germinal centres with enduring affinity maturation and clonal migration. Nature. 10.1038/s41586-022-05216-9.

Lee, P.P., Fitzpatrick, D.R., Beard, C., Jessup, H.K., Lehar, S., Makar, K.W., Perez-Melgosa, M., Sweetser, M.T., Schlissel, M.S., Nguyen, S., et al. (2001). A critical role for Dnmt1 and DNA methylation in T cell development, function, and survival. Immunity 15, 763-774. 10.1016/s1074-7613(01)00227-8.

Li, Y., O'Dell, S., Walker, L.M., Wu, X., Guenaga, J., Feng, Y., Schmidt, S.D., McKee, K., Louder, M.K., Ledgerwood, J.E., et al. (2011). Mechanism of neutralization by the broadly neutralizing HIV-1 monoclonal antibody VRC01. J Virol 85, 8954-8967. 10.1128/JVI.00754-11.

Lin, Y., Wong, K., and Calame, K. (1997). Repression of c-myc transcription by Blimp-1, an inducer of terminal B cell differentiation. Science 276, 596-599. 10.1126/science.276.5312.596.

Lindahl, T., Ljungquist, S., Siegert, W., Nyberg, B., and Sperens, B. (1977). DNA N-glycosidases: properties of uracil-DNA glycosidase from Escherichia coli. J Biol Chem 252, 3286-3294.

Linterman, M.A., Beaton, L., Yu, D., Ramiscal, R.R., Srivastava, M., Hogan, J.J., Verma, N.K., Smyth, M.J., Rigby, R.J., and Vinuesa, C.G. (2010). IL-21 acts directly on B cells to regulate Bcl-6 expression and germinal center responses. J Exp Med 207, 353-363. 10.1084/jem.20091738.

Linterman, M.A., Pierson, W., Lee, S.K., Kallies, A., Kawamoto, S., Rayner, T.F., Srivastava, M., Divekar, D.P., Beaton, L., Hogan, J.J., et al. (2011). Foxp3+ follicular regulatory T cells control the germinal center response. Nat Med 17, 975-982. 10.1038/nm.2425.

Liu, B., Lin, Y., Yan, J., Yao, J., Liu, D., Ma, W., Wang, J., Liu, W., Wang, C., Zhang, L., and Qi, H. (2021). Affinity-coupled CCL22 promotes positive selection in germinal centres. Nature 592, 133-137. 10.1038/s41586-021-03239-2.

Liu, D., Xu, H., Shih, C., Wan, Z., Ma, X., Ma, W., Luo, D., and Qi, H. (2015). T-B-cell entanglement and ICOSL-driven feed-forward regulation of germinal centre reaction. Nature 517, 214-218. 10.1038/nature13803.

Liu, Y., Fang, Y., Shao, H., Lindsey-Boltz, L., Sancar, A., and Modrich, P. (2010). Interactions of human mismatch repair proteins MutSalpha and MutLalpha with proteins of the ATR-Chk1 pathway. J Biol Chem 285, 5974-5982.

10.1074/jbc.M109.076109.

Liu, Y.J., Xu, J., de Bouteiller, O., Parham, C.L., Grouard, G., Djossou, O., de Saint-Vis, B., Lebecque, S., Banchereau, J., and Moore, K.W. (1997). Follicular dendritic cells specifically express the long CR2/CD21 isoform. J Exp Med 185, 165-170. 10.1084/jem.185.1.165.

Liu, Y.J., Zhang, J., Lane, P.J., Chan, E.Y., and MacLennan, I.C. (1991). Sites of specific B cell activation in primary and secondary responses to T cell-dependent and T cell-independent antigens. Eur J Immunol 21, 2951-2962. 10.1002/eji.1830211209.

Long, Z., Phillips, B., Radtke, D., Meyer-Hermann, M., and Bannard, O. (2022). Competition for refueling rather than cyclic reentry initiation evident in germinal centers. Sci Immunol 7, eabm0775. 10.1126/sciimmunol.abm0775.

Luo, W., Hawse, W., Conter, L., Trivedi, N., Weisel, F., Wikenheiser, D., Cattley, R.T., and Shlomchik, M.J. (2019). The AKT kinase signaling network is rewired by PTEN to control proximal BCR signaling in germinal center B cells. Nat Immunol 20, 736-746. 10.1038/s41590-019-0376-3.

Luo, W., Weisel, F., and Shlomchik, M.J. (2018). B Cell Receptor and CD40 Signaling Are Rewired for Synergistic Induction of the c-Myc Transcription Factor in Germinal Center B Cells. Immunity 48, 313-326 e315. 10.1016/j.immuni.2018.01.008.

Ma, X., Liu, Y., Wang, Q., Chen, Y., Liu, M., Li, X., Xiang, R., Wei, Y., Duan, Y., and Han, J. (2015). Tamoxifen induces the development of hernia in mice by activating MMP-2 and MMP-13 expression. Biochim Biophys Acta 1852, 1038-1048. 10.1016/j.bbadis.2015.02.006.

MacLean, A.J., Richmond, N., Koneva, L., Attar, M., Medina, C.A.P., Thornton, E.E., Gomes, A.C., El-Turabi, A., Bachmann, M.F., Rijal, P., et al. (2022). Secondary influenza challenge triggers resident memory B cell migration and rapid relocation to boost antibody secretion at infected sites. Immunity 55, 718-733 e718. 10.1016/j.immuni.2022.03.003.

MacLennan, I.C. (1994). Germinal centers. Annu Rev Immunol 12, 117-139. 10.1146/annurev.iy.12.040194.001001.

MacLennan, I.C., Toellner, K.M., Cunningham, A.F., Serre, K., Sze, D.M., Zuniga, E., Cook, M.C., and Vinuesa, C.G. (2003). Extrafollicular antibody responses. Immunol Rev 194, 8-18. 10.1034/j.1600-065x.2003.00058.x.

Madden, S.K., de Araujo, A.D., Gerhardt, M., Fairlie, D.P., and Mason, J.M. (2021). Taking the Myc out of cancer: toward therapeutic strategies to directly inhibit c-Myc. Mol Cancer 20, 3. 10.1186/s12943-020-01291-6.

Mandel, T.E., Phipps, R.P., Abbot, A.P., and Tew, J.G. (1981). Long-term antigen retention by dendritic cells in the popliteal lymph node of immunized mice. Immunology 43, 353-362.

Marchingo, J.M., Kan, A., Sutherland, R.M., Duffy, K.R., Wellard, C.J., Belz, G.T., Lew, A.M., Dowling, M.R., Heinzel, S., and Hodgkin, P.D. (2014). T cell signaling. Antigen affinity, costimulation, and cytokine inputs sum linearly to amplify T cell expansion. Science 346, 1123-1127. 10.1126/science.1260044.

Marin, T.M., Keith, K., Davies, B., Conner, D.A., Guha, P., Kalaitzidis, D., Wu, X., Lauriol, J., Wang, B., Bauer, M., et al. (2011). Rapamycin reverses hypertrophic cardiomyopathy in a mouse model of LEOPARD syndrome-associated PTPN11 mutation. J Clin Invest 121, 1026-1043. 10.1172/JCI44972.

Martin, A., Bardwell, P.D., Woo, C.J., Fan, M., Shulman, M.J., and Scharff, M.D. (2002). Activation-induced cytidine deaminase turns on somatic hypermutation in hybridomas. Nature 415, 802-806. 10.1038/nature714.

Maruyama, M., Lam, K.P., and Rajewsky, K. (2000). Memory B-cell persistence is independent of persisting immunizing antigen. Nature 407, 636-642. 10.1038/35036600.

Mayer, C.T., Gazumyan, A., Kara, E.E., Gitlin, A.D., Golijanin, J., Viant, C., Pai, J., Oliveira, T.Y., Wang, Q., Escolano, A., et al. (2017). The microanatomic segregation of selection by apoptosis in the germinal center. Science 358. 10.1126/science.aao2602.

McCoy, L.E., and Weiss, R.A. (2013). Neutralizing antibodies to HIV-1 induced by immunization. J Exp Med 210, 209-223. 10.1084/jem.20121827.

Merkenschlager, J., Finkin, S., Ramos, V., Kraft, J., Cipolla, M., Nowosad, C.R., Hartweger, H., Zhang, W., Olinares, P.D.B., Gazumyan, A., et al. (2021). Dynamic regulation of TFH selection during the germinal centre reaction. Nature 591, 458-463. 10.1038/s41586-021-03187-x.

Mesin, L., Ersching, J., and Victora, G.D. (2016). Germinal Center B Cell Dynamics. Immunity 45, 471-482. 10.1016/j.immuni.2016.09.001.

Meyer-Hermann, M. (2021). A molecular theory of germinal center B cell selection and division. Cell Rep 36, 109552. 10.1016/j.celrep.2021.109552.

Meyer-Hermann, M., Mohr, E., Pelletier, N., Zhang, Y., Victora, G.D., and Toellner, K.M. (2012). A theory of germinal center B cell selection, division, and exit. Cell Rep 2, 162-174. 10.1016/j.celrep.2012.05.010.

Meyers, G., Ng, Y.S., Bannock, J.M., Lavoie, A., Walter, J.E., Notarangelo, L.D., Kilic, S.S., Aksu, G., Debre, M., Rieux-Laucat, F., et al. (2011). Activation-induced cytidine deaminase (AID) is required for B-cell tolerance in humans. Proc Natl Acad Sci U S A 108, 11554-11559. 10.1073/pnas.1102600108.

Migliazza, A., Martinotti, S., Chen, W., Fusco, C., Ye, B.H., Knowles, D.M., Offit, K., Chaganti, R.S., and Dalla-Favera, R. (1995). Frequent somatic hypermutation of the 5' noncoding region of the BCL6 gene in B-cell lymphoma. Proc Natl Acad Sci U S A 92, 12520-12524. 10.1073/pnas.92.26.12520.

Mikell, I., Sather, D.N., Kalams, S.A., Altfeld, M., Alter, G., and Stamatatos, L. (2011). Characteristics of the earliest cross-neutralizing antibody response to HIV-1. PLoS Pathog 7, e1001251. 10.1371/journal.ppat.1001251.

Mombaerts, P., Clarke, A.R., Rudnicki, M.A., Iacomini, J., Itohara, S., Lafaille, J.J., Wang, L., Ichikawa, Y., Jaenisch, R., Hooper, M.L., and et al. (1992). Mutations in T-cell antigen receptor genes alpha and beta block thymocyte development at

different stages. Nature 360, 225-231. 10.1038/360225a0.

Moran, I., Nguyen, A., Khoo, W.H., Butt, D., Bourne, K., Young, C., Hermes, J.R., Biro, M., Gracie, G., Ma, C.S., et al. (2018). Memory B cells are reactivated in subcapsular proliferative foci of lymph nodes. Nat Commun 9, 3372. 10.1038/s41467-018-05772-7.

Mueller, J., Matloubian, M., and Zikherman, J. (2015). Cutting edge: An in vivo reporter reveals active B cell receptor signaling in the germinal center. J Immunol 194, 2993-2997. 10.4049/jimmunol.1403086.

Murphy, D.B., Lo, D., Rath, S., Brinster, R.L., Flavell, R.A., Slanetz, A., and Janeway, C.A., Jr. (1989). A novel MHC class II epitope expressed in thymic medulla but not cortex. Nature 338, 765-768. 10.1038/338765a0.

Nakagawa, R., Toboso-Navasa, A., Schips, M., Young, G., Bhaw-Rosun, L., Llorian-Sopena, M., Chakravarty, P., Sesay, A.K., Kassiotis, G., Meyer-Hermann, M., and Calado, D.P. (2021). Permissive selection followed by affinity-based proliferation of GC light zone B cells dictates cell fate and ensures clonal breadth. Proc Natl Acad Sci U S A 118. 10.1073/pnas.2016425118.

Natsume, T., Kiyomitsu, T., Saga, Y., and Kanemaki, M.T. (2016). Rapid Protein Depletion in Human Cells by Auxin-Inducible Degron Tagging with Short Homology Donors. Cell Rep 15, 210-218. 10.1016/j.celrep.2016.03.001.

Nieuwenhuis, P., and Opstelten, D. (1984). Functional anatomy of germinal centers. Am J Anat 170, 421-435. 10.1002/aja.1001700315.

Nishikawa, Y., Hikida, M., Magari, M., Kanayama, N., Mori, M., Kitamura, H., Kurosaki, T., and Ohmori, H. (2006). Establishment of lymphotoxin beta receptor signaling-dependent cell lines with follicular dendritic cell phenotypes from mouse lymph nodes. J Immunol 177, 5204-5214. 10.4049/jimmunol.177.8.5204.

Nowosad, C.R., Spillane, K.M., and Tolar, P. (2016). Germinal center B cells recognize antigen through a specialized immune synapse architecture. Nat Immunol 17, 870-877. 10.1038/ni.3458.

Oberdoerffer, P., Otipoby, K.L., Maruyama, M., and Rajewsky, K. (2003). Unidirectional Cre-mediated genetic inversion in mice using the mutant loxP pair lox66/lox71. Nucleic Acids Res 31, e140. 10.1093/nar/gng140.

Ochiai, K., Maienschein-Cline, M., Simonetti, G., Chen, J., Rosenthal, R., Brink, R., Chong, A.S., Klein, U., Dinner, A.R., Singh, H., and Sciammas, R. (2013). Transcriptional regulation of germinal center B and plasma cell fates by dynamical control of IRF4. Immunity 38, 918-929. 10.1016/j.immuni.2013.04.009.

Oellerich, T., Bremes, V., Neumann, K., Bohnenberger, H., Dittmann, K., Hsiao, H.H., Engelke, M., Schnyder, T., Batista, F.D., Urlaub, H., and Wienands, J. (2011). The B-cell antigen receptor signals through a preformed transducer module of SLP65 and CIN85. EMBO J 30, 3620-3634. 10.1038/emboj.2011.251.

Okada, T., Miller, M.J., Parker, I., Krummel, M.F., Neighbors, M., Hartley, S.B., O'Garra, A., Cahalan, M.D., and Cyster, J.G. (2005). Antigen-engaged B cells undergo chemotaxis toward the T zone and form motile conjugates with helper

T cells. PLoS Biol 3, e150. 10.1371/journal.pbio.0030150.

Okazaki, I.M., Hiai, H., Kakazu, N., Yamada, S., Muramatsu, M., Kinoshita, K., and Honjo, T. (2003). Constitutive expression of AID leads to tumorigenesis. J Exp Med 197, 1173-1181. 10.1084/jem.20030275.

Ozaki, K., Spolski, R., Feng, C.G., Qi, C.F., Cheng, J., Sher, A., Morse, H.C., 3rd, Liu, C., Schwartzberg, P.L., and Leonard, W.J. (2002). A critical role for IL-21 in regulating immunoglobulin production. Science 298, 1630-1634. 10.1126/science.1077002.

Pae, J., Ersching, J., Castro, T.B.R., Schips, M., Mesin, L., Allon, S.J., Ordovas-Montanes, J., Mlynarczyk, C., Melnick, A., Efeyan, A., et al. (2021). Cyclin D3 drives inertial cell cycling in dark zone germinal center B cells. J Exp Med 218. 10.1084/jem.20201699.

Palm, A.E., and Henry, C. (2019). Remembrance of Things Past: Long-Term B Cell Memory After Infection and Vaccination. Front Immunol 10, 1787. 10.3389/fimmu.2019.01787.

Pape, K.A., Catron, D.M., Itano, A.A., and Jenkins, M.K. (2007). The humoral immune response is initiated in lymph nodes by B cells that acquire soluble antigen directly in the follicles. Immunity 26, 491-502. 10.1016/j.immuni.2007.02.011.

Pasqualucci, L., Kitaura, Y., Gu, H., and Dalla-Favera, R. (2006). PKA-mediated phosphorylation regulates the function of activation-induced deaminase (AID) in B cells. Proc Natl Acad Sci U S A 103, 395-400. 10.1073/pnas.0509969103.

Paus, D., Phan, T.G., Chan, T.D., Gardam, S., Basten, A., and Brink, R. (2006). Antigen recognition strength regulates the choice between extrafollicular plasma cell and germinal center B cell differentiation. J Exp Med 203, 1081-1091. 10.1084/jem.20060087.

Pereira, J.P., Kelly, L.M., Xu, Y., and Cyster, J.G. (2009). EBI2 mediates B cell segregation between the outer and centre follicle. Nature 460, 1122-1126. 10.1038/nature08226.

Pham, P., Bransteitter, R., Petruska, J., and Goodman, M.F. (2003). Processive AID-catalysed cytosine deamination on single-stranded DNA simulates somatic hypermutation. Nature 424, 103-107. 10.1038/nature01760.

Phan, R.T., and Dalla-Favera, R. (2004). The BCL6 proto-oncogene suppresses p53 expression in germinal-centre B cells. Nature 432, 635-639. 10.1038/nature03147.

Phan, R.T., Saito, M., Basso, K., Niu, H., and Dalla-Favera, R. (2005). BCL6 interacts with the transcription factor Miz-1 to suppress the cyclin-dependent kinase inhibitor p21 and cell cycle arrest in germinal center B cells. Nat Immunol 6, 1054-1060. 10.1038/ni1245.

Phan, T.G., Amesbury, M., Gardam, S., Crosbie, J., Hasbold, J., Hodgkin, P.D., Basten, A., and Brink, R. (2003). B cell receptor-independent stimuli trigger immunoglobulin (Ig) class switch recombination and production of IgG autoantibodies by anergic self-reactive B cells. J Exp Med 197, 845-860. 10.1084/jem.20022144.

Phan, T.G., Grigorova, I., Okada, T., and Cyster, J.G. (2007). Subcapsular encounter and complement-dependent transport of immune complexes by lymph node B cells. Nat Immunol 8, 992-1000. 10.1038/ni1494.

Phan, T.G., Paus, D., Chan, T.D., Turner, M.L., Nutt, S.L., Basten, A., and Brink, R. (2006). High affinity germinal center B cells are actively selected into the plasma cell compartment. J Exp Med 203, 2419-2424. 10.1084/jem.20061254.

Pierce, S.K., and Liu, W. (2010). The tipping points in the initiation of B cell signalling: how small changes make big differences. Nat Rev Immunol 10, 767-777. 10.1038/nri2853.

Pikor, N.B., Morbe, U., Lutge, M., Gil-Cruz, C., Perez-Shibayama, C., Novkovic, M., Cheng, H.W., Nombela-Arrieta, C., Nagasawa, T., Linterman, M.A., et al. (2020). Remodeling of light and dark zone follicular dendritic cells governs germinal center responses. Nat Immunol 21, 649-659. 10.1038/s41590-020-0672-y.

Piskurich, J.F., Lin, K.I., Lin, Y., Wang, Y., Ting, J.P., and Calame, K. (2000). BLIMP-I mediates extinction of major histocompatibility class II transactivator expression in plasma cells. Nat Immunol 1, 526-532. 10.1038/82788.

Pohl, T., Gugasyan, R., Grumont, R.J., Strasser, A., Metcalf, D., Tarlinton, D., Sha, W., Baltimore, D., and Gerondakis, S. (2002). The combined absence of NF-kappa B1 and c-Rel reveals that overlapping roles for these transcription factors in the B cell lineage are restricted to the activation and function of mature cells. Proc Natl Acad Sci U S A 99, 4514-4519. 10.1073/pnas.072071599.

Qi, H., Egen, J.G., Huang, A.Y., and Germain, R.N. (2006). Extrafollicular activation of lymph node B cells by antigen-bearing dendritic cells. Science 312, 1672-1676. 10.1126/science.1125703.

Qin, D., Wu, J., Vora, K.A., Ravetch, J.V., Szakal, A.K., Manser, T., and Tew, J.G. (2000). Fc gamma receptor IIB on follicular dendritic cells regulates the B cell recall response. J Immunol 164, 6268-6275. 10.4049/jimmunol.164.12.6268.

Quast, I., Dvorscek, A.R., Pattaroni, C., Steiner, T.M., McKenzie, C.I., Pitt, C., O'Donnell, K., Ding, Z., Hill, D.L., Brink, R., et al. (2022). Interleukin-21, acting beyond the immunological synapse, independently controls T follicular helper and germinal center B cells. Immunity 55, 1414-1430 e1415. 10.1016/j.immuni.2022.06.020.

Radtke, D., and Bannard, O. (2018). Expression of the Plasma Cell Transcriptional Regulator Blimp-1 by Dark Zone Germinal Center B Cells During Periods of Proliferation. Front Immunol 9, 3106. 10.3389/fimmu.2018.03106.

Ramezani-Rad, P., Chen, C., Zhu, Z., and Rickert, R.C. (2020). Cyclin D3 Governs Clonal Expansion of Dark Zone Germinal Center B Cells. Cell Rep 33, 108403. 10.1016/j.celrep.2020.108403.

Ranuncolo, S.M., Polo, J.M., Dierov, J., Singer, M., Kuo, T., Greally, J., Green, R., Carroll, M., and Melnick, A. (2007). Bcl-6 mediates the germinal center B cell phenotype and lymphomagenesis through transcriptional repression of the DNA-damage sensor ATR. Nat Immunol 8, 705-714. 10.1038/ni1478.

Ranuncolo, S.M., Polo, J.M., and Melnick, A. (2008). BCL6 represses CHEK1

and suppresses DNA damage pathways in normal and malignant B-cells. Blood Cells Mol Dis 41, 95-99. 10.1016/j.bcmd.2008.02.003.

Razzaghi, R., Agarwal, S., Kotlov, N., Plotnikova, O., Nomie, K., Huang, D.W., Wright, G.W., Smith, G.A., Li, M., Takata, K., et al. (2021). Compromised counterselection by FAS creates an aggressive subtype of germinal center lymphoma. J Exp Med 218. 10.1084/jem.20201173.

Rehwinkel, J., and Gack, M.U. (2020). RIG-I-like receptors: their regulation and roles in RNA sensing. Nat Rev Immunol 20, 537-551. 10.1038/s41577-020-0288-3.

Reid, J.M., Goetz, M.P., Buhrow, S.A., Walden, C., Safgren, S.L., Kuffel, M.J., Reinicke, K.E., Suman, V., Haluska, P., Hou, X., and Ames, M.M. (2014). Pharmacokinetics of endoxifen and tamoxifen in female mice: implications for comparative in vivo activity studies. Cancer Chemother Pharmacol 74, 1271-1278. 10.1007/s00280-014-2605-7.

Reif, K., Ekland, E.H., Ohl, L., Nakano, H., Lipp, M., Forster, R., and Cyster, J.G. (2002). Balanced responsiveness to chemoattractants from adjacent zones determines B-cell position. Nature 416, 94-99. 10.1038/416094a.

Reimold, A.M., Iwakoshi, N.N., Manis, J., Vallabhajosyula, P., Szomolanyi-Tsuda, E., Gravallese, E.M., Friend, D., Grusby, M.J., Alt, F., and Glimcher, L.H. (2001). Plasma cell differentiation requires the transcription factor XBP-1. Nature 412, 300-307. 10.1038/35085509.

Reynaud, C.A., Mackay, C.R., Muller, R.G., and Weill, J.C. (1991). Somatic generation of diversity in a mammalian primary lymphoid organ: the sheep ileal Peyer's patches. Cell 64, 995-1005. 10.1016/0092-8674(91)90323-q.

Robbiani, D.F., Bothmer, A., Callen, E., Reina-San-Martin, B., Dorsett, Y., Difilippantonio, S., Bolland, D.J., Chen, H.T., Corcoran, A.E., Nussenzweig, A., and Nussenzweig, M.C. (2008). AID is required for the chromosomal breaks in c-myc that lead to c-myc/IgH translocations. Cell 135, 1028-1038. 10.1016/j.cell.2008.09.062.

Sage, P.T., and Sharpe, A.H. (2016). T follicular regulatory cells. Immunol Rev 271, 246-259. 10.1111/imr.12411. Saito, M., Gao, J., Basso, K., Kitagawa, Y., Smith, P.M., Bhagat, G., Pernis, A., Pasqualucci, L., and Dalla-Favera, R. (2007). A signaling pathway mediating downregulation of BCL6 in germinal center B cells is blocked by BCL6 gene alterations in B cell lymphoma. Cancer Cell 12, 280-292. 10.1016/j.ccr.2007.08.011.

Saito, M., Novak, U., Piovan, E., Basso, K., Sumazin, P., Schneider, C., Crespo, M., Shen, Q., Bhagat, G., Califano, A., et al. (2009). BCL6 suppression of BCL2 via Miz1 and its disruption in diffuse large B cell lymphoma. Proc Natl Acad Sci U S A 106, 11294-11299. 10.1073/pnas.0903854106.

Sander, S., Chu, V.T., Yasuda, T., Franklin, A., Graf, R., Calado, D.P., Li, S., Imami, K., Selbach, M., Di Virgilio, M., et al. (2015). PI3 Kinase and FOXO1 Transcription Factor Activity Differentially Control B Cells in the Germinal Center Light and Dark Zones. Immunity 43, 1075-1086. 10.1016/j.immuni.2015.10.021.

Saribasak, H., Maul, R.W., Cao, Z., Yang, W.W., Schenten, D., Kracker, S., and Gearhart, P.J. (2012). DNA polymerase zeta generates tandem mutations in

immunoglobulin variable regions. J Exp Med 209, 1075-1081. 10.1084/jem.20112234.

Schieffelin, J.S., Costin, J.M., Nicholson, C.O., Orgeron, N.M., Fontaine, K.A., Isern, S., Michael, S.F., and Robinson, J.E. (2010). Neutralizing and non-neutralizing monoclonal antibodies against dengue virus E protein derived from a naturally infected patient. Virol J 7, 28. 10.1186/1743-422X-7-28.

Sciammas, R., Li, Y., Warmflash, A., Song, Y., Dinner, A.R., and Singh, H. (2011). An incoherent regulatory network architecture that orchestrates B cell diversification in response to antigen signaling. Mol Syst Biol 7, 495. 10.1038/msb.2011.25.

Sciammas, R., Shaffer, A.L., Schatz, J.H., Zhao, H., Staudt, L.M., and Singh, H. (2006). Graded expression of interferon regulatory factor-4 coordinates isotype switching with plasma cell differentiation. Immunity 25, 225-236. 10.1016/j.immuni.2006.07.009.

Sengupta, S., Peterson, T.R., and Sabatini, D.M. (2010). Regulation of the mTOR complex 1 pathway by nutrients, growth factors, and stress. Mol Cell 40, 310-322. 10.1016/j.molcel.2010.09.026.

Shaffer, A.L., Rosenwald, A., Hurt, E.M., Giltnane, J.M., Lam, L.T., Pickeral, O.K., and Staudt, L.M. (2001). Signatures of the immune response. Immunity 15, 375-385. 10.1016/s1074-7613(01)00194-7.

Shi, J., Hou, S., Fang, Q., Liu, X., Liu, X., and Qi, H. (2018). PD-1 Controls Follicular T Helper Cell Positioning and Function. Immunity 49, 264-274 e264. 10.1016/j.immuni.2018.06.012.

Shinnakasu, R., Inoue, T., Kometani, K., Moriyama, S., Adachi, Y., Nakayama, M., Takahashi, Y., Fukuyama, H., Okada, T., and Kurosaki, T. (2016). Regulated selection of germinal-center cells into the memory B cell compartment. Nat Immunol 17, 861-869. 10.1038/ni.3460.

Shlomchik, M.J. (2018). Do Memory B Cells Form Secondary Germinal Centers? Yes and No. Cold Spring Harb Perspect Biol 10. 10.1101/cshperspect.a029405.

Shlomchik, M.J., Luo, W., and Weisel, F. (2019). Linking signaling and selection in the germinal center. Immunol Rev 288, 49-63. 10.1111/imr.12744.

Shulman, Z., Gitlin, A.D., Targ, S., Jankovic, M., Pasqual, G., Nussenzweig, M.C., and Victora, G.D. (2013). T follicular helper cell dynamics in germinal centers. Science 341, 673-677. 10.1126/science.1241680.

Shulman, Z., Gitlin, A.D., Weinstein, J.S., Lainez, B., Esplugues, E., Flavell, R.A., Craft, J.E., and Nussenzweig, M.C. (2014). Dynamic signaling by T follicular helper cells during germinal center B cell selection. Science 345, 1058-1062. 10.1126/science.1257861.

Signer, R.A., Magee, J.A., Salic, A., and Morrison, S.J. (2014). Haematopoietic stem cells require a highly regulated protein synthesis rate. Nature 509, 49-54. 10.1038/nature13035.

Silver, J., Zuo, T., Chaudhary, N., Kumari, R., Tong, P., Giguere, S., Granato, A., Donthula, R., Devereaux, C., and Wesemann, D.R. (2018). Stochasticity enables

BCR-independent germinal center initiation and antibody affinity maturation. J Exp Med 215, 77-90. 10.1084/jem.20171022.

Smith, K.G., Light, A., O'Reilly, L.A., Ang, S.M., Strasser, A., and Tarlinton, D. (2000). bcl-2 transgene expression inhibits apoptosis in the germinal center and reveals differences in the selection of memory B cells and bone marrow antibody-forming cells. J Exp Med 191, 475-484. 10.1084/jem.191.3.475.

Smith, K.G., Light, A., O'Reilly, L.A., Ang, S.M., Strasser, A., and Tarlinton, D. (2000). bcl-2 transgene expression inhibits apoptosis in the germinal center and reveals differences in the selection of memory B cells and bone marrow antibody-forming cells. J Exp Med 191, 475-484. 10.1084/jem.191.3.475.

Sok, D., and Burton, D.R. (2018). Recent progress in broadly neutralizing antibodies to HIV. Nat Immunol 19, 1179-1188. 10.1038/s41590-018-0235-7.

Stamatatos, L., Morris, L., Burton, D.R., and Mascola, J.R. (2009). Neutralizing antibodies generated during natural HIV-1 infection: good news for an HIV-1 vaccine? Nat Med 15, 866-870. 10.1038/nm.1949.

Stewart, I., Radtke, D., Phillips, B., McGowan, S.J., and Bannard, O. (2018). Germinal Center B Cells Replace Their Antigen Receptors in Dark Zones and Fail Light Zone Entry when Immunoglobulin Gene Mutations are Damaging. Immunity 49, 477-489 e477. 10.1016/j.immuni.2018.08.025.

Suan, D., Krautler, N.J., Maag, J.L.V., Butt, D., Bourne, K., Hermes, J.R., Avery, D.T., Young, C., Statham, A., Elliott, M., et al. (2017). CCR6 Defines Memory B Cell Precursors in Mouse and Human Germinal Centers, Revealing Light-Zone Location and Predominant Low Antigen Affinity. Immunity 47, 1142-1153 e1144. 10.1016/j.immuni.2017.11.022.

Suan, D., Nguyen, A., Moran, I., Bourne, K., Hermes, J.R., Arshi, M., Hampton, H.R., Tomura, M., Miwa, Y., Kelleher, A.D., et al. (2015). T follicular helper cells have distinct modes of migration and molecular signatures in naive and memory immune responses. Immunity 42, 704-718. 10.1016/j.immuni.2015.03.002.

Takemori, T., Kaji, T., Takahashi, Y., Shimoda, M., and Rajewsky, K. (2014). Generation of memory B cells inside and outside germinal centers. Eur J Immunol 44, 1258-1264. 10.1002/eji.201343716.

Tam, H.H., Melo, M.B., Kang, M., Pelet, J.M., Ruda, V.M., Foley, M.H., Hu, J.K., Kumari, S., Crampton, J., Baldeon, A.D., et al. (2016). Sustained antigen availability during germinal center initiation enhances antibody responses to vaccination. Proc Natl Acad Sci U S A 113, E6639-E6648. 10.1073/pnas.1606050113.

Tas, J.M., Mesin, L., Pasqual, G., Targ, S., Jacobsen, J.T., Mano, Y.M., Chen, C.S., Weill, J.C., Reynaud, C.A., Browne, E.P., et al. (2016). Visualizing antibody affinity maturation in germinal centers. Science 351, 1048-1054. 10.1126/science.aad3439.

Taylor, J.J., Pape, K.A., Steach, H.R., and Jenkins, M.K. (2015). Humoral immunity. Apoptosis and antigen affinity limit effector cell differentiation of a single naive B cell. Science 347, 784-787. 10.1126/science.aaa1342.

Thomas, M.J., Klein, U., Lygeros, J., and Rodriguez Martinez, M. (2019). A

Probabilistic Model of the Germinal Center Reaction. Front Immunol 10, 689. 10.3389/fimmu.2019.00689.

Tiller, T., Tsuiji, M., Yurasov, S., Velinzon, K., Nussenzweig, M.C., and Wardemann, H. (2007). Autoreactivity in human IgG+ memory B cells. Immunity 26, 205-213. 10.1016/j.immuni.2007.01.009.

Todd, D.J., McHeyzer-Williams, L.J., Kowal, C., Lee, A.H., Volpe, B.T., Diamond, B., McHeyzer-Williams, M.G., and Glimcher, L.H. (2009). XBP1 governs late events in plasma cell differentiation and is not required for antigen-specific memory B cell development. J Exp Med 206, 2151-2159. 10.1084/jem.20090738.

Tolar, P., Sohn, H.W., and Pierce, S.K. (2005). The initiation of antigen-induced B cell antigen receptor signaling viewed in living cells by fluorescence resonance energy transfer. Nat Immunol 6, 1168-1176. 10.1038/ni1262.

Treanor, B. (2012). B-cell receptor: from resting state to activate. Immunology 136, 21-27. 10.1111/j.1365-2567.2012.03564.x.

Treanor, B., Depoil, D., Gonzalez-Granja, A., Barral, P., Weber, M., Dushek, O., Bruckbauer, A., and Batista, F.D. (2010). The membrane skeleton controls diffusion dynamics and signaling through the B cell receptor. Immunity 32, 187-199. 10.1016/j.immuni.2009.12.005.

Tunyaplin, C., Shaffer, A.L., Angelin-Duclos, C.D., Yu, X., Staudt, L.M., and Calame, K.L. (2004). Direct repression of prdm1 by Bcl-6 inhibits plasmacytic differentiation. J Immunol 173, 1158-1165. 10.4049/jimmunol.173.2.1158.

Turner, J.S., Benet, Z.L., and Grigorova, I.L. (2017). Antigen Acquisition Enables Newly Arriving B Cells To Enter Ongoing Immunization-Induced Germinal Centers. J Immunol 199, 1301-1307. 10.4049/jimmunol.1700267.

Turner, J.S., Ke, F., and Grigorova, I.L. (2018). B Cell Receptor Crosslinking Augments Germinal Center B Cell Selection when T Cell Help Is Limiting. Cell Rep 25, 1395-1403 e1394. 10.1016/j.celrep.2018.10.042.

Ventura, A., Kirsch, D.G., McLaughlin, M.E., Tuveson, D.A., Grimm, J., Lintault, L., Newman, J., Reczek, E.E., Weissleder, R., and Jacks, T. (2007). Restoration of p53 function leads to tumour regression in vivo. Nature 445, 661-665. 10.1038/nature05541.

Viant, C., Weymar, G.H.J., Escolano, A., Chen, S., Hartweger, H., Cipolla, M., Gazumyan, A., and Nussenzweig, M.C. (2020). Antibody Affinity Shapes the Choice between Memory and Germinal Center B Cell Fates. Cell 183, 1298-1311 e1211. 10.1016/j.cell.2020.09.063.

Victora, G.D., Dominguez-Sola, D., Holmes, A.B., Deroubaix, S., Dalla-Favera, R., and Nussenzweig, M.C. (2012). Identification of human germinal center light and dark zone cells and their relationship to human B-cell lymphomas. Blood 120, 2240-2248. 10.1182/blood-2012-03-415380.

Victora, G.D., and Nussenzweig, M.C. (2012). Germinal centers. Annu Rev Immunol 30, 429-457. 10.1146/annurev-immunol-020711-075032.

Victora, G.D., and Nussenzweig, M.C. (2022). Germinal Centers. Annu Rev Immunol 40, 413-442. 10.1146/annurev-immunol-120419-022408.

Victora, G.D., Schwickert, T.A., Fooksman, D.R., Kamphorst, A.O., Meyer-Hermann, M., Dustin, M.L., and Nussenzweig, M.C. (2010). Germinal center dynamics revealed by multiphoton microscopy with a photoactivatable fluorescent reporter. Cell 143, 592-605. 10.1016/j.cell.2010.10.032.

Vinuesa, C.G., Tangye, S.G., Moser, B., and Mackay, C.R. (2005). Follicular B helper T cells in antibody responses and autoimmunity. Nat Rev Immunol 5, 853-865. 10.1038/nri1714.

Vos, Q., Lees, A., Wu, Z.Q., Snapper, C.M., and Mond, J.J. (2000). B-cell activation by T-cell-independent type 2 antigens as an integral part of the humoral immune response to pathogenic microorganisms. Immunol Rev 176, 154-170. 10.1034/j.1600-065x.2000.00607.x.

Walker, L.M., Sok, D., Nishimura, Y., Donau, O., Sadjadpour, R., Gautam, R., Shingai, M., Pejchal, R., Ramos, A., Simek, M.D., et al. (2011). Rapid development of glycan-specific, broad, and potent anti-HIV-1 gp120 neutralizing antibodies in an R5 SIV/HIV chimeric virus infected macaque. Proc Natl Acad Sci U S A 108, 20125-20129. 10.1073/pnas.1117531108.

Wang, X., Cho, B., Suzuki, K., Xu, Y., Green, J.A., An, J., and Cyster, J.G. (2011). Follicular dendritic cells help establish follicle identity and promote B cell retention in germinal centers. J Exp Med 208, 2497-2510. 10.1084/jem.20111449.

Wang, Y., Shi, J., Yan, J., Xiao, Z., Hou, X., Lu, P., Hou, S., Mao, T., Liu, W., Ma, Y., et al. (2017). Germinal-center development of memory B cells driven by IL-9 from follicular helper T cells. Nat Immunol 18, 921-930. 10.1038/ni.3788.

Wardemann, H., Yurasov, S., Schaefer, A., Young, J.W., Meffre, E., and Nussenzweig, M.C. (2003). Predominant autoantibody production by early human B cell precursors. Science 301, 1374-1377. 10.1126/science.1086907.

Watanabe, M., Fujihara, C., Radtke, A.J., Chiang, Y.J., Bhatia, S., Germain, R.N., and Hodes, R.J. (2017). Co-stimulatory function in primary germinal center responses: CD40 and B7 are required on distinct antigen-presenting cells. J Exp Med 214, 2795-2810. 10.1084/jem.20161955.

Weisel, F.J., Zuccarino-Catania, G.V., Chikina, M., and Shlomchik, M.J. (2016). A Temporal Switch in the Germinal Center Determines Differential Output of Memory B and Plasma Cells. Immunity 44, 116-130. 10.1016/j.immuni.2015.12.004.

Xu, Z., Pone, E.J., Al-Qahtani, A., Park, S.R., Zan, H., and Casali, P. (2007). Regulation of aicda expression and AID activity: relevance to somatic hypermutation and class switch DNA recombination. Crit Rev Immunol 27, 367-397. 10.1615/critrevimmunol.v27.i4.60.

Yeh, C.H., Nojima, T., Kuraoka, M., and Kelsoe, G. (2018). Germinal center entry not selection of B cells is controlled by peptide-MHCII complex density. Nat Commun 9, 928. 10.1038/s41467-018-03382-x.

Young, C., and Brink, R. (2021). The unique biology of germinal center B cells. Immunity 54, 1652-1664. 10.1016/j.immuni.2021.07.015.

Young, R.M., and Staudt, L.M. (2013). Targeting pathological B cell receptor signalling in lymphoid malignancies. Nat Rev Drug Discov 12, 229-243. 10.1038/nrd3937.

Yusuf, I., Kageyama, R., Monticelli, L., Johnston, R.J., Ditoro, D., Hansen, K., Barnett, B., and Crotty, S. (2010). Germinal center T follicular helper cell IL-4 production is dependent on signaling lymphocytic activation molecule receptor (CD150). J Immunol 185, 190-202. 10.4049/jimmunol.0903505.

Yusuf, I., Zhu, X., Kharas, M.G., Chen, J., and Fruman, D.A. (2004). Optimal B-cell proliferation requires phosphoinositide 3-kinase-dependent inactivation of FOXO transcription factors. Blood 104, 784-787. 10.1182/blood-2003-09-3071.

Zaretsky, I., Atrakchi, O., Mazor, R.D., Stoler-Barak, L., Biram, A., Feigelson, S.W., Gitlin, A.D., Engelhardt, B., and Shulman, Z. (2017). ICAMs support B cell interactions with T follicular helper cells and promote clonal selection. J Exp Med 214, 3435-3448. 10.1084/jem.20171129.

Zhang, Y., Tech, L., George, L.A., Acs, A., Durrett, R.E., Hess, H., Walker, L.S.K., Tarlinton, D.M., Fletcher, A.L., Hauser, A.E., and Toellner, K.M. (2018). Plasma cell output from germinal centers is regulated by signals from Tfh and stromal cells. J Exp Med 215, 1227-1243. 10.1084/jem.20160832.

Zhao, Y., Gregory, M.T., Biertumpfel, C., Hua, Y.J., Hanaoka, F., and Yang, W. (2013). Mechanism of somatic hypermutation at the WA motif by human DNA polymerase eta. Proc Natl Acad Sci U S A 110, 8146-8151. 10.1073/pnas.1303126110.

Zikherman, J., Parameswaran, R., and Weiss, A. (2012). Endogenous antigen tunes the responsiveness of naive B cells but not T cells. Nature 489, 160-164. 10.1038/nature11311.

Zotos, D., Coquet, J.M., Zhang, Y., Light, A., D'Costa, K., Kallies, A., Corcoran, L.M., Godfrey, D.I., Toellner, K.M., Smyth, M.J., et al. (2010). IL-21 regulates germinal center B cell differentiation and proliferation through a B cell-intrinsic mechanism. J Exp Med 207, 365-378. 10.1084/jem.20091777.

Zotos, D., Quast, I., Li-Wai-Suen, C.S.N., McKenzie, C.I., Robinson, M.J., Kan, A., Smyth, G.K., Hodgkin, P.D., and Tarlinton, D.M. (2021). The concerted change in the distribution of cell cycle phases and zone composition in germinal centers is regulated by IL-21. Nat Commun 12, 7160. 10.1038/s41467-021-27477-0.

Zuba-Surma, E.K., Kucia, M., Abdel-Latif, A., Lillard, J.W., Jr., and Ratajczak, M.Z. (2007). The ImageStream System: a key step to a new era in imaging. Folia Histochem Cytobiol 45, 279-290.